UNIVERSITÀ DEGLI STUDI FIRENZE

Doctoral Programme in Industrial Engineering

Dottorato di Ricerca in Ingegneria Industriale

XXX

Belted Safety Jacket: a new concept in motorcycle passive safety

ING/IND-14

Doctoral Candidate
Ing. Alessandro Grassi

Supervisors
Prof. Niccolò Baldanzini

Ing. Daniele Barbani

External Referees
Prof. Massimiliano Avalle

Prof. Ugo Galvanetto

Dean of the Doctoral Programme
Prof. Maurizio De Lucia

Years 2014/2017

Dedicated to myself

Summary

Powered Two Wheelers (PTWs) offer a viable solution to reduce traffic congestion and promote personal mobility. However, vehicle characteristics and conspicuity issues lead to an overrepresentation of PTWs in accident statistics. This work presents an innovative approach for concept design of new passive safety devices and their development. The landscape of possible design solutions was examined with an in-depth analysis of the state of the art and using conceptual design tools. Candidate solutions underwent a feasibility assessment and they were crossed-checked with rider needs, identified via a specific on-line survey. The concept of a new passive safety device was born: a Belted Safety Jacket (BSJ).

An initial assessment of the device effectiveness for the reduction of riders' injuries was performed by comparison of the main biomechanical indexes (HIC, N_{ijmax}, Chest Deflection and Viscous Criterion) in a relevant accident configuration, reproduced in a virtual environment, with and without the device. Later a full factorial Design of Experiment (DOE) was carried out to understand the influence of the device geometrical variables (i.e. possible design parameters) on the biomechanical indexes. The results demonstrated that the BSJ fitted into the vehicle has the potential to significantly reduce the occurrence of serious injuries during a PTW accident versus a car, since it prevents the contact of the rider with the opponent vehicle. The analysis of the accident kinematic with BSJ suggests that the device will be beneficial also in accidents with other vehicle types.

In the second part of the study, first steps of the device development were carried out. The best device geometrical configuration, emerged from an optimization activity on the factors analysed with DOE, was used to test the device effectiveness in other impact configurations. In order to define which are the most common and representative impact configurations of the European daily life, in a depth analysis on a motorcycle accident databases was conducted. From this activity, it emerged that only three of the seven impact configurations reported in the standard reference (ISO 13232), are still representative. Instead, the other four were different. Subsequently, a new vehicle impact speed assessment for each impact configuration was done.

Thanks to this work, it was possible to establish the speed pair able to guarantee a good representativity of the harmfulness of the impact configuration. The numerical simulations showed interesting results and, allowed to observe that the integration of the passive safety device, developed and assessed in this research activity, can reduce significantly the probability to incur in serious injuries during an accident. In general, the results showed that with the device fitted onto PTW, the rider's chest did not impact against the handlebar. This allowed a good reduction of chest bio-mechanical indexes. Furthermore, the dummy final position always resulted less dangerous for possible secondary impacts. In the majority of the tested configurations, the head and neck injury indexes decreased considerably. On the other hand for rear-end and head-on collision, the restraint force exerted by BSJ was too high, and it may lead to an increase of the neck index but with a contained effect on head dynamic actions. Also in these cases, the final position taken by the dummy is safer in presence of the device. Indeed, even if, the MC impact speed was low, the displacement of the dummy was high, and the dummy loses the physical contact with the PTW. Contrary, for higher impact speed, the effectiveness of the device resulted most obvious. As already emerged from the preliminary impact configuration assessed, if the MC speed is higher, the benefits of device for the injury reduction were evident. The work done laid the basis for future Belted Safety Jacket development and it opened the way to new opportunities in this field. Future works will be able to tackle and pass the limits highlighted in this preliminary study. Moreover, only seven impact configurations are not sufficient to uniquely establish the device effectiveness in the injuries reduction, but the results obtained were quite interesting and for this reason further tests in different configurations and with different impact speeds would be necessary to deeply investigate the issue. Furthermore, it could be interesting to evaluate the device possible integration with other safety systems, to further increase the safety level.

Contents

List of Figures

List of Tables

Glossary

ACEM Association des Constructeurs Europeens de Motocycles.

AIS Abbreviated Injury Scale.

ASV-3 Advanced Safety Vehicule 3.

C.R.I. Configuration Risk Index.

DM Decision Matrix.

DOE Design of Experiment.

EEVC European Enhanced Vehicle-Safety Committee.

GSI Gadd Severity Index.

HIC Head Injury Criterion.

Hybrid III Standard crash test dummy for frontal crash tests.

IRTAD International Traffic Safety Data and Analysis Group.

ISO International Standard of Organization.

ISQ Innovation Situation Questionnaire.

MAIDS Motorcycle Accidents In Depth Study.

MC Motorcycle.

MCS Motorcycle Speed.

MIPS Multi-direction Impact Protection System.

$\mathbf{N_{ij}}$ Biomechanical Neck Injury Predictor.

NHTSA National Highway Traffic Safety Administration.

NoP Network of Problem.

OECD Organization for Economic and Co-operation and Development.

OTSM Obshtchaya Teorya Silnogo Myshlenia - General Theory of Powerful Think-ing.

OV Opposing Vehicle.

OVS Opposing Vehicle Speed.

PHPS Phillips Head Protection System.

PMHS Post Mortem Human Subject.

PTW Powered Two Wheeler.

RHA Relative Heading Angle.

SDI Speed Damage Index.

SO System Operator.

TI Tibia Index.

TRIZ Teoriya Resheniya Izobretatelskikh Zadach - Theory of Inventive Problem Solving.

TRL Transport Research Laboratory.

V*C Viscous Criterion.

WHO World Health Organization.

WSM Weighted Sum Method.

WSTC Wayne State Tolerance Curve.

Introduction

In the last years, in Italy and in Europe, the Powered Two-Wheelers (PTWs) circulating park suffered a sudden drop in sales, but their presence on the roads is still relevant. This big diffusion is strictly linked to the user's unremitting demand for mobility. Specifically motorcycles, scooters and mopeds play a significant role in cities around the world, where traffic congestion and parking spaces represent a relevant daily problem. As such, PTWs are becoming a more and more important component of the transport system. However, PTWs inherent instability, the low use of passive safety protective devices (non-mandatory) and the absence of structures represent a challenge for safety. Riders are at far more risk than car drivers per kilometre ridden in terms of fatalities and severe injuries compared with car occupants (Holgate et al. (2015)). Moreover, although the holistic approach to safety includes different factors (e.g. safe road, improved user training, safe vehicle, etc.), protective systems are still a cornerstone to ensure more tolerance in case of riders' or other road users' errors.

This study aims to deepen previous knowledge in Powered Two-Wheeler passive safety with an innovative approach in this field, capable to systematically explore all possible design solutions, in order to find new devices/systems able to increase rider's safety. The backbone of this work is comprised of several activities, which are summarized in the schematic diagram of figure 1.

In regard of this, in the first sections, a general statistic overview of PTWs world (accident, market and spread) is reported, in order to contextualize this work from a global point of view. Subsequently, the standards adopted, the tools and methods employed in the research are presented. After this first introductory part, the research focuses on the *"Research and development of a new passive safety device for motorcycle/motorcyclist"*.

As shown in figure 1, this aim is pursued through three different and simultaneous activities. The analysis of the state of the art is fundamental to understand previous research activities in this sector, what is missing and where research is heading, but also to extrapolate evaluation criteria for solutions that arise from the Network of Problem.

Later, a specific survey, based on the principles of Kano's theory (Kano (1984)), is created to evaluate candidate factors to improve customers' level of satisfaction on passive safety devices: the survey is targeted to understand stakeholders' habits and needs. It also helps to translate them in selection/decision criteria for the Network of Problem solutions, focusing the attention on the device features to be

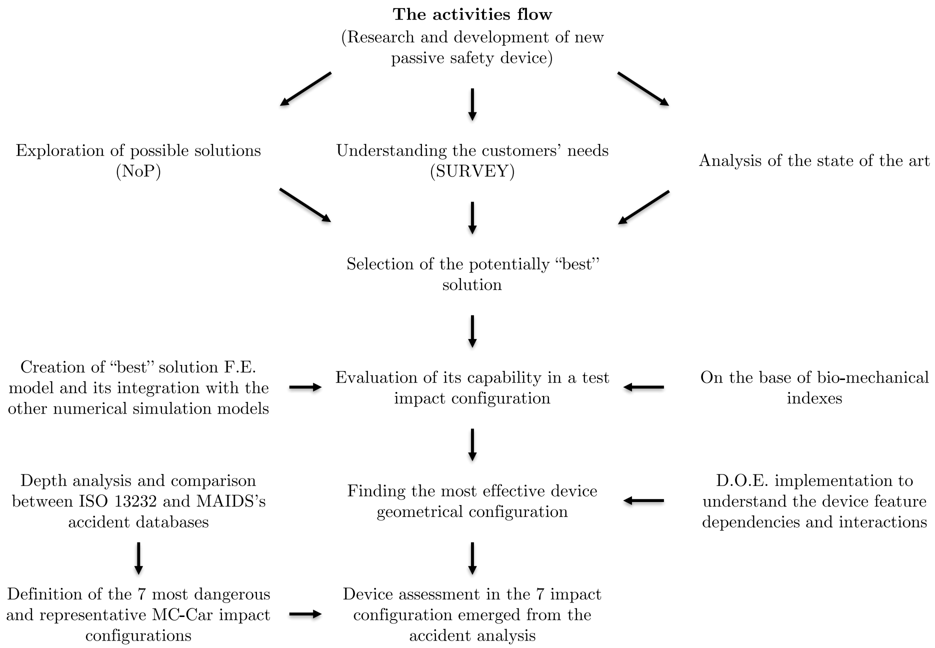

Figure 1: Research flowchart

implemented or not during the new device design phase.

Subsequently, the implementation of the NoP (Khomenko et al. (2007)) using TRIZ and OTSM tools, are introduced. In general, NoP represents a network of plausible solutions to the problem, which allows to find new development paths and solutions.

From the information and criteria extracted from the state of the art and the survey, it is possible to analyse the NoP solutions and to select the best potential one. In order to define which is the best solution, a very common tool called Weighted Sum Method (WSM), combined with a Decision Matrix (DM), is used.

A FE model of the solution found is generated and integrated with PTW, car, dummy and helmet models into a specific crash test simulation. Analysing the bio-mechanical injury indexes variation, extracted from the simulation, the device capability to reduce rider's injuries is evaluated.

In the second section, the new safety device is introduced, describing the rationale and the overall working principle as well as each component. The device is tested in a Finite Element (FE) virtual environment against a passenger car for a specific crash configuration. A comparative analysis (i.e. with and without the chosen device fitted on the PTW) is performed to evaluate its protective efficacy.

Later a full factorial DOE (Design Of Experiment) is implemented to understand possible correlations of device parameters, and their interactions with its protective performance. DOE results allow to identify the best performing design of the device with reference to the specific tested impact configuration.

In the end, the behaviour and the results, obtained testing the device in other impact configurations, are described. To this end, an in-depth motorcycle accident database analysis is conducted, in order to verify if the set of the seven most relevant configurations, proposed within the ISO 13232 ISO (2005), are effectively representative of the European context. Comparing the obtained results from MAIDS (MAIDS (2009)) database with the outcomes of the ISO 13232 ISO (2005), it is possible to choose, on the basis of a new objective evaluation method, which are the most important and the most dangerous impact scenarios for the rider. Thanks to this activity it is possible to define a new impact configurations set.

The new device (Belted Safety Jacket) is tested in the new proposed set. For each of these new configurations, a comparison of the most used bio-mechanical indexes, with and without the device fitted on PTW-rider, is presented. Furthermore, a brief critical analysis of results and simulation frames obtained is carried out. From the results obtained, useful indications for future device development and improvement are extrapolated.

Chapter 1

Background

In statistical analyses conducted by ACEM (Association des Constructeurs Europeens de Motocycles), within “Motorcycle Accidents In Depth Study” (MAIDS), and by the International Traffic Safety Data and Analysis Group (IRTAD), the use of motorcycles as means of transport is significantly more risky than other vehicles (figure 1.1). The relative risk of motorcyclist is on average nineteenth times higher than car occupants. Consequently the number of injured people is generally higher, both from a physical and/or economic point of view. For this reason, in the last decades and in particular in the last few years, research focused its efforts to improve safety. To do this, it is necessary to broaden the spectrum of analysis and intervention. In this optic, many countries tend to think more in terms of the “Safe System approach”. Indeed, by focusing the attention only on the behaviour of the road users involved, the road safety issues is impossible to solve. This new approach is not opposed to that focused on road users, but it simply provides a wider understanding of the risk factors and the spectrum of interventions, which may address them efficiently. The philosophy of the last 30 years was focused on the enforcement of some important factors such as speed, alcohol, use of safety systems/devices as seat-belt or helmet and, more generally, non-compliance with the basic safety rules.

The Safe System approach bases its focus on avoiding the most severe traffic crashes taking into account the main road system components (ITF (2015)). In the specific:

- promote safe behavior of road users;
- offer the capacity to correct their errors;
- protect them when these errors cannot be corrected.

To protect road users by their errors remains the last resource to mitigate the consequences of an inevitable collision. In order to respond to this point, this thesis is aimed to research and develop a new passive safety device. It could represent a little, but fundamental step, towards a Safe System approach. The Safe System approach (see figure 1.2) addresses risk factors and interventions related to road users, vehicles, road environment, and post-crash response, in an integrated manner (Belin (2012); OECD (2008); WHO (2005)). The Safe System approach

	Car Occupant	Motorcyclists	Mopeds (when distinction is made in statistics)	Relative risk of motorcyclists vs. car occupants
Australia	5.2	71.8		14
Austria (2010)	4.7	59.7	56.1	13 for motorcyclists 12 for mopeds
Belgium (2010)	5.9	76.9		13
Canada (2010)	4.9	62.9		13
Czech Republic (2010)	10.5	252.6		24
Denmark	4.2	49.5		12
France	4.9	72.4	64.7	15 for motorcyclists 13 for mopeds
Germany	3.3	59.5	14.6	18 for motorcyclists 4 for moped
Ireland	2.5	60.8		24
Israel (2010)	5.1	45.7	26.8	9 for motorcyclists 5 for mopeds
Netherlands (2004-08)	3.0	64	63	21
Slovenia	4.3	112.5		26
Sweden (2010)	2.2	43.9		20
Switzerland	2.3	39.2	29.6	17 for motorcyclists 12 for mopeds
United Kingdom (Great Britain) (2012)	2.1	72		34
United States	5.0	155.0		31

Figure 1.1: Deaths per billion vehicle-kilometres in 2011 (*Source:* IRTAD).

to road safety recognizes that transport is important to society, and that travel should be safe for all road users while they interact with roads and vehicles. The Safe System approach aims to eliminate fatal crashes and reduce serious injuries through provision of a safe transport system that is forgiving of human error and takes into account people's vulnerability to serious injury. This is done through a policy focus on road infrastructure, vehicles and travel speeds, and is supported by a range of activities in education, regulation, enforcement and penalties. The Safe System approach has been shown to be applicable in several settings around the world, in some cases facilitating road safety gains where progress had stalled (Mooren et al. (2011)).

The key principles of the Safe System approach are summarized as follows (OECD (2008)):

Recognition of human error in the transport system. People will make mistakes in traffic that can easily lead to injuries and death. The Safe System approach does not ignore road user behaviour interventions but emphasizes that behaviour is just one of many essential prevention focus areas.

Recognition of human physical vulnerability and limits. People have a limited tolerance to violent force, beyond which serious injury or death occurs.

Promotion of a system approach. Combined road safety measures yield better results than single measures.

Promotion of a shared responsibility. Responsibility for traffic safety must be shared between road users and system designers. While road users are expected to comply with traffic regulations, system designers and operators

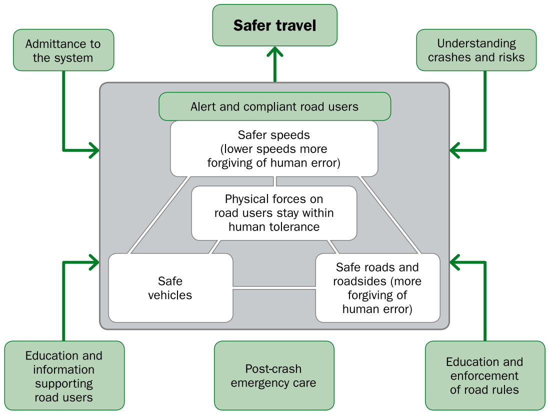

Figure 1.2: The Safe System approach (*Source:* WHO (2017)).

have a responsibility to develop a transport system that is as safe as possible for users.

Promotion of ethical values in road safety. The ethical value underlying the Safe System approach is that any level of serious trauma arising from the road transport system is unacceptable. Humans can learn to behave more safely, but errors will inevitably occur on some occasions. The errors may lead to crashes, but death and serious injury are not inevitable consequences.

As noted in the Decade of Action on Road Safety, 2010-2020 (WHO (2005)), the principles of the Safe System approach are upheld via coordination across five pillars of action: road safety management, safer roads and mobility, safer vehicles, safer road users and post-crash response. The approach sees a shift from the view of individual responsibility of the road user to a shared responsibility by many different arms of government, politicians and industry. The approach aims to not only reduce road user errors, but importantly to reduce the risk of serious injury if an error occurs, through coordinated planning addressing all pillars of action.

1.1 Statistical point of view

Concentrating the attention on two and three wheeler motorized vehicles, it is possible to see that, they represent the second most deadly means of transportation after occupants' car, with a world average percentage of 23%. In specific regions this value can exceed 33% becoming the most common case of death. From Figure 1.1 and Figure 1.3, it is clear that, in the short term, the research of new systems to protect the motorcyclists must be a priority. Nowadays, the technological development has enabled the integration of more and more powerful security devices, especially for four-wheelers vehicles. On the contrary, the high number of possible collision scenarios that may occur, and the complex dynamics of the motorcyclist's movement, still characterize the two-wheeled world.

Annually, some 1.24 million people are killed on the world's roads and up to 50 million are severely injured. This represents big economic costs for many countries. Like all road traffic crashes, those involving powered two and three-wheelers (PTWs) such as motorcycles and e-bikes are often predictable and preventable, and should not be accepted as inevitable. The main factors for motorcycle traffic injuries are represented by: non-use of helmets; vehicle speed; alcohol use; mixed traffic conditions; lack of protection from the vehicle itself during a crash; and lack of safe infrastructure for PTWs, such as poor road surfaces and roadside hazards (WHO (2017)). WHO data show that globally more than 286000 motorcyclists were killed in road traffic crashes in 2013 (WHO (2015)). This represents almost a quarter of all road traffic deaths in that year. While the majority (90%) of PTW-related deaths globally occurred in lowland middle-income countries, PTW safety is a concern to all regions (figure 1.3).

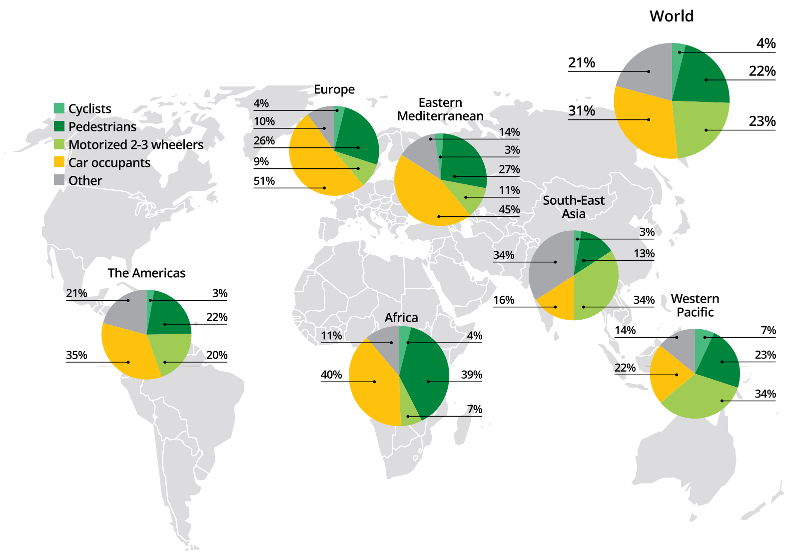

Figure 1.3: Road traffic deaths by type of road user, by WHO region (*Source:*WHO (2015)).

On average, the African region has the lowest fatality rate (7%) while Cambodia and Thailand, where there is a large PTW fleet, motorcycle fatalities in 2013 accounted for 70% and 73% of total road fatalities respectively, while in the same region, in high-income countries such as Australia and the Republic of Korea, motorcycle fatalities accounted for less than 18% of all traffic-related deaths (WHO (2015)). Furthermore, from this figure, it is possible to see that half of all road traffic deaths involve vulnerable road users, including: pedestrians, motorcyclists and cyclists. Around 17% of road traffic deaths in Organization for Economic and Co-operation and Development (OECD) countries in 2010 involved PTW users. Between 2010 and 2013 the proportion of motorcyclist deaths remained largely unchanged in the African Region and South-East Asia Region, while there was a slight decrease in motorcyclist deaths in the Eastern Mediterranean Region, European Region and the Western Pacific Region. The Americas Region is the only region that experienced an increase (see figure 1.4)

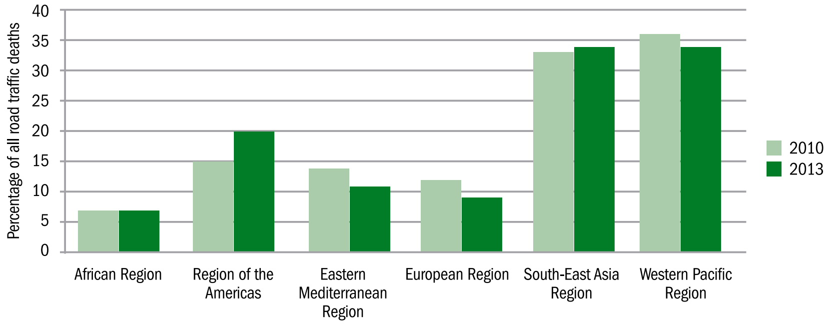

Figure 1.4: Proportion of motorcyclist deaths by WHO region (*Source:*WHO (2017)).

The demographic and socioeconomic profile of seriously and fatally injured PTW users greatly varies by region and country-income level. In low- and middle-income countries, most PTW users are aged 15-34 years, while in high-income countries, PTWs are widely used by people aged 35 years or older. As such, in low- and middle-income countries the majority of PTW crash casualties are those in their most productive years of life, with a mean age of 25 years. The peak age for motorcycle-related injury in low- and middle-income countries is in the early to late twenties ITF (2015).The majority of fatalities in low- and middle-income countries also falls into the same young adult age group (i.e. aged 15-34 years), while in high-income countries the mean age for PTW users killed as a result of a crash is about 55 years. This profile in high-income countries partially reflects that PTWs are used more as recreational vehicles than in low- and middle-income countries, where they are used as the primary mode of transport ITF (2015). Figure 1.5 shows data of 2015 (the most recent year available) from selected countries on the distribution of PTW-related deaths by age group, highlighting the variation between countries. In low- and middle-income countries (such as Argentina, Brazil, Colombia, Mexico, Thailand and Venezuela), young adults aged 15-34 years accounted for over 60% of all of PTW-related deaths. In high-income countries (such as the United States of America (USA) and the United Kingdom), almost 50% of the deaths occurred in adults aged 35-59 years; in Japan, those aged over 60 years accounted for 34% of deaths whereas those aged 35-59 years accounted for 36%.

Focusing the attention to European data, in 2014 about 26.000 people were killed in road accidents. Motorcycle and moped fatalities, together referred to as Powered Two Wheelers (PTW), accounted for 17% of those fatalities (16% in 2005). In 2014, at least 723 riders of mopeds were killed in the EU in accidents. As compared to 2005, this count has decreased by almost 56%. Regarding

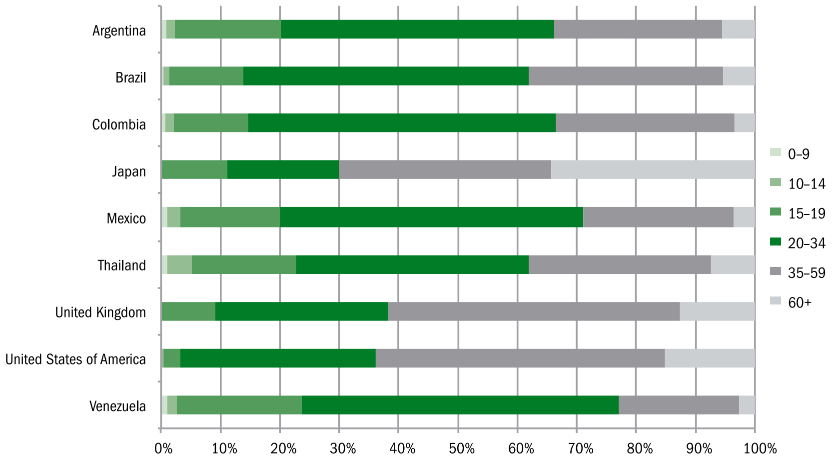

Figure 1.5: Age distribution of PTW users killed (*Source:*WHO (2017), WHO Mortality database).

drivers and passengers of motorcycle, at least 3.841 were killed in road accidents with a decrease of 32% compared to 2005 (Source:EU Commission (2016)). The distribution of road fatalities in EU from 2005 to 2014 is illustrated in figure 1.6

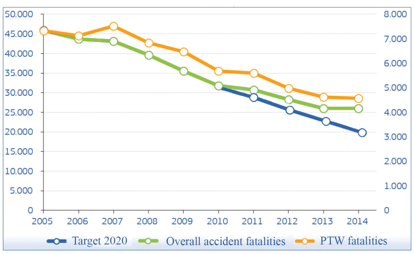

Figure 1.6: Distribution of road fatalities in the EU, 2005-2014 (*Source:*EU Commission (2016), CARE).

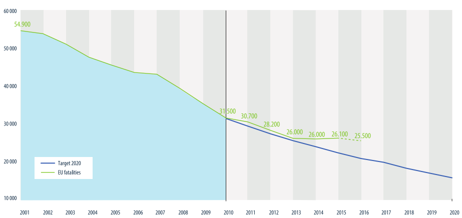

Figure 1.7: Road fatalities in the EU since 2001 (*Source:* European Commission, CARE).

Here, it is possible to observe that, the decrease trend of accident fatalities for all motor vehicles and the PTW, is void. After two years of stagnation (2013 and 2014), in 2015 fatalities increased (figure 1.7), while in 2016 a little decrease, but not in line with the target, was registered. As already seen in figure 1.1, also European data highlight the fatality of motorcycle respect to the other means of transport (see figure 1.8).

Figure 1.8 shows that the trend for motorcycle riders' fatalities differs somewhat from the trend for other modes of transport. Motorcycling is the only mode of transport for which the number of fatalities has increased during the period

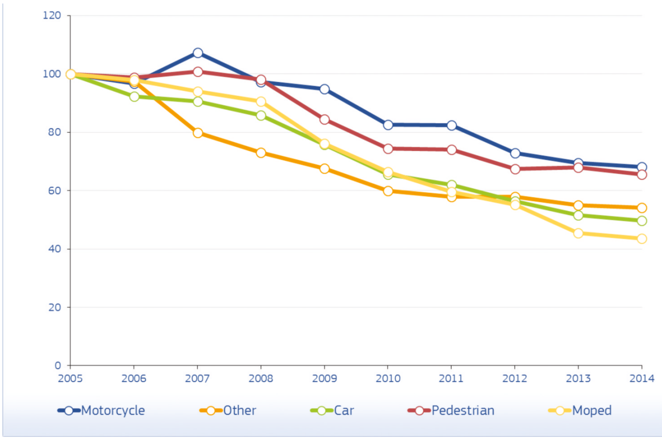

Figure 1.8: Index (2004=100) of motorcycle and moped fatalities compared with other modes of transport in the EU, 2005-2014 (*Source:*EU Commission (2016), CARE).

studied and only after 2007 a decrease set in. While figure 1.9 shows the fatality rate by age group in the EU. The rates for moped riders aged 15-17 and motorcycle riders aged 18-24 are particularly high.

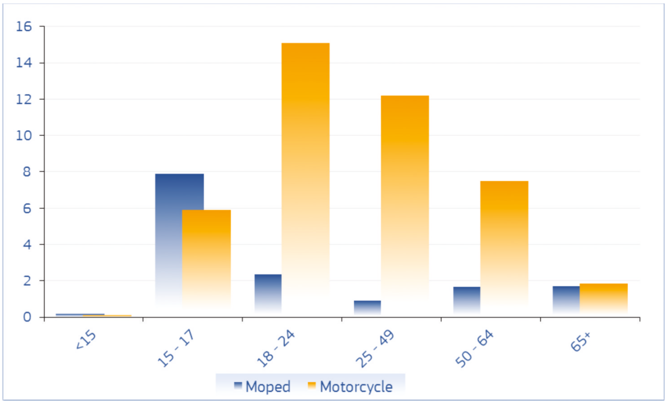

Figure 1.9: Motorcycle and moped fatalities per million population by age group in the EU, 2014 (*Source:*EU Commission (2016), CARE.).

1.2 Two wheelers choice

In the previous section, it was possible to see a little overview on: new strategies and existing policies to reduce severe or fatal road accidents, and distribution of world deaths cases divided by vehicle type. An important consideration could be understand why road users choose a specific type of vehicle Regarding motorcycles, scooters and mopeds, the citizens daily mobility demand is the reason of their heavy usage. Every day, across Europe, millions of citizens use the two wheels in everyday life, and the ever-increasing shortage of parking spaces in urban centres, makes the use of two-wheeled vehicles almost a compulsory choice. In addition, uncommon transport systems provide mobility to a large number of urban and rural residents in low and middle income countries, often because of a lack of affordable and accessible organized public transport. In India for example, only about 100 of the more than 5000 cities and towns have formal public transport systems. In some settings, ubiquitous but more expensive informal carriers are the only form of public transport available, for example, motorcycle taxis, auto-rickshaws (three-wheeled motorized vehicles), and four-wheeled jeepneys and jitneys (WHO (2017)). PTWs have a negative impact on the environment, and so factors such as air pollution should be taken into account when assessing and addressing the role of PTWs in mobility. In view of the overwhelming overpopulation of metropolitan areas has imposed a considerable motorcycle and mopeds CO_2 emissions reduction (figure1.10). In the last few years, their greater environmental sustainability compared to motor vehicles, places PTWs as favorite vehicles for private use. In summary the main factors contributing to the increase of PTWs fleet are:

- growing income levels in different regions;
- an unmet transport demand;
- increasing traffic congestion in urban areas;
- increasing cost of other forms of transport (e.g. in the form of high fuel prices);
- convenience and ease of parking and maintenance; and
- lower fuel consumption.

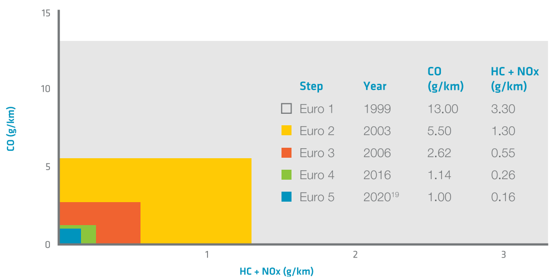

Figure 1.10: Emission reduction process for motorcycles (*Source:* ACEM).

In recent years, due to the economic crisis, the motorcycle market suffered a sudden drop in sales. Some countries as Italy limited, at least initially, this trend encouraging new purchases with financial aids, but it was not enough to stop recession on new registrations. In 2013, they reached the lowest in all countries, including Italy and Spain (see figure 1.11).

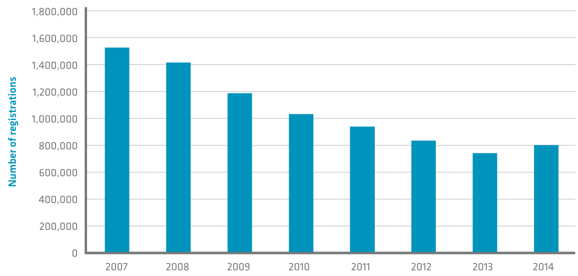

Figure 1.11: Motorcycle registrations in EU countries (2007-2014) (*Source:* ACEM).

This trend was already confirmed in the previous years. Regarding motorcycle, in 2014 saw a slight recovery, while for mopeds the trend remained unchanged (see figure 1.12).

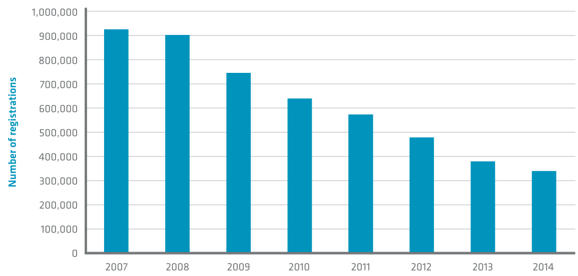

Figure 1.12: Moped registrations in EU countries (2007-2014) (*Source:* ACEM).

From the analysis of ACEM's market data, in 2016, EU motorcycles and mopeds sold increased by 9.1%, compared to the previous year. In 2016 European registrations of motorcycles (i.e. vehicles with two- or three wheels and an engine capacity of more than 50cc) grew by 13.3% compared to 2015. The largest market for motorcycles in Europe was Italy, with 195,290 units registered. Other large European motorcycle markets also showed positive trends: like Germany, France, Spain and UK. While regarding mopeds registration (i.e. vehicles with two or three wheels and an engine capacity of 50cc or less) a total of 327,826 mopeds were registered in Europe in 2016, representing a decrease of 3.5% confirming the trend in this segment. Registrations increased only in some of the major European markets such as Spain, Netherlands, and remained stable in France and Italy.

Regarding the last ACEM's available data (see figure 1.13), between January and June 2017 registrations of motorcycles reached 520,846 units marking -4.9% compared to the same period of 2016.

Italy and France result the only countries with a positive trend, while in Ger-

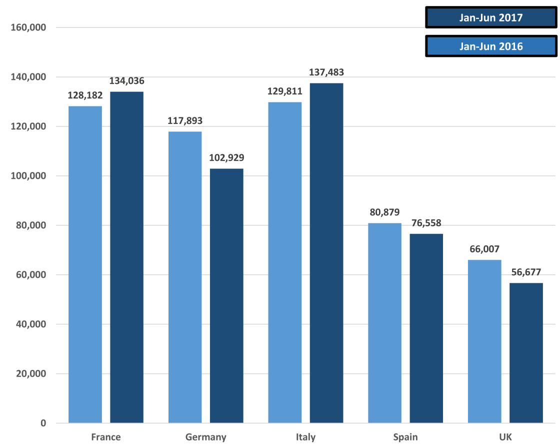

Figure 1.13: Cumulative registrations of mopeds and motorcycles in key EU markets January-June 2017 (*Source:* ACEM).

many, Spain and the UK a negative evolution was registered. The moped registration increased by 3.66% (161,162 units), led by strong growth in France and the Netherlands. Moped registrations declined in Germany, but remained stable in Poland and Italy.

1.3 Details of the standard ISO 13232:2005

In recent years, the improvement of active and passive safety has become an increasingly important topics in powered two-wheelers vehicles (PTWs) safe strategies. The main problem is related to the wide range of possible consequences of an accident resulting from the high complexity of the motorcycle-motorcyclist combined motion and the associated mechanisms of injury (considerably different from those typically highlighted in auto-vehicle occupants).

The collision of a motorcycle against a car is described by a large number of variables, such as the speed of the involved vehicles, the contact points between them etc. For many years a confusion ruled on methods used by the various research institutes to assess the injuries and the benefit/cost of a safety device. For this reason, the first ISO standard was developed and published in 1996, in order to standardize the assessment methods. A large description of the most important parts of the ISO 13232 (ISO (2005)), an insight of injury mechanisms and injury indexes (safe and widespread use) are given below.

The ISO 13232 (ISO (2005)) is a specific standard that describes the procedures for testing and analyse impact-protection equipment for motorcyclists. The 2005 version, which replaces the previous one (1996), describes the standardized methods and procedures for the development and evaluation of rider's crash protective devices fitted to motorcycles. Its application has no legislative purpose, but the procedures, outlined above, must be used to verify the applicability and the feasibility of a certain motorcycle protection device. However, experiments outside this standard are not prohibited. In these cases, it is necessary to specify, when and how, the experiment did not follow the procedures indicated therein. The need to standardize the tests is fundamental to be able to compare results and solutions obtained from different research groups. Indeed, during the research, it can be possible to use different types of dummy, different impact conditions and different measurement methods, that may lead to opposite results evaluating the same solution. The ISO 13232 (ISO (2005)) tries to avoid these ambiguities.

The standard is made up of 8 parts and it can be applied to the impact tests that involve:

- two-wheeled vehicles (MC);
- a specific type of opposing vehicle (OV);
- either a stationary and a moving vehicle or two moving vehicles;
- for any moving vehicle, a steady speed and straight-line motion immediately prior to impact;
- one helmeted dummy in a normal seating position on an upright motorcycle;
- the measurement of the potential for specified types of injury by body region and
- evaluation of the results of paired impact tests (i.e. comparisons between motorcycles with and without the proposed devices).

1.3.1 Part 1 - Definitions, symbols and general considerations

Motorcycle MC, two-wheeled vehicle with an engine cylinder capacity in the case of a thermal engine exceeding $50cm^3$ or whatever the means of propulsion a maximum design speed exceeding $50km/h$.

Opposing Vehicle OV, saloon type passenger car, against which the MC is impacted.

Fitted to the motorcycle, attached in a permanent manner to a structural element of the motorcycle.

Impact conditions, five variables which characterize and define the positions, orientations and velocities of the MC and OV immediately prior to impact in a full-scale impact test, a computer simulation of an impact or in MC/OV accident data.

RHA, angle between the MC x axis and the OV x axis measured in a clockwise direction from the MC x axis as viewed from above, immediately prior to first MC/OV contact.

MCS and OVS, magnitude of the OV and MC velocities relative to the ground, immediately prior to first MC/OV contact.

OV or MC contact point, for accident analysis, point representing the region of main and presumably initial structural damage to the OV in a given accident with an MC and vice versa.

Time of first MC/OV contact, first instant in time when a part of the MC or the dummy contacts the OV.

Here, it was reported only and excerpt of all definitions present in the standard. Any other definition are available in the first standard section.

1.3.2 Part 2 - Definition of impact conditions in relation to accident data

Fundamental purpose of the second part of the ISO 13232 (ISO (2005)) is to specify the minimum requirements for the collection and analysis of all motorcycle accident data, in order to provide:

- standardized and representative sub-set of car/motorcycle accident data; and
- a sub-set of car/motorcycle impact conditions based on the analysis of this standardized accident data.

The target is to understand, which impact configurations occur relatively frequently in the real world and which configurations result in relatively frequent injuries to certain body regions, based upon actual, large, randomized samples of motorcycle accidents. Two specific [1] accident databases were processed. During this work, five variables are necessary to define an impact test or an impact data for an accident, in the specific:

- relative heading angle; and
- opposing vehicle (OV) impact speed;
- motorcycle (MC) impact speed;
- OV contact point;
- MC contact point.

From the categorization and sorting method, defined in this section of the standard and applied to the combined Los Angeles and Hannover databases, 200 impact configurations were defined as combination of the five previous variables. Considering also injury frequencies, seven main configuration were extracted. These seven impact configurations are shown in Figure 1.14 and listed in Table 1.1.

The impact configuration code shall comprise a series of three digits describing the OV contact point, the MC contact point, and the relative heading angle, respectively, as generally defined in Figures 1.15(a), 1.15(b), and 1.15(c), followed by a hyphen (-), the OV impact speed, and the MC impact speed (see columns 5 and 6 of table 1.1).

Full-scale tests shall include the impact configuration shown in Figure 1.14 and listed in Table 1.1, with the following general rules:

[1] The accident database shall include at least 200 MC accidents and shall be uniformly sampled data from all reporting facilities for a given region (i.e., a randomized sample). The samples shall be the result of in depth investigations including on-site measurements and reconstructions. The subsample used, shall consist only of those accidents involving impacts between motorcycles and passenger cars.

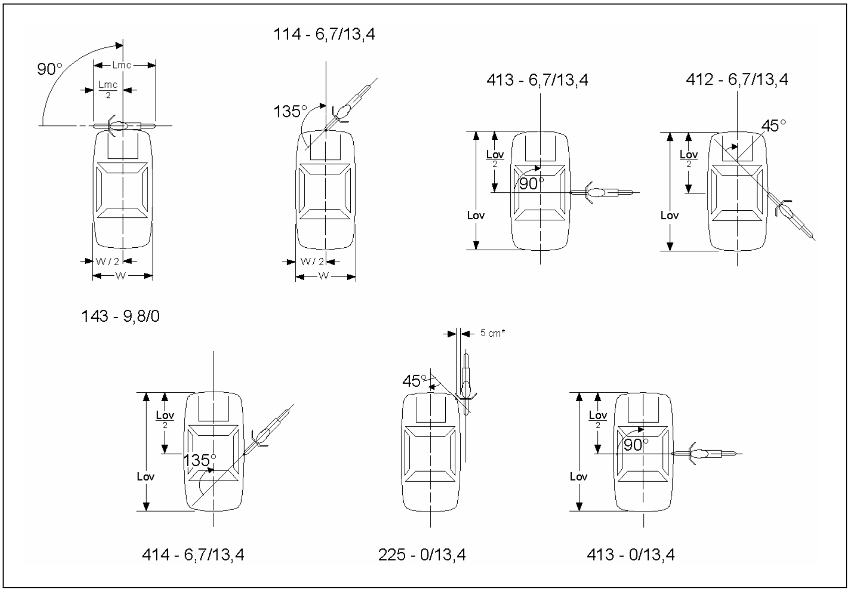

Figure 1.14: Target impact geometries at first MC/OV contact for seven required impact configurations. (*Source:*ISO (2005))

Table 1.1: Impact configurations for preliminary assessment.

Configuration number	**OV contact point code** (figure 1.15(a))	**Mc contact point code** (figure 1.15(b))	**RHA**	**OVS** $[m/s]$	**MCS** $[m/s]$
1	1	4	3	9,8	0
2	1	1	4	6,7	13,4
3	4	1	3	6,7	13,4
4	4	1	2	6,7	13,4
5	4	1	4	6,7	13,4
6	2	2	5	0	13,4
7	4	1	3	0	13,4

- OV corner contact points shall be the 45° tangent points, as shown in Figure 1.14;
- OV front and rear contact points shall be at the center line of the OV;
- OV side front, side middle, and side rear contact points shall be the points corresponding to 1/4, 1/2 and 3/4 of the overall length of the OV, respectively, as measured from the foremost point on the OV;
- MC front contact point shall be such that the projection of the MC center line, forward of the foremost part of the front wheel, at first contact between any portion of the MC or dummy and the OV, intersects a vertical line through the specified OV contact point;
- MC rear contact point shall be such that the projection of the MC center line,

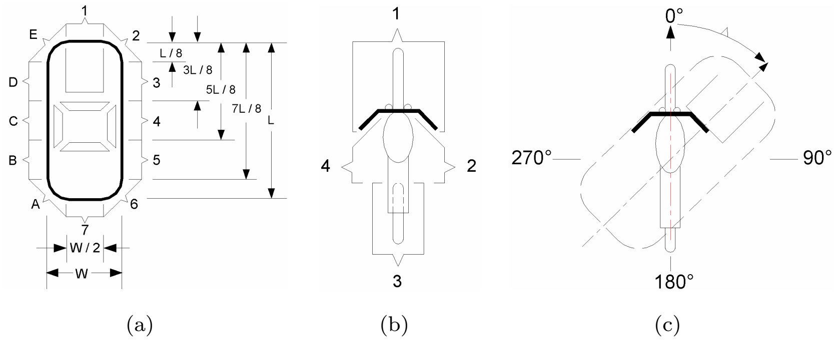

Figure 1.15: The impact configuration code defined by: (a) OV contact point codes; (b) MC contact point codes and (c) relative heading angle. (*Source:*ISO (2005))

rearward of the rearmost part of the rear wheel, at first contact between any portion of the MC or dummy and the OV, intersects a vertical line through the specified OV contact point;

- MC side contact shall use the conventions shown in Figure 1.14 (i.e., for OV front or rear contact use the 143-9,8/0 type of geometry; for OV corner contact use the 225-0/13,4 type of geometry);
- The relative heading angles shall be at the nominal values defined in Figure 1.15(c).

1.3.3 Part 3 - Motorcyclist anthropometric impact dummy

The third part of the standard specifies the minimum requirements for the dummy and in the specific:

- its biofidelity;
- its compatibility with motorcycles, helmets, multi-directional impacts, and the instrumentation;
- repeatability and reproducibility of its properties and responses.

Furthermore, the ISO 13232 (ISO (2005)) specifies that the basis dummy shall be the Hybrid III 50th percentile male dummy[2]. The dummy shall be equipped with:

- the sit/stand construction;
- the head/neck assembly which is compatible with the six axis upper neck load cell which is specified in the part 4 of the ISO (2005);
- standard, non-sliding knees.

[2]Basis dummy as specified in 49 CFR Part 572 (NHTSA (1993)), subpart E, or equivalent.

In 1989, the Hybrid III 50th percentile male dummy was identified as being the most thoroughly researched, contemporary, biofidelic, well documented, available dummy as a starting point for a motorcyclist dummy, on a worldwide basis. In addition, however, a number of modifications to it were needed, in order for it to be useable in motorcycle impact research. In the specific, a frangible femur and tibia bones, knee and solid abdominal insert are necessary. These modifications are needed because the standard Hybrid III is designed for passenger car (sitting). Other important changes are located in the neck zone (as a result of experimentation on motorcycle airbag). The complete assembly of the neck, nodding blocks, head attachment pin, bib simulator, and the upper half of the serrated lower neck mount shall have a mass of 1.55kg. The neck should be designed to meet simultaneously biofidelity criteria in frontal flexion and extension, lateral bending and torsion. In conclusion, skins, spine, hands and elbow, were modified to increase the biofidelity and the compatibility for example with the helmet, fuel tanks and so on. In figure 1.16 are reported the main components of the dummy Hybrid III.

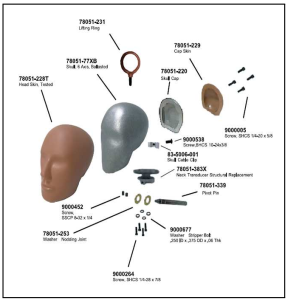
(a) Head components.

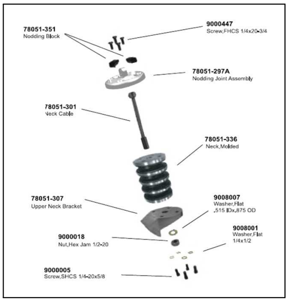
(b) Neck components.

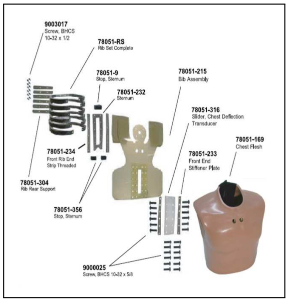
(c) Chest components.

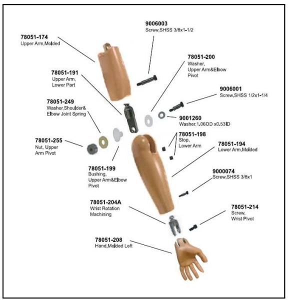
(d) Left arm components.

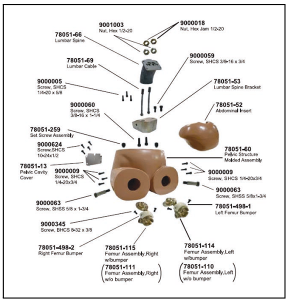
(e) Pelvis components.

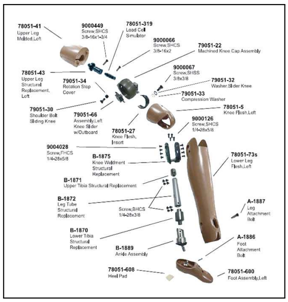
(f) Left leg components.

Figure 1.16: Hybrid III main components.

1.3.4 Part 4 - Variables to be measured, instrumentation and measurement procedures

This part specifies requirements for the:

- repeatability and reproducibility of the dynamic measurement procedures for the motorcycle, the opposing vehicle, and the dummy; and
- dummy instrumentation.

In all full-scale impact tests, the electronically recorded variables listed below shall be recorded:

- first MC/OV contact occurrence;
- nine linear head accelerations;
- sternum upper, lower, right and left displacements;
- antero-posterior shear force ($F_{x,n}$), lateral shear force ($F_{y,n}$), tension/compression force ($F_{z,n}$) and lateral bending ($M_{x,n}$), flexion/extension ($M_{y,n}$), torsional ($M_{z,n}$) moments, acting on the neck;
- axial force, bending moment and antero-posterior bending moment acting on the left and right femur;
- bending moment and antero-posterior bending moment acting on the left and right tibia.

It also defines the sensor specifications and positioning of the targets on the various components for photographic acquisition.

1.3.5 Part 5 - Injury indices and risk/benefit analysis

In the fifth part of the ISO 13232 (ISO (2005)) are defined:

- performance indices which can be correlated with human injuries;
- formulae which relate injury indices to probable injury cost;
- a consistent means of interpreting impact test results;
- a means of relating the results obtained from film analysis and instrumentation of the dummy to injuries sustained in accidents;
- a means of assessing both the combined and relative effects of multiple injuries;
- an objective means of quantifying injury cost using a single index;
- a means of verifying the analysis; and
- a means of doing risk/benefit analysis of protective devices fitted to motorcycles, based upon the population of impact conditions identified in the second part of this standard.

1.3.6 Part 6 - Full-scale impact-test procedures

The sixth part specifies minimum requirements for:

- paired comparison tests;
- the preparation of the dummy, motorcycle and opposing vehicle;
- the repeatability and reproducibility of impact test conditions within and between test sites;
- the minimization of variation in secondary test variables;
- realistic and representative impact conditions for full-scale impact tests;
- a means to verify analytical evaluations of proposed rider crash protective devices fitted to motorcycles, such as computer simulation.

Regarding the OV, for all tests in a given test series, it shall be a single make, model, year and version of any four door saloon having a kerb mass ranged from $1238kg$ and $1450kg$, and having an overall height not less than $137cm$ and not greater than $147cm$.

For the motorcycles many adjustments are necessary, from the fuel, chain or belt removal, to MC steering system freedom, to steer after release from the guidance system, in order to allow for self stabilization of the MC, and improved accuracy of the impact point.

The motorcyclist impact dummy used shall meet all of the requirements described in the part three of the standard. Prior to use in impact testing the dummy head, thorax, and knees shall be tested to conform to the calibration requirements and procedures.

The dummy shall be fitted with a Bieffe model B12R correctly helmeted. The helmet shall be new and with small ($56cm$) or medium ($58cm$) size. It shall be certified to ECE Reg 22-03 (United Nations (2000)) on a $57cm$ headform and helmets from the same production lot should be used for all tests within a paired comparison.

High speed cameras having the capabilities given in the fourth part shall be used. The cameras used for pre-test and pre-impact frames may be remotely triggered. Photographic targets shall be placed on the MC, OV, ground and dummy at the locations described in this and in the previous part.

As regards the air temperature of the area used for long term storage of the dummy, it should be between $13°C$ and $30°C$. For the test set-up, both the MC and the OV must have the wheels free to move at impact time, if they are moving.

For the OV, the battery cable and fuel removal are necessary. Also in this case the steering wheel and steering system should be free to steer, and transmission in neutral gear. Completely close all doors, windows, the bonnet, and the boot lid.

If only one pair of tests is carried out, a test must be carried out with the motorcycle equipped with the protective device and one without the device.

1.3.7 Part 7 - Standardized procedures for performing computer simulations of motorcycle impact tests

The purposes of this part are to provide:

- conventions for calibrating and documenting the important features of the simulation models;
- guidelines for definition and use of mathematical models for motorcycle impact simulations, which can be correlated against data for full-scale tests;
- a means for identifying possible additional impact conditions for full-scale testing; and
- a standardized tool, of optional use, for risk/benefit analysis of rider crash protective devices fitted to motorcycles, based upon the population of impact conditions identified in the second part of the standard.

The simulation model shall be based upon accepted laws and principles of physics and mechanics and it shall consist of portions describing a motorcycle (MC) and the opposing vehicle (OV), the dummy, the dummy mounting position, joint tensions, and helmet, the protective device, if present, and the road surface. In the model, the MC impact speed, OV impact speed, MC contact point, OV contact point and relative heading angle shall be able to be varied.

Regarding the construction of individual models, legislation imposes constraints on their composition. It lists the minimum parts to be formed and the minimum requirements that must match the actual ones, for example: mass, center of gravity, moments of inertia, position and orientation of the dummy joints, degrees of freedom, etc.

When the components have been completed, the correct output variables (forces, moments, speeds, accelerations, deformations, etc.) must be established to allow the calculation of the damage indexes. Output data should be considered from the instant $t = 1ms$ until the dummy comes into contact with the ground or in any case up to $t = 500ms$ after the first contact between the motorcycle and the vehicle depending on which of the two conditions occurs first. Next, the three dimensional animation should be used to display, graphically, the motions of MC, OV, dummy and protective device. The animation shall only show the modelled components as rigid bodies or finite elements with their own shape, orientation and relative position. Optional markers could be inserted to facilitate comparison between simulations and tests, in which case they shall match the photographic targets used in real impact tests.

When comparing experimental and virtual video, it is advisable to place the observation point at the same angle and distance from the cameras used in the real test. Among the frames that need to be collected in the simulation documentation are: the first contact moment between MC and OV, the first contact time between the dummy head and OV or the security device and the instants $t = 250ms$ and $t = 500ms$ after the first contact between MC and OV.

The injury analysis, the risk/benefit analysis and the performance of the protection device in the impact condition range shall be performed by means of computer simulations and may be performed as indicated in Part 3 using the conventions highlighted in Part 5.

The simulation shall be calibrated with tests, and the calibration results shall be documented in Part 8. If necessary, laboratory tests on the individual models or their components, can be performed for calibration.

The simulation must be carried out with all available data corresponding to the tests carried out in real scale according to the ISO 13232 (ISO (2005)) and using the same initial test conditions.

The comparison with experimental data shall be carried out in accordance with the methods set out in Part 4 and the graphs shall be presented in accordance with Part 8. Where data of 14 or more tests are available, a quantitative statistical analysis of the grade of correlation between experimental and numerical cases is necessary.

1.3.8 Part 8 - Documentation and reports

This part describes the documentation needed to properly compile test reports (real and/or virtual scale) according to the standard. In the appendices there are the tabs to be compiled for each phase of the experiment.

1.4 Injury evaluation

1.4.1 Injuries description

In this section some of the main topics are briefly addressed, to better understand: the connection between certain accidents and their resulting injuries and also the criteria used to evaluate them.

Main types of PTW accidents

As already mentioned, in the PTW sector, except for sporadic cases, the vehicle does not offer any protection to the users. The only protections are protective clothings worn by the rider (helmet, gloves, jacket, boots, etc.), which are not always able to limit injuries caused by strains of compression, twisting and cutting, generated as a result of an accident. Statistically we know that the most common accidents for motorcycles are those involving the front of the PTW (MAIDS (2009)). Figure 1.17) shows the line of sight to the OV as seen from the PTW rider at the time of the precipitating event.

Figure 1.18 shows frequencies associated with the most common motorcycle incident types.

In case of frontal impact with possible ejection, it is generally noted that the frontal wheel is the first contact point with the other vehicle. This one is generally located below the vehicle center of gravity. This condition causes the vehicle rotation by projecting the pilot in forward direction. Even in the case of a scooter, it is found that, after the impact, the rider moves forward banging the knees and lower limbs on handlebars, dissipating some of the kinetic energy possessed by the

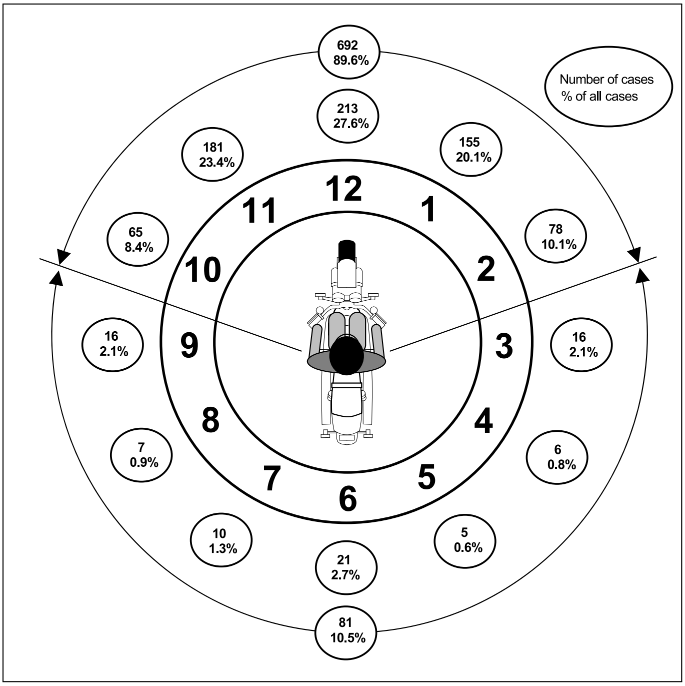

Figure 1.17: PTW line of sight to OV (*Source:* MAIDS (2009)).

body, and injuring more or less severely ankles, femur and knees. The problem is represented by the remaining energy. Indeed, the lower limbs do not completely dissipate all the kinetic energy of the body, this causes the upper part of the body to keep on moving, leading the chest and abdomen to possible impacts with the handlebars, the fairing and so on. The head, on the other hand, depending on the type of clash, can violently impact against the windscreen, OV or, in the case of ejection, it can disastrously landing by stressing the spine and neck. This scenario has generally serious consequences such as: cranial trauma, distortion or fractures of the cervical spine.

By analyzing the lateral impact it is easy to find the same lesions detected in the case of frontal impact. However, in this case the possibility of ejection is higher even at lower speed. The ejection often leads the top of the pilot's body, especially the head and lateral area of the chest, to hit against the bonnet the windscreen or the side of the OV with serious consequences, which can also evolve in secondary collisions with the ground.

PTW falling is usually recorded as a result of abrupt braking or loss of balance, and it involves the sliding of the motorcyclist as the vehicle lays on one side. In the most fortunate cases, the driver separates from the vehicle and beyond the initial impact, it can undergo cuts and abrasions due to the slippage resulting therefrom. In other cases, other parts of the body, usually feet, can remain locked, for example in the pedal cranks, dragging the pilot in event of rolling. This situation can be

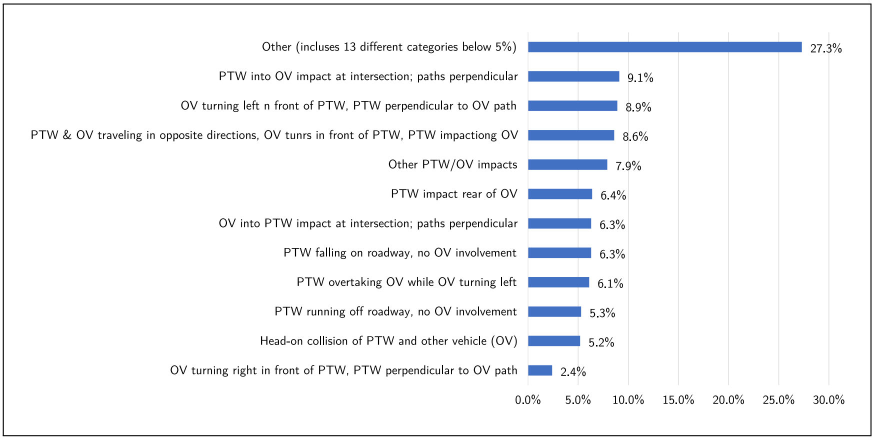

Figure 1.18: PTW accident configuration (*Source:* MAIDS (2009)).

very dangerous and can seriously damage the joints of the legs.

1.4.2 Main types of motorcyclist injuries

The following sections describe the types of injuries most frequently diagnosed for riders and passengers of powered two-wheeled vehicles involved in road accidents. Furthermore, they will also briefly describe the physical phenomena that have consequences for the most affected parts of the body.

Head injuries

The brain, contained within the skull, is suspended in the cefalorachid fluid and wrapped in meninges, as shown in figure 1.19. The main cause of head injury is caused by the relative movement between the brain and the skull. This phenomena is due to inertial effects. Inertia phenomena occur when the head, which has a certain traveling speed (the same as the rider and the vehicle), comes into contact with objects having a certain relative speed relative to it or simply undergoes accelerations or decelerations.

Skull fracture is the typical contact consequence between the cranial box and another object, clash that can often lead to a series of lesions. Typically, these injuries are represented by brain damage, vascular lesions and hematomas under the inner skull surface.

Cervical lesions reported as a result of an impact, are due to the compressive stresses following the introflection of the cranial bone. In event of collision, it is not unusual to detect a recoil injury; which occurs in the area diametrically opposite to where the contact took place. This effect is related to the local depression that is introduced in the cerebral fluid, subjecting the tissues to the major tensile stress. Scholars, P.Lubock and W.Goldsmith (Lubock and Goldsmith (1980)) argue that the great depressions that may be generated, can even lead to cavitation of cerebral fluid. The marked unevenness of the deformation velocity, that the various tissues

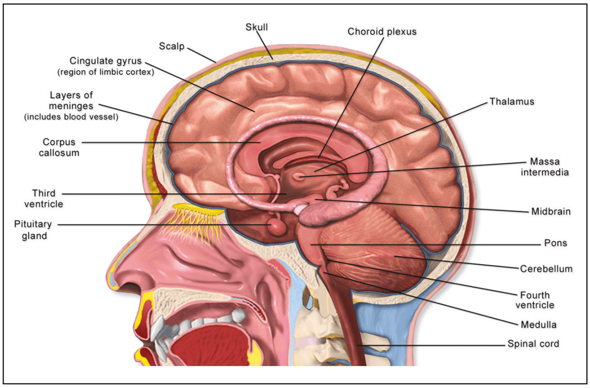

Figure 1.19: Human brain picture.

present, is associated with the intensity, the gradient, and duration at which tissues are subjected. If the impact develops on large and hard surfaces, generally, high acceleration gradients and reduced times, are observed.

Often, the energy associated with impacts does not lead to cranial fractures, but the accelerations of the brain mass can cause high traction and shear forces in the vessels between the meninges. These are sensitive to deformation speed, thereby generating subdural hematomas. The impact against softer surfaces causes lower gradients than those just described, but with extension of persistence times. In this scenario the most widespread consequence is to report a widespread axonal damage, that means, multiple damage on most of the nerve fibers, such as tearing and interruptions to microscopic level.

Cervical spine injuries

The cervical segment of the column consists of 7 vertebrae ($C1$ to $C7$) (figure 1.20), the 5 lower structurally identical ones, while the first (atlas) and the second (axis or epistafeo) have a very different conformation from the others, and in adults are fused together forming the occipital joint.

The vertebrae are kept apart from each other thanks to inter-vertebral disks and they are linked to each other by ligament bundles. The injuries reported in this area are direct consequences of dynamic stresses as a result of an impact. The stress components found are generally of axial type, both compression and traction, bending moments, both front and side, torque moments and cutting stress. Phenomena of frontal and lateral hyperflexion and those of hyperextension are particularly important, because they can cause vertebral fractures and compression along the concave section of the curve (figure 1.21).

Shear actions can lead to vertebral dislocation without fracturing. Excessive rotation of the head, combined with other movements, can injure the ligaments and lead to muscle strain. Cervical vertebrae lesions are of utmost importance, because within them, there is the spinal cord, and the nerves that control the upper limbs and the respiration.

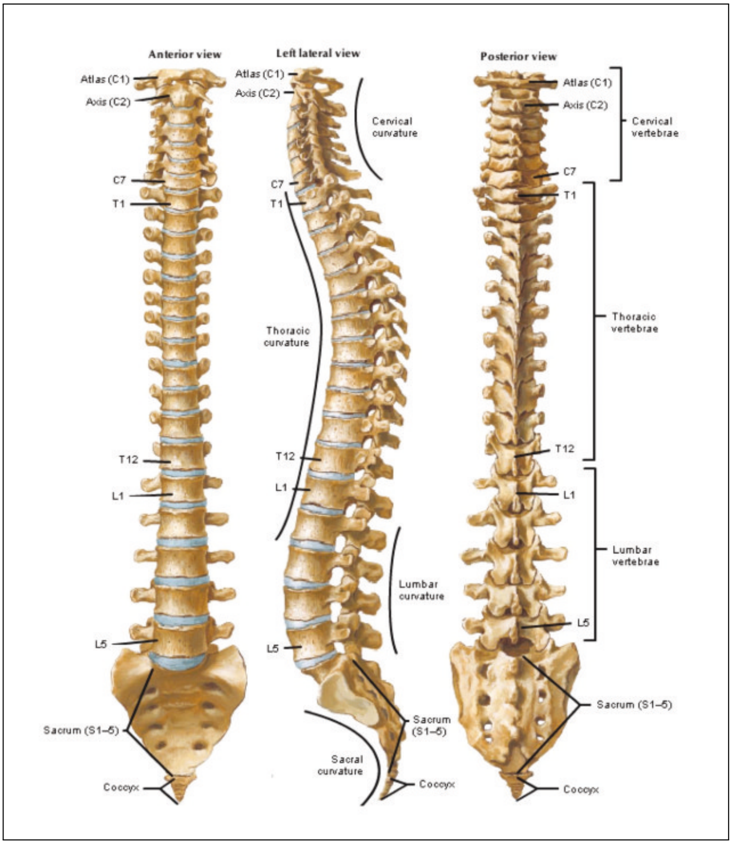

Figure 1.20: Three different views of the spine.

Thorax injuries

The chest cage (figure 1.22) consists of 12 vertebrae ($T1$-$T12$), and as many pairs of ribs, seven of which are connected to the sternum, the others are floating, finally, there are, the manubrium and the intercostal musculature. The purpose of the thoracic cage is to protect the internal organs, by ensuring, at the same time, appropriate flexibility for the respiration and the movements.

During the accidents, it is common to report fractures, even displaced, of one or more ribs due to compression loads, viscous and inertial loads. In these cases, pulmonary lesions, myocardial lacerations for overpressure and thoracic wall tear, may occur. Furthermore, it can still be seen a diaphragm and an aortic perforation, and respiratory insufficiency in the case of multiple fractures. Naturally, the above mentioned phenomena may occur, without necessarily have suffered ribs' fractures and vice versa. The internal structure of the chest is very sensitive to the deformation speed and therefore, when its deformation speed increases, the maximum tolerable deformation is reduced.

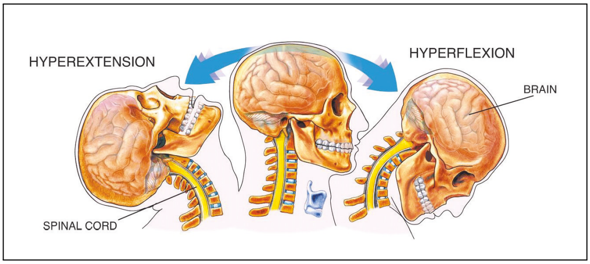

Figure 1.21: Neck hyperextension and hyperflextion phenomena.

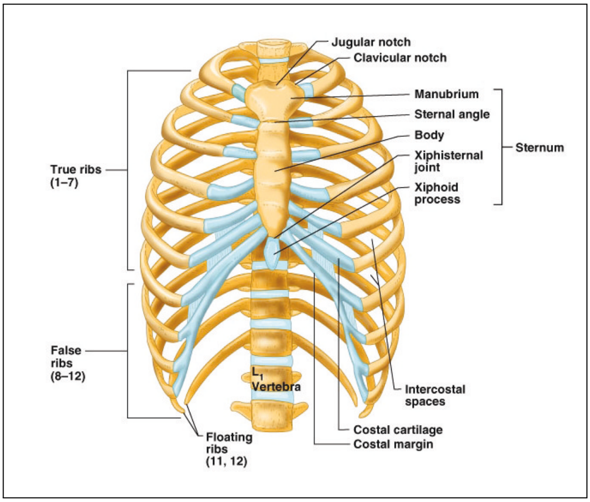

Figure 1.22: Rib cage picture.

Thoracic and lumbar spine injuries

The thoracic spine is made up of 12 vertebrae ($T1$-$T12$), while the lumbar of 5 ($L1$-$L5$) (figure 1.20). These are all very similar to those of the cervical section, although the lumbar ones are larger in size, as their function is to support the abdomen. The typical lesion for this zone is the compression rupture, which, being the last stretch of spinal cord, results in loss of lower limbs motility.

Pelvis and lower limbs injuries

Pelvis and lower limbs injuries are generally due to direct contact with an obstacle, and they rarely are fatal. Contrary, they are very common, especially for legs, feet and knees, and they may in any case could result in permanent invalidity.

1.4.3 Injury indexes and injury criteria

The need to define a direct link between the injury type, acting on a specific body part, and the relative injury severity, it was for many years, a central aim of biomechanicanics of impacts. In practice, drawing up a table that relates the cause to the effect is anything but easy, because, at the same stress, the response in terms of injury may be significantly different depending on sex, age and on the health of the subject. For this purpose, in 1969, the standardized scale called AIS (Abbreviated Injury Scale) was compiled (table 1.2 Gennarelli and Wodzin (2015)).

Table 1.2: AIS, Abbreviate Injury severity Scale.

AIS code	Description
1	Minor
2	Moderate
3	Serious
4	Severe
5	Critical
6	Maximal

This work was based on experiments and empirical criteria performed on corpses and volunteers, introducing other extirpation variables, (e.g. those linked to the tissues and their inevitable degradation), but not considering muscular reactions.

The injury criteria and the injury indexes, following reported, instead, they are mainly based on accelerations and deformations of regions containing vital organs, forces, and moments acting on the bone segments. With the injury index/criterion values, extracted from the impact simulations (simulated or real), it is possible to establish the degree of the injury severity. This is possible thanks to specific correlation curves, which link a injury index/criteria value with an associate probability of having a certain injury severity (AIS value).

Head Injury Criterion

As previously cited, the head is definitely one of the vital organs to be safeguarded in the event of an accident. Indeed, head injury continues to be a leading cause of death and disability; although a considerable advancement in the understanding of head injury mechanisms and the reduction of the number and severity of head injuries thanks to the introduction of safety systems (e.g. helmet for PTW). In spite of these advancements the only injury criteria in wide use is the Head Injury Criterion (HIC), which was adopted over forty-five years ago. This criterion was developed starting from the work of (Gurdjian et al. (1955)), who used the clinically observed prevalence of concomitant concussions in skull fracture cases (80% of all concussion cases also had linear skull fractures) to relate cadaver impacts to brain injury. With their study Gurdjian and co-workers concluded that by measuring the skull fracture tolerance, it is effectively inferring the tolerance to brain injury. Subsequently, Lissner and his co-workers (1960) developed a relationship between the magnitude of the translational anterior-posterior acceleration and the load duration that became known as the *WSTC* (Wayne State Tolerance Curve), which is fundamentally based on the average resultant translational head acceleration. In his study, Gadd (1962) developed what became known as the Gadd severity index *GSI* (Gadd (1966)); only afterwards Versace (1971) proposed the current version of the HIC in 1971 as measure of average acceleration that correlates it with the $WSTC$. HIC was then proposed by NHTSA as a replacement for the GSI and is computed according to the following expression:

$$HIC = \max\left[\left(\frac{1}{t_2 - t_1}\int_{t_1}^{t_2} a(t)dt\right)^{2.5} \cdot (t_2 - t_1)\right] \tag{1.1}$$

Where:

- t_1 and t_2 are two arbitrary times during the acceleration pulse expressed in $[s]$
- $a(t)$ is the acceleration, measured in multiples of the gravity acceleration $[g]$ and time is measured in seconds.

Initially, NHTSA proposed to limit this HIC time interval to 36 milliseconds. Subsequent studies have shown that this range may be excessively high if calculated on crash test dummies (Prasad and Mertz (1985); Mertz et al. (1994)). It is possible to differentiate two indexes with different ranges for which the limits are:

- $HIC_{36} = 1000$
- $HIC_{15} = 700$

The HIC_{36} value equal to 1000 corresponds to a probability of 18% to get an injury of AIS4 or higher. Figure 1.23 shows the correlation curve between the HIC value and the associated AIS4+ probability, proposed in Yoganandan et al. (2005).

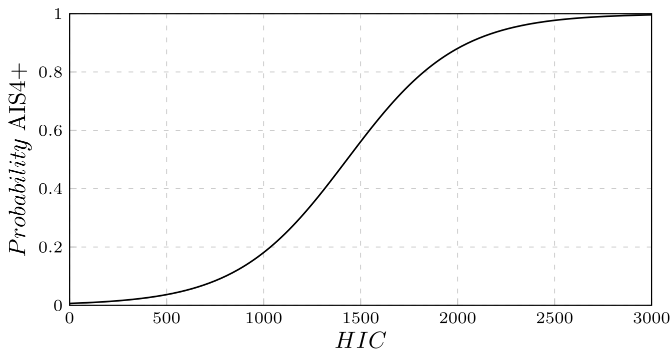

Figure 1.23: Correlation between HIC and probability of AIS4+.

The research shows that when the HIC value is greater than 1000, there is a high risk of fatal damage. Additional conditions for the equation 1.1 is that an acceleration of more than $3ms$ should not exceed the $80g$ value.

Neck injury criteria

The injury criteria for the neck consist in individual tolerance limits for different stresses. These tolerance values are based on studies conducted in the last forty years on volunteer, cadaver, and dummy tests. The first study on tolerance levels for flexion and extension bending moments was carried out, on volunteers and cadavers, by Mertz and Patrick (1971). From this first tests it emerged that the moment tolerance limits are strictly dependent on the biofidelity of the dummy neck in bending. Afterwards, Mertz et al. (1978) conducted a study, using a Hybrid III 50% male dummy, to investigate the football players neck injuries in a block event by establishing that the compression tolerance varies with the duration of the load application, with a peak value of 40 kN. Nyquist et al. (1980) developed the current tolerance levels for tension and shear loads (33 kN and 30 kN, respectively) testing, in frontal collisions, a belted Hybrid III 50% male dummy.

Subsequently, the concept that a composite neck injury indicator based on a linear combination of axial tension loads and extension (rearward) bending moments was developed. Prasad and Daniel (1984), using their results from experimental tests on porcine subjects defined an area (shaded in figure 1.24) above which the tension/extension actions exceed the tolerance levels.

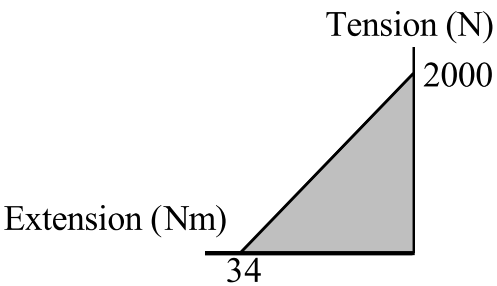

Figure 1.24: Linear combination of axial and tension loads for porcine subjects representing the size of a three year old child (Prasad and Daniel (1984)).

Then, the concept of neck criteria based on a linear combination of loads and moments was expanded to include the four major classifications of combined neck loading modes; namely tension-extension, tension-flexion, compression-extension, and compression-flexion. The resulting criteria are referred to as $\mathrm{N_{ij}}$ (Biomechanical Neck Injury Predictor), and it was submitted for the first time in 1996 by Klinich et al.. Inside to "*ij*" they are present four indexes for four different injury mechanisms: N_{TE}, N_{TF}, N_{CE}, and N_{CF} where the first subscript index represents the axial load (tension or compression) while the second one represents the sagittal plane bending moment (flexion or extension).

In general for any given loading of the dummy, the standard 6-axis upper neck load cell dynamically records loads and moments in all the three directions at the top of the neck. In a frontal collision, the primary motion and the measured neck reactions occur in the sagittal plane while, out of the motion plane, the reactions are typically of secondary importance. As a result, only the two measurements associated with sagittal plane motion are used in the current formulation of the N_{ij} neck injury criteria, namely axial load (F_Z) and flexion/extension bending moment at the occipital condyles (M_Y). Shear load (F_x) is only used to calculate the effective moment at the occipital condyles.

$$N_{ij} = \frac{F_z}{F_{int}} + \frac{M_y}{M_{int}} \tag{1.2}$$

Where:

- F_z is the axial load
- F_{int} is the corresponding critical intercept value of load used for normalization (table 1.3)
- M_y is the flexion/extension bending moment computed at the occipital condyles, whose value is defined by:

$$M_y = M - F_x \cdot D \tag{1.3}$$

  - M bending moment
  - F_x shear force
  - D distance between the load cell and the condyles

- M_{int} is the corresponding critical intercept value for moment used for normalization (table 1.3)

Table 1.3: Cervical spine load limits.

Load type	Max load values
Traction force	$6810N$
Compression force	$6160N$
Bending moment - flexion	$310Nm$
Bending moment - extension	$135Nm$

The following conditions determine the index values for which there is a high percentage risk of serious damage:

$$N_{ij} \leq 1 \tag{1.4}$$

- If $N_{ij} = 1.0$ there is a 15% probability of occurring in severe neck damage (AIS4 or more) IIHS (2009)
- If $N_{ij} = 1.4$ there is a 30% probability of occurring in severe neck damage (AIS4 or more) IIHS (2009)

In Kleinberger et al. (1998); Eppinger et al. (1999) are proposed methods for calculating the probability of AIS scale according to N_{ij} value. (figure 1.25 Kleinberger et al. (1998), RTO (2007)).

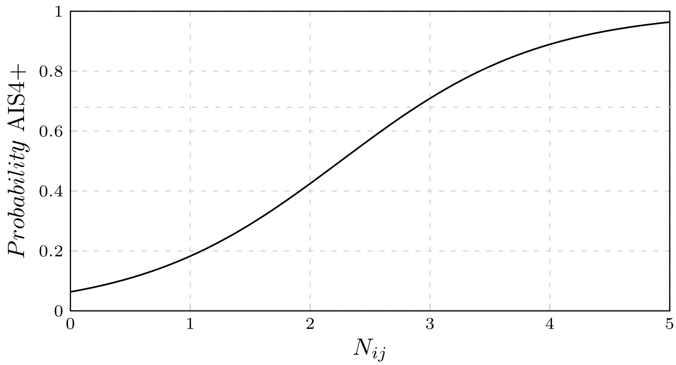

Figure 1.25: Correlation between N_{ij} and probability of AIS4+.

Thorax injury critera

Chest injuries are less common than those of the head, abdomen and extremities but, the chest is an important body region to protect because it contains organs that are essential for life, such as the heart and lungs. In general, two main mechanisms occur for chest injury: localised forces applied directly to the chest due to an impact (including the restraint system) or sudden chest deceleration and its effect on the internal organs. The discussion about using chest deflection or chest acceleration in frontal impact thoracic injury prediction started in the '70s when the first results of human volunteer rocket sled testing by Stapp (1970) were published. Thanks to this research, and that conducted by Mertz and Gadd (1971) the following year on instrumented stunt diver, the fundations were laid for the development of the injury threshold for chest acceleration of 60 g.

At the same time, Kroell et al. (1971, 1974) demonstrated the importance of chest deformation, using blunt thoracic impacts of unembalmed (adult) cadavers. Based on this tests Neathery et al. (1975) developed an assessment recommendation for the rib cage and internal organs using chest deflection, while, Stalnaker et al. (1973) determined that a linear combination of normalized chest deflection, and the subject age, correlated best with injury response. Nahum et al. (1975)) compared sternal and spinal acceleration of Post Mortem Human Subjects (PMHS), concluding that none of the sternal acceleration parameters correlated well with the AIS ratings in the analyzed database.

Wiechel et al. (1985) analyzed the data of Kroell et al.(1971, 1974) using Viano's thoracic injury risk curve (Viano (1978)) defining two injury predictors. The first based on the chest deflection for lower injuries (AIS 1-3). The second, based on spinal acceleration, to predict the higher injury severity levels (AIS 4-6). The following year, Lau and Viano (1986) presented a Viscous Criterion (V*C) and defined as:

$$VC = k \cdot \frac{Y}{D'} \cdot \frac{dY}{dt} \tag{1.5}$$

Where:

- $k\,(1.3 \div 1.0)$ and $D'\,(138 \div 254mm)$ are constants dependent on the subject (age, gender)
- Y is the thoracic cage deflection

The limit is equal to $1m/s$.

As reported by the same Lau and Viano in Viano and Lau (1988), $VC = 1m/s$ corresponds to a probability of 25% to register injuries with AIS4 or major.The correlation curve is shown in figure 1.26.

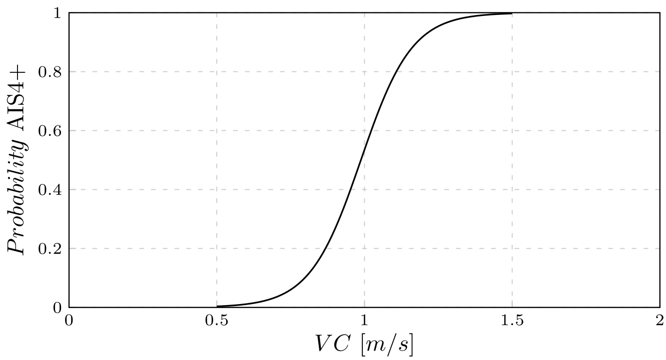

Figure 1.26: Correlation between VC and probability of AIS4+.

Through subsequent studies, it was found that one of the factors most influencing chest damage is deflection of the chest, due to interaction with the seat belts or with other rigid object. The deflection limit is $50mm$.

Lower extremity criteria

Femur injury Foot and ankle are the most injured body parts and their injury mechanisms are complex. During the years, to better understand them, many research were conducted. In the last years, new dummy legs are allowing to deepen this argument. Generally, in the motorcycling context, the field is reduced to the forces in action on the femurs in axial direction. As biomechanical damage index, the absolute values (Kuppa et al. (2001)), with a limit value equal to 9.1kN can be simply used. This limit value corresponds to a probability of 12% to lead a damage with AIS value of level 3 or higher (Kuppa et al. (2001)) (figure 1.27).

Leg injury The Tibia Index (*TI*) was originally proposed by Mertz (1993) as an injury tolerance criterion for the leg which combines bending moment and axial compressive loads on the leg as measured by the Hybrid III tibia load cell. The modified version of TI adopted by EEVC (European Enhanced Vehicle-Safety Committee) (Hobbs et al. (1997)) is given by:

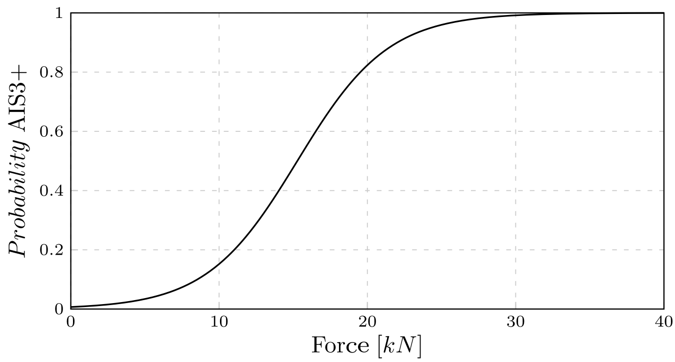

Figure 1.27: Correlation between femur axial force and probability of AIS3+.

$$TI = 1.3 \cdot \frac{F}{F_c} \cdot \frac{M}{M_c} \tag{1.6}$$

where:

- F is the compressive axial force (kN) in the superior-inferior direction
- M is the resultant moment of the medial-lateral and the anterior-posterior moments
- F_c and M_c are the critical axial compressive force and the critical bending moment.

Those ones are presented in the following table 1.4:

Table 1.4: Critical moment and compressive axial force (*Source:* Eppinger et al. (1999)).

	Hybrid III 5^{th} percentile female	Hybrid III 50^{th} percentile male	Hybrid III 95^{th} percentile male
M_c [Nm]	115	225	307
F_c [kN]	22.9	35.9	44.2

The values of MC and FC for the 50th percentile male are based on human bone tolerance values obtained from Yamada and Evans (1970). The critical values for the 5^{th} percentile female and the 95^{th} percentile male were obtained by using scaling relations proposed by Mertz et al. (1989). A TI threshold of 1.3 was recommended and adopted by Hobbs et al. (1997), based on analysis of crash test data.

Chapter 2

State of the art of passive safety devices

This chapter aims to give a general overview on the most common passive safety devices developed over the years, what was done since today, and which is their development direction. Thanks to this analysis, it will be possible to understand the strengths and limits of the solutions found, helping us in the new device ideation and design. Finally, fundamental part of the analysis of the state of the art is extrapolating evaluation criteria for solutions that will arise from the Network of Problem (a parallel activity carried out in this study).

Past research activities on PTW/rider passive safety clearly highlight the difficulty to find safety solutions truly efficient in every accident configuration or at least solutions which are neutral (i.e. not harmful) in off-design scenarios. Over the years, the device development was focused on the protection of specific body parts and the solution of specific problems. A rider almost often sustains multiple injuries in an accident (Rogers et al. (1991)) and head injuries are among the leading causes of death in PTW crashes (Ankarath et al. (2002) figure 2.1 and Piantini et al. (2016)).

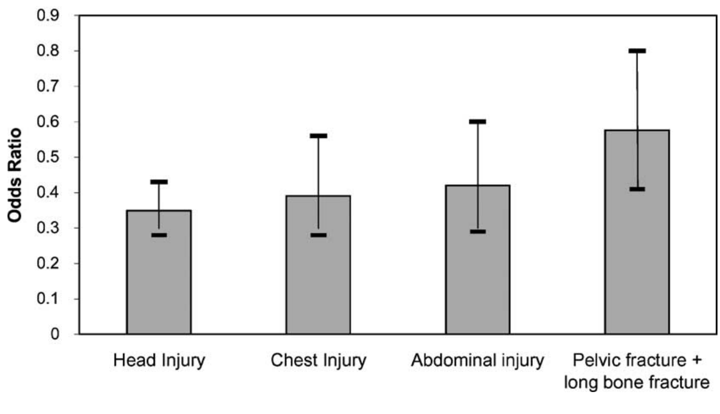

Figure 2.1: Odds ratio for factors related to mortality (*Source:* Ankarath et al. (2002)).

Helmets

Despite the efforts made by researchers to improve helmet efficiency head injuries are still often fatal (Aare and Holst (2003)). Helmet is the oldest and the most used PTW passive safety device (the first hard shell of modern PTW helmet dates to the 1930s). Indeed, helmets can reduce fatal injuries by around 44% (Elvik (2009)) and the risk of head injury by 69% (Liu et al. (2008)). Over decades its effectiveness increased due to the improvement in helmet design and materials (Deutermann (2004)). Nowadays, there are four main types of helmets available in the market.

According to recent studies conducted by (EU Commission (2001) and Aare and Holst (2003)), full face helmets provide a better protection than others (modular, open face and half helmet) especially from chin injuries. Indeed, 16% of total helmet damages are located at the chin guard (Richter et al. (2001)). In the last decades, research efforts were focused on the implementation of new solutions to enhance the absorption of rotational forces due to oblique impact (Otte et al. (1999); Aare et al. (2004); Kis et al. (2004),2013). With reference to this problem, Halldin et al. (2001) presented the Multi-direction Impact Protection System (MIPS) (see figure 2.11), while Phillips (Phillips (2004)) proposed the Phillips Head Protection System (PHPS).

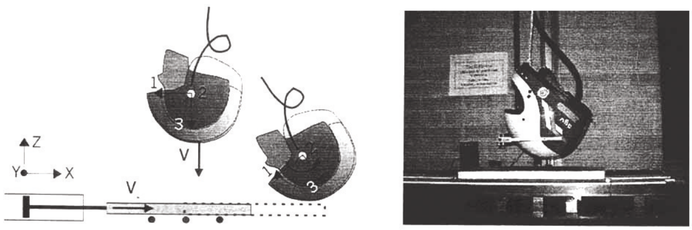

Figure 2.2: Halldin laboratory tests (*Source:* Halldin et al. (2001)).

Both solutions are based on the friction reduction, introducing an easy-shear layer, outside the helmet shell or between the liner and the shell respectively. More recently, researches investigated smart helmets, able to monitor vital signs (von Rosenberg et al. (2015)) (figure 2.3) or to estimate the amount of impact (Veena et al. (2014)) (figure 2.4), in order to promptly assess the rider's accident injuries and to communicate the emergency through GSM communication.

Rider's kinematics after impact depends on several variables (e.g. relative position and speed of the vehicles, if an opposing vehicle is involved) and on the rider's actions before the impact. In the same scenario a loss of control or a controlled fall of the vehicle can drastically change the accident consequences and the reported injuries. Finnis (Finnis (1990)) claims that, in frontal collision, a rider's trajectory control and the related speed reduction could be a good way to decrease injuries.

Figure 2.3: Electrodes attached to five locations on the face (*Source:* von Rosenberg et al. (2015)).

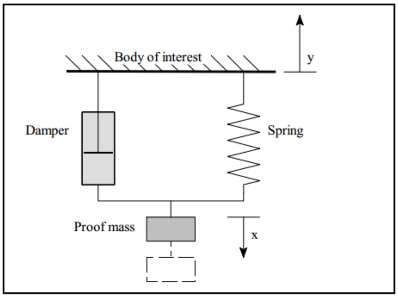

Figure 2.4: Principle of operation of a sensing element of an accelerometer (*Source:* Veena et al. (2014)).

Airbags

The airbag represents an effective device to reduce the impact velocity preventing rider's injuries. Despite the difficulty of installation on PTWs, the first works carried out by Hirsch and Bothwell (Hirsch and Bothwell (1973)) in the 1970s indicated that an airbag could be effective in frontal crashes (figure 2.5).

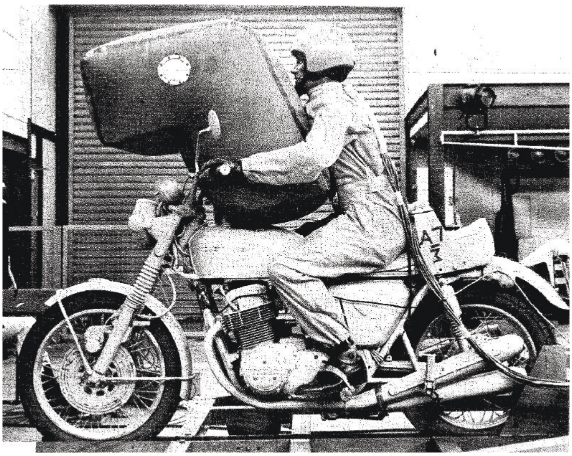

Figure 2.5: Hirsch and Bothwell test apparatus.

This topic was not further developed until 1985 when Chinn published ”Motorcycle rider protection in frontal impacts” (Chinn et al. (1985)), and subsequently in the early 1990s, when tests were completed in the UK at the Transport Research Laboratory (TRL) . The publications of Finnis (Finnis (1990)) and Happian-Smith with Chinn (Happian-Smith and Chinn (1990)) described the tests of three different types of PTWs fitted with an airbag. Finnis (Finnis (1990)) noted that a conventional airbag design produced a controlled deceleration of the rider and, by increasing the exit height of the rider, it could avoid the impact against the car; in parallel hitting the ground from a greater height it could result in more serious injuries.

The Happian-Smith’s (Happian-Smith and Chinn (1990)) results showed that a full restraint was not possible above a speed of 30 mph, though reducing the speed and controlling the rider’s trajectory it could still be beneficial. In 2004, Honda developed with TRL the first airbag system for PTWss (Chinn et al. (1996)), which was made available since 2006 on the new Honda Gold Wing: a unit in the airbag, positioned to the right of the module, analyses signals from the crash sensors to determine whether or not to inflate the airbag. Four crash sensors, attached on both sides of the front fork, detected changes in acceleration caused by frontal impacts (figure 2.6).

Figure 2.6: The Honda Goldwing equipped with the motorcycle airbag system.

In 2004 Berg (Berg et al. (2004)) published the results of tests on an integrated motorcycle airbag. The main purpose was to investigate the effectiveness of airbags for medium-sized motor vehicles. Berg explained that it was not generally possible to apply a car airbag directly to a motor vehicle (although a passenger side airbag had very similar volumes), since it is necessary to take into account the pilot’s trajectory, that is not subject to any retention system as it happens in motor vehicles. So, Yamaha carried out a research on the airbag, and in 2007 presented a work by Kanbe (Kanbe et al. (2007)) inside the project ASV-3 (Advanced Safety Vehicle 3) .

The authors explained that to reduce the driver damage indexes, in a wide range of collision configurations, it was fundamental to avoid collisions of every part of the body (especially head and chest) against the vehicle, but also to decelerate the rider. To this end, the airbag was made smaller and was placed closer to the pilot than the previous versions. To decelerate the rider, an innovative multi chamber airbag coupled with a back plate was tested (figure 2.7).

Figure 2.7: Yamaha ASV-3 research vehicle incorporating an airbag system.

In general, airbags were found to be more effective in 90-degree collisions with a stationary car. Oblique collisions or collisions with a moving car tend to result in a rider's sliding around the side of the bag, producing only a modest reduction in rider's impact energy (Berg et al. (2005)). In addition, the cost of fitting an airbag was too expensive in proportion with the PTW cost.

In the last decade, the airbag development focused on wearable devices. Although the motorbike airbag jacket was a Hungarian invention (patent registered in 1976 by Tamás Straub), only recently wearable inflatable safety systems for riders caught on. In simpler implementation, these airbags are connected to the PTW by a cable and they are deployed when the cable is detached from its mounting clip. Most recent models are activated by an electronic control unit. Helite (figure 2.8(a)), and all major rider's garment manufacturers (as Spidi (figure 2.8(b)), Brembo, Alpinestars (figure 2.8(c)), Dainese (figure 2.8(d)) developed airbag jackets for PTW riders. These devices are capable to reduce injuries to important body parts, such as spine, chest, neck and major organs of the upper body, wearable airbags are beneficial also for snowmobile riders and horseback riders.

Leg protectors

Injuries to the lower extremities are less severe but more frequent, thus they are relevant for the economic impact. For this reason, several research activities were conducted to protect the lower extremities and some solutions were proposed (figure 2.9).

A proposed solution incorporated a crash bar into the PTW to prevent the intrusion into the space generally occupied by legs. Craig (Craig et al. (1983)) observed that these type of protectors were not able to protect the lower extremities. He considered that some forms of shell (e.g. fairing) could help to protect

(a) Helite airbag system.

(b) Spidi airbag system.

(c) AlpinestarR airbag system.

(d) Dainese airbag system.

Figure 2.8: Wearable airbag marketed.

the legs against impacts. Previously also Ouellet obtained similar results (Ouellet (1982)): he investigated 131 crashes involving crash bar equipped motorcycles, and he concluded that the occurrence of leg injuries was not directly related with leg space preservation, because the legs moved out of the initial volume during the accidents.

Subsequently, other studies were conducted (Chinn and Macaulay (1984); Chinn et al. (1985); Tadokoro et al. (1985)) to reduce injuries to the lower extremities using protective components installed onto the PTW. These solutions, designed to increase lower limb protection, were often criticized and disputed (Watson (1990)). Ouellet (Ouellet (1990)) stated that leg protection structures could worsen overall

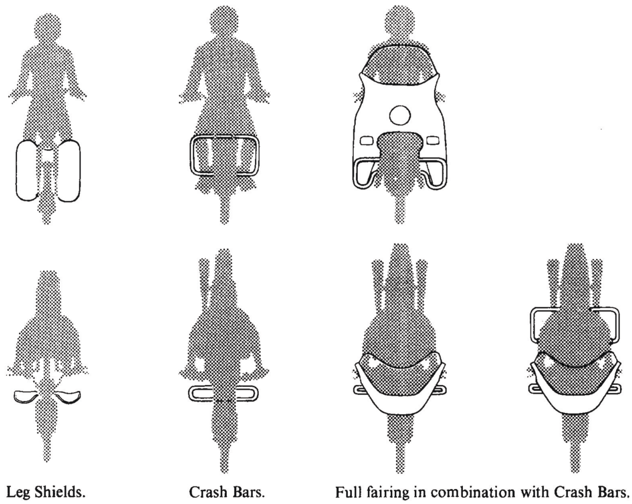

Figure 2.9: Categories of leg protector (*Source:* Ross (1983)).

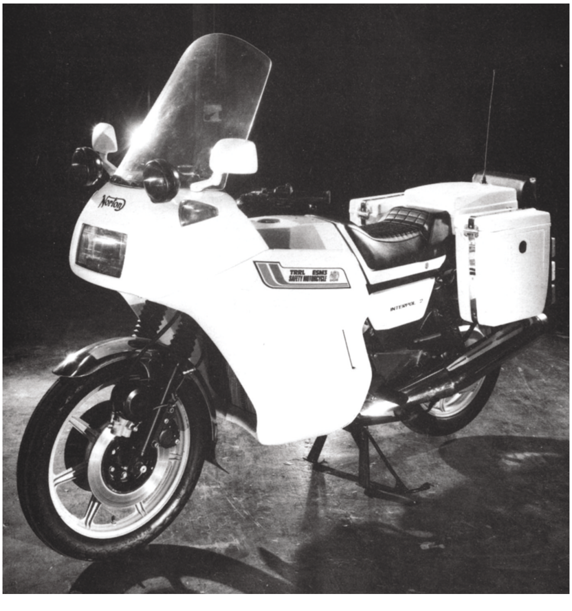

Figure 2.10: Motorcycle fitted with leg protecting fairing.

rider's injuries by increasing head and chest impact loads.

On the contrary, Nairn (Nairn (1993)) argued that, in accidents with serious leg injuries, their severity could be reduced by approximately 50% if leg protectors were fitted. Subsequent studies showed different possibilities to optimize leg protectors (Otte (1994)), and an overall evaluation of motorcycle leg protectors, based on ISO 13232 (ISO (2005)), was carried out by Rogers and Zellner (Rogers and Zellner (1998)). Nonethelss Hobbs et al. (Hobbs (2001)), suggested that further work on these devices was necessary to ensure that leg protectors do not change rider's trajectory and result in negative side effects.

Protective clothings

Another important field in PTW safety protection is represented by protective clothings. For protective clothings mean certain types of jackets, gloves, boots, pants and suits, typically made of leather which include heavy padding (in Kevlar, carbon fiber or plastic) on the elbow, spine, shoulder, knee, ankle and toe regions, in order to prevent or limit the injuries. Their effectiveness to reduce rider injuries was initially stated in 1976 by Feldkamp et al (Feldkamp et al. (1977)). They reported results on the reduction of serious injuries in motorcycle crashes thanks to the use of protective clothings. Since then, many studies confirmed the effective of protective clothings in reducing the frequency and severity of some types of injury (Zettas et al. (1979); Aldman et al. (1981); Hurt et al. (1981); Schuller et al. (1982);(1986); Otte and Middelhauve (1987); Hell and Lob (1993)). In the specific, protective clothings are effective to protect soft tissue injuries such as lacerations, contusions and abrasions. In addition, they can prevent or reduce many other injuries including exhaust pipe burns, friction burns, muscle stripping and de-gloving. Another important effect is the reduction of risk infection due to wound contamination and consequent complications in the healing of severe injuries.

Schuller et al.(Schuller et al. (1986)) collected crashes and interviews at injured riders to assess the protection provided by these cloths. He concluded that there was a significant injuries reduction, especially for skin and soft tissues. Otte et al. (Otte et al. (2001)) found that protective clothing can reduce the leg and foot injuries comparing two crashes at the same speed (with and without the device fitted on the rider), and he also reported that riders without protective clothing sustained injuries even in collisions at low speeds. Furthermore, protective clothing can also prevent accidents by maximizing the conspicuity of the rider (Hole et al. (1996)). In Europe, standards were developed for motorcycle protective clothing to promote more abrasion-resistant clothings (gloves CSN EN (2015), jackets, trousers and combi-units (CSN EN (2002)), shoes (DIN EN (2016), limb protectors (DIN EN (2013)), back protectors (CNS EN (2014) and chest protectors (DIN EN (2015)).

Also de Rome et al. (de Rome et al. (2011)) found strong correlation between the use of protective clothing and the mitigation of the injury consequences in terms of post-crash health and well-being.

Neck brace

Over the years, other protective concepts were developed. Neck braces (Geisinger et al. (2007); Leatt et al. (2012)) were developed because conventional clothing (helmets, jackets and back protectors) were not reputed to adequately protect this body region (figure 2.11).

Figure 2.11: Leatt-Brace® Moto GPX.

Despite neck injuries are less frequent than other injury types, they may have serious consequences for the rider. However there is an ongoing debate in the scientific community on neck braces, since it is not clear if their use truly mitigates the risk of neck injuries (Khosroshahi et al. (2016)).

Innovative vehicles

Another important branch, in motorcycle passive safety, is represented by innovative vehicles with special safety features. BMW C1 is the first vehicle presented in this review (Kalliske and Albus (1998); Osendorfer and Rauscher (2001)) (figure 2.12). It is a scooter with an exceptionally high level of passive safety performance.

Figure 2.12: BMW-C1 new electric version (2009).

The vehicle was equipped with an aluminium space frame, safety belts with load limiter and energy absorption elements mounted to the space frame. Thanks to these features, in several countries it was approved for use without a helmet. After selling over 10k units in 2001, BMW only sold 2k units in 2002 and ceased production in October 2002. In general, customers are divvied up between those who love it and those who do not understand its "character". After C1 concept, other projects were carried out. The first was ZEDIS (Gehre et al. (2001)), a vehicle likewise equipped with safety cell and restraint systems. In the design of this PTW, the lower leg protection section was specially developed by testing plastic foam supports and airbags for the knee area. Another one was the CLEVER project (Hollmotz et al. (2005)) (figure 2.13).

Figure 2.13: CLEVER.

The vehicle, classified as a three-wheeler, was characterized by a technologically advanced tilting system. In crash tests, it received a USNCAP 3 stars safety rating by ensuring a good head and chest protection. Another PTW with above average safety performance is Piaggio Mp3 (Di Genova et al. (2007); Sponziello et al. (2008); Santucci et al. (2009)) (see figure 2.14). It is a tilting three-wheelers scooter with innovative front suspension. The two frontal wheels offer an increased stability and thus an implicit higher safety performance.

In conclusion, many studies and ideas on protective safety devices/equipment for PTW and riders were conceived, but rarely they were developed and marketed. Many factors have to be considered for the commercial success of a protective device, apart from the safety performance. If these factors are not taken into account and included into the design process, a bright idea may not be accepted by the market. With this in mind, exploring new opportunities in this sector with an open-minded approach, or importing existing solutions from other matters, may be a good way to find solutions to be implemented.

Figure 2.14: Piaggio Mp3.

Chapter 3

Device definition

In this chapter they will be presented two central activities, which led to the first device development. In the specific:

- SURVEY - to understanding the customers' needs;
- NoP - to explore the landscape of possible solutions.

3.1 Survey

This activity was fundamental to define the evaluation criteria to assess the solutions that will emerge from the NoP, and to extrapolate fundamental information and features for the device design. With this objective, customer's needs, extracted from a survey structured on Kano's theory, were considered a good choice. Kano's theory (Kano (1984)) is usually employed to discover customer's needs. It can offer a better understanding of how customers evaluate a product, and it assists companies to focus on the most important attributes to be improved (Gustafsson et al. (1999)). In recent years, Kano's model was widely and successfully applied in strategic thinking, business planning, and product development to provide guidance with respect to innovation, competitiveness, and product compliance (Watson (2003)). Kano's model explains how the relationship between the degree of sufficiency and the customer's satisfaction of a quality attribute can be classified into six categories of perceived quality:

- Attractive (A)
- One-dimensional (O)
- Must-be (M)
- Questionable (Q)
- Indifferent (I)
- Reverse (R)

Where A indicates that attribute is an attractive requirement from the customer's point of view and it increase the product success; O means that the attribute results in satisfaction when fulfilled and dissatisfaction when not fulfilled;

M category is for requirements that the customers expect and that are taken for granted; *Q* is for conflicting responses (probably, the interviewed person did not understand the question or marked out a wrong answer by mistake); *I* means that the customer is indifferent to the attribute and probably he is not willing to pay more for this feature; *R* indicates that this product feature is not only unwanted by the customer but he even expects the opposite. Kano's theory was applied in this work to create an on-line survey for powered two-wheeler users. The questionnaire was proposed only in Italian language and it was promoted on the main Italian rider forums.

As suggested by Sauerwein et al. (Sauerwein et al. (1996)), the first step to implement a Kano's questionnaire is the identification of the product requirements. To fulfil this task, over 20 customer's interviews in homogenous segments were carried out, in order to determine approximately 90 - 95% of all possible product requirements (Griffin and Hauser (1993)). These interviews were based on 5 main questions to identify customer's problems, as suggested by Shiba et al. (Shiba (1993)).

1. Which associations does the customer make when using the passive safety device/system?
2. Which problems/defects/complaints does the customer associate with the use of the passive safety device/system?
3. Which criteria does the customer take into consideration when buying the passive safety device/system?
4. Which new features or services would better meet the expectations of the customer?
5. What would the customer change in passive safety device/system?

Before starting the interview, it was fundamental to understand if the participants were aware of passive safety devices/systems. In case of vague responses, explanations and examples were provided. From these interviews potential problems to solve and some product requirements to be implemented were identified.

The survey was organized in two main parts: the first one focused on the definition of rider's profile, including its mobility habits and its general use of passive safety systems; the second one to collect rider's requirements regarding basic features of new passive safety systems for PTWs. For the second part, a pair of questions were formulated for each product feature: the first question considers the customer's reaction if the product feature was implemented, the second (dysfunctional form of the question) concerns the reaction if the feature was not implemented. By combining the two answers in the evaluation table (table 3.1), every product feature could be classified.

Out of 228 answers, only 180 were complete and were considered for the analysis. The first results were on general information about riders: 90% of the participants were men and the remaining 10% women; they were between 19 and 67 years old. Participants were distributed on the Italian territory as follows: 39.8% from the North, 50.6% from the Centre and the remaining 9.6% were from the South.

Table 3.1: Kano's evaluation table.

Customer requirements		Dysfunctional (negative) question				
		1.like	2. must be	3.neutral	4. live with	5. dislike
Functional (positive) question	1.like	Q	A	A	A	O
	2. must be	R	I	I	I	M
	3.neutral	R	I	I	I	M
	4. live with	R	I	I	I	M
	5. dislike	R	R	R	R	Q

In figure 3.1 four pie charts representative of owned PTW type (a), years of riding experience (b), kilometres driven per year (c); estimated use of the PTWs (d) are shown. All results are expressed in percentage of the total answers. In these graphs, it is possible to see a good representation of all PTW styles (figure 3.1a), and a uniform distribution of kilometres driven (figure 3.1c). Most of the people exceeded 10 years of riding experience (74.44%; figure 3.1b). Three use types represented more than 97% of usage: tourism, leisure/hobby/sport, and commuting (i.e. go to work/school/university) (figure 3.1d).

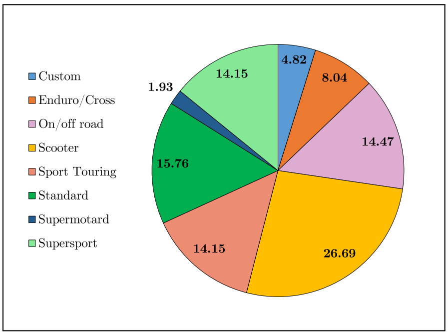

(a) Motorbike types owned (%).

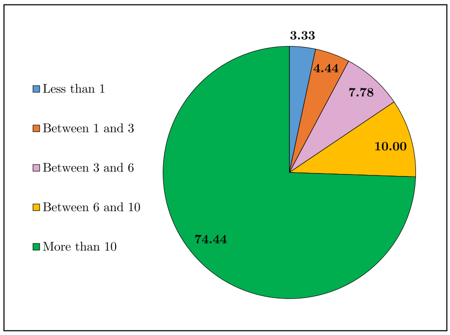

(b) Years of riding experience (%).

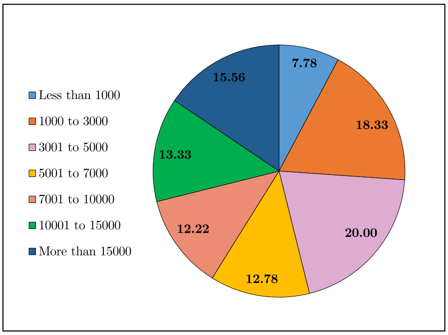

(c) Kilometers driven per year (%).

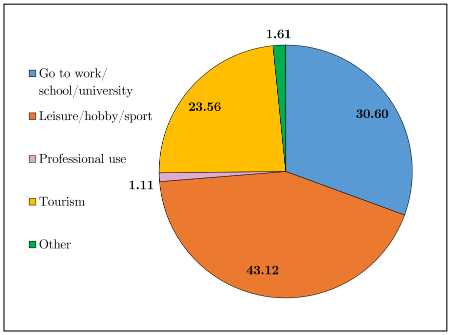

(d) PTWs average use (%).

Figure 3.1: Survey's general results.

Concerning passive safety devices and systems, the results showed that participants know all of them (Figure 3.2 left side), but their daily use rate was low (Figure 3.2 right side), especially for those more recently introduced into the market. Lastly the willingness to pay for personal safety equipment was tested. Answers highlighted that over 60% of the participants would be willing to spend between 100€ and 500€ for the new device (30.6% between 100-300€ and 31.7% between 300-500€); the remaining 40% was divided among the other 5 options (5.6% less than 100€, 8.9% between 500-700€, 11.1% between 700-1000€, 9.4% more than 1000€ and 2.7% is not willing to spend for not mandatory safety devices). The last question of the first part of the survey asked to the participants of estimating their weekly use of the various transport means. The results are shown in figure 3.3. PTWs are used almost as much as the car. Naturally, these data are relative to a sample of motorcycle owners and this indicates that MC owners use it regularly.

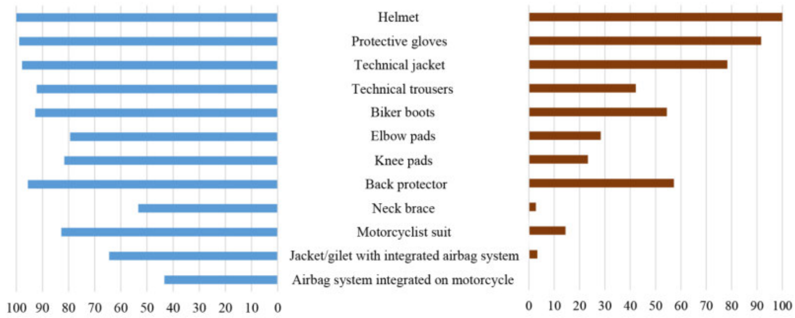

Figure 3.2: Knowledge of passive safety devices/systems (%) [Left]; daily use of passive safety devices/systems (%) [Right].

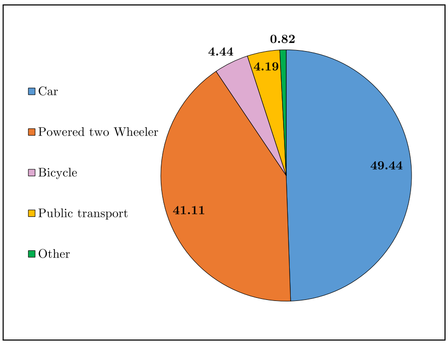

Figure 3.3: Weekly use of various transport means (%) .

The first question of the second part of the survey was to understand which impact scenario and which consequences the participants think that the device should be able to mitigate. This question proposed alternatives for three impact scenarios (showed in figure 3.4 a,b,c), plus two additional answers: the first claims that the three scenarios have the same importance, and the second one that the participants do not know the answer. In figure 3.4d are shown the share of replies. Over 60% of the participants thinks that the three scenarios have the same importance, while 6.67% doesn't know the answer. Lateral and frontal impacts result approximately equal (Over 15%) and only 1.67% considers rear impact the most important.

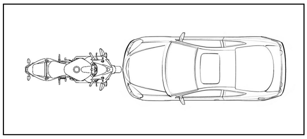

(a) Frontal impact.

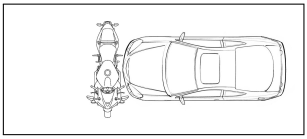

(b) Lateral impact.

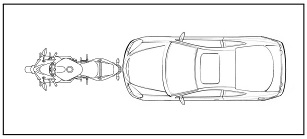

(c) Rear impact.

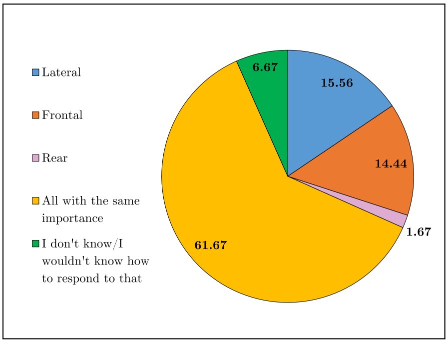

(d) Partecipants'replies (%).

Figure 3.4: Customers' sense of the .

In the second part of the survey, fourteen pairs of questions, formulated according to Kano's method, were included to establish customers' priorities regarding the main features of the passive security systems. In the specific, the fourteen pairs of questions focused on the following features of the safety device:

- integration on the PTW;
- obligation to wear it;
- partial limitation of the movements during its use;
- possible re-use after a crash;
- possibility to use/transfer it on other motorcycles;
- functionality dependent on other devices;
- comfort limitation;
- influence on PTW handling;
- influence on PTW performance;
- modification of the “classic” PTW aesthetic;

- its inexpensiveness (device cost);
- increase of the PTW cost;
- limitation of visibility;
- integration of multimedia features.

The graphical results of each couple of questions are reported in appendix A. To process the results of the survey, Customer Satisfaction Coefficients (CSCs) were used. Each coefficient indicates the strength of a product feature to influence customer satisfaction or, in case of its non-fulfillment, customer dissatisfaction (Berger et al. (1993); Matzler and Hinterhuber (1998); Zhu et al. (2010); Mote et al. (2016)). To calculate the average impact on satisfaction, it is necessary to add the attractive and one-dimensional answers and divide by the total number of attractive, one-dimensional, must-be and indifferent responses (equation 3.1). For the calculation of the average impact on dissatisfaction the sum of the must-be and one-dimensional columns has to be divided by the same normalizing factor (equation 3.2). A minus sign in the Dissatisfaction Index (DI) emphasizes its negative influence on customer satisfaction.

$$Customer's\ Satisfaction\ coefficient\ (SI) = \frac{A+O}{A+O+M+I} \tag{3.1}$$

$$Customer's\ Dissatisfaction\ coefficient\ (DI) = \frac{O+M}{A+O+M+I}(-1) \tag{3.2}$$

In figure 3.5 the CSCs obtained from the product quality assessment are plotted. The diagram is divided into four quadrants according to the four types of requirements (Attractive, Must-be, Indifferent and One Dimensional). Attractive and Must-be categories are the most relevant as they have the major impact on customers' satisfaction.

In this study, it is possible to see that no One Dimensional or Must-be features were found. Four attractive and four indifferent characteristics were identified. Movement restriction, comfort limitation, influence on performance, vehicle cost increase and influence on aesthetic are totally or almost totally indifferent categories. For this reason, they were not subsequently considered. Visibility limitation category was neglected because its influence is not defined being in the axes origin. Conversely Attractive and Indifferent categories will be used, with different weights, as decision criteria in the solution assessment phase.

3.2 Network Of Problem

Analyses of complex problems, as may be motorcyclist's injury reduction using a passive safety device, could be viewed as a journey into unknown territories for which no map exists. So, the successful development of a map, based on a thought process, can guide "the explorer" through complex problem situations.

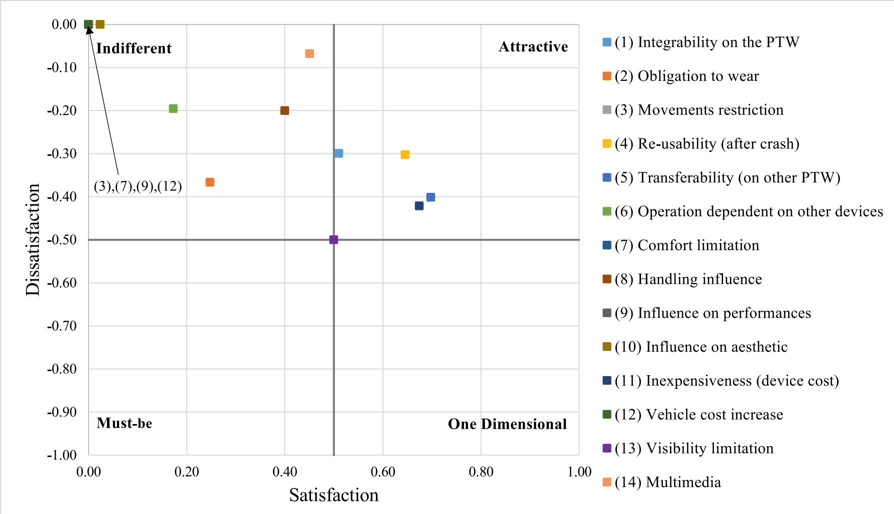

Figure 3.5: Influence of product features on customers' satisfaction or dissatisfaction.

It can help to collect a set of partial solutions that could be used in order to develop satisfactory solutions, but also to get a generic view of the links between the problems.

In the past, several problem-solving methods based on the idea of a map were proposed in engineering systems like loops diagram and KJ diagram (Senge (1990); Sage and Rouse (1999)). They were not able to solve the cognitive gap between the description of the problem and the description of the solution. Theories like TRIZ (Altshuller (1969, 1984, 1986, 1999)) and OTSM (Khomenko (1984, 1987, 1988a, 1988b, 1988c, 1997, 1999), Khomenko et al. (1988, 2002, 2006, 2007, 2007), Cavallucci et al. (2005)) can help, with their tools and algorithms, to overcome this problem. TRIZ and OTSM shall make available to techniques to deepen the problem, to see/analyse the problem in other respects, to think and approach the problem in a different way, in order to obtain an overall picture of the problem to solve. For this study the Network of Problems (NoP) was selected to represent the problem solutions. The NoP is a semantic map (blocks diagram) of relationships among problems, partial solutions to the problems or a reached objective, each represented by a block, where the focus is to create a network of contradictions to be cleared in order to solve the problem.

The first step in a NoP development is to state which is the main problem to be solved. According to Terninko (Terninko et al. (1998)), in this preliminary stage, the Innovation Situation Questionnaire (ISQ) can help to have the right understanding of the problem: it provides the structure to gather the necessary information for an in-depth understanding of the problem and reformulate and break it down into several smaller problems. As suggested by Khomenko, when the main problem to solve is clear, a list of the most painful known problems and their potential or partial solutions will be reported (Khomenko (2014); Terninko et al. (1998)), in a three column table (figure 3.6).

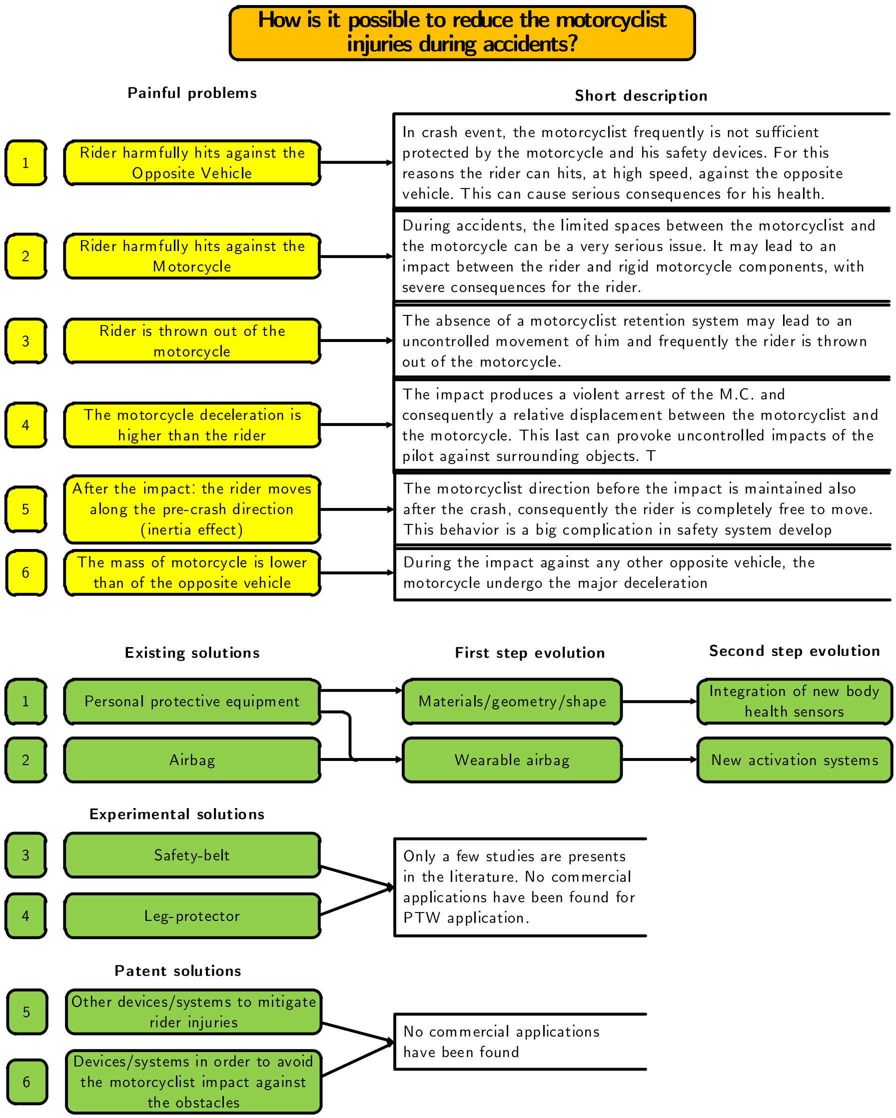

Figure 3.6: NoP: first development step.

In this case study, the main problem is: *"how is it possible to reduce the motorcyclist's injuries during accidents?"*. Examples of painful problems may be: *"a rider harmfully hits against the opposite vehicle"* or *"a rider is thrown out of the motorcycle"* and so on. About potential/partial solutions: the use of *"personal protective equipment"*, that is maybe the most obvious. Numbers beside the painful problems and the existing solutions (picture 3.6), are only identifiers, any connection between problems and solutions, is present. The numbers on the first column simply represent a progressive numeration.

In this first step, problems and potential solutions reported are those emerged from the analysis of the state of the art and the previous knowledge of passive safety devices. Based on this information, previous solutions to the problem were listed and an overview on potential drawbacks, occurred during the use of these devices and systems, was generated. In addition, an in-depth analysis carried out on all technical solutions found in the state of the art, relatively to driver/rider's protection (in general), led to the definition of three common macro-functions able to solve the problem. From our point of view, they were considered, not as possible solutions but as new main problems to resolve. In the specific, from the main problem ("how is it possible to reduce the motorcyclist's injuries during accidents?"), three problems were obtained at a higher abstraction level. This process is the basis of the generic problem solving approach (figure 3.7):

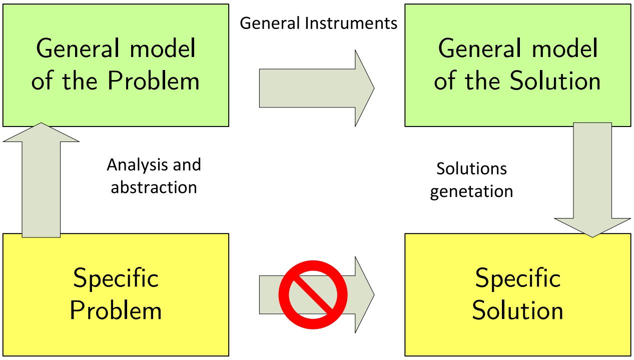

Figure 3.7: Problem solving approach.

In this approach a specific problem (in our case: "how is it possible to reduce the motorcyclist's injuries during accidents?") was analysed (in our case with the analysis of the state of the art), and it was abstracted passing to other three sub-problem apparently more specific but really, more abstracted. Therefore, they result are more usable considering the TRIZ database effects (Object-Action) suggested by the Oxford Creativity. The three sub problems are:

- Protect the motorcyclist;
- Slow-down the motorcyclist;
- Motorcyclist's displacement control.

Obviously, the NOP division is purely conceptual, since each solution could implement more than one function/problem. For each macro-function/problem, a "classical" System Operator (SO) was prepared, to find any resources in the various detail levels and in the time-line (see example of the motorcyclist's displacement control in figure 3.8).

Figure 3.8: System Operator for "the motorcyclist's displacement control" case.

In figure 3.8 different detail levels are visible. Resources for each level were identified by different colours (super-system, system and sub-system from the top to the bottom respectively). While, from the left to the right, the columns labeled past, present, future. This information should help the user to think of alternative solutions for the analysed problem. In this application, the power of the SO tool was not completely exploited because "passive safety" foresees obligatory the accident event. This limited the focus on the "Present", and even more "Future" time sections. Then, all possible solutions, potentially able to avoid the accident, were discarded since they would be in the domain of the active safety. For two of the partial solutions identified in the preliminary NoP (airbag on motorcycle and wearable airbag (in figure 3.6)), a series of functional models were developed (see two specific examples in figure 3.9).

In these diagrams are shown:

- the main elements (in yellow);
- the useful action (arrows in black);
- the insufficient useful action (arrow with dashed line in black);

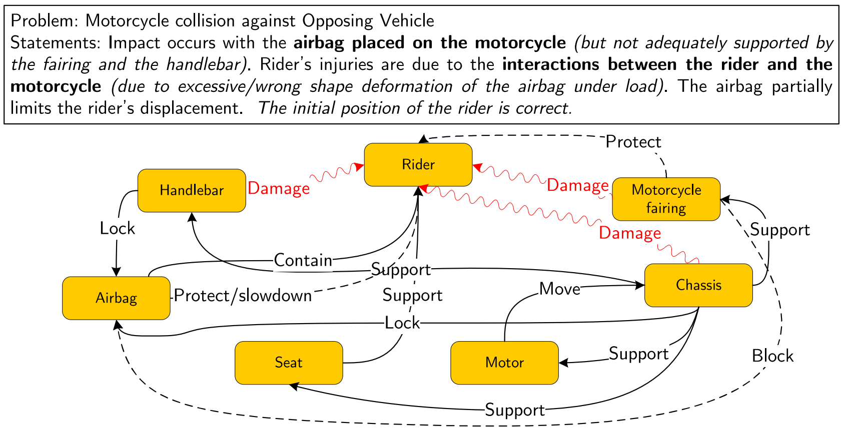

(a) PTW airbag.

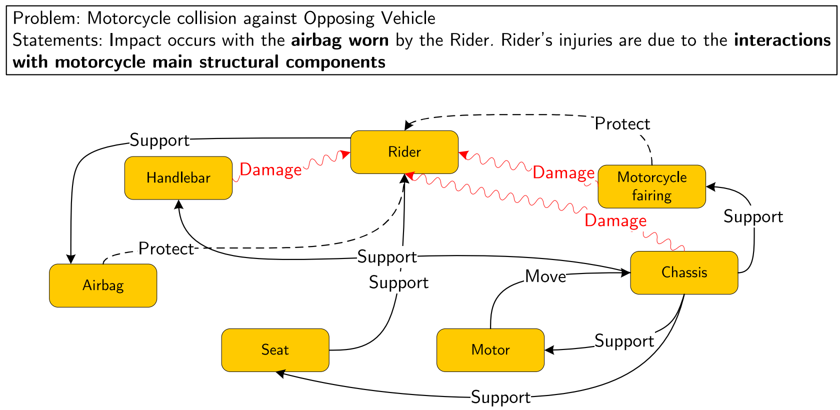

(b) Wearable airbag.

Figure 3.9: Example of functional model.

- the harmful action (arrows in red).

To determine which are the interactions between each couple of elements, it is necessary to "interrogate" them. Each element is individually analysed, to understand as it interacts with the other ones. This operation allows to identify which type of interaction there is between two elements and it highlights where the main problem is. The use of this tool was limited to specific problems/situations relative to the airbags because, from the state of the art, it was possible to identify and understand which were the problems in their use. The functional model allows to identify the possible interactions among the "system" elements and to highlight specific problems of the technical solutions analysed. TRIZ effects database was used to find a solution to specific problems. Through this procedure, the network was further extended with other branches. Each contradiction was isolated and analyzed with the classical tools like functional model and matrix of solutions, based on the 40 TRIZ principles. At the end of the implementation process, all solutions were going to be assessed on the base of criteria extracted from Kano's survey, and from technical considerations identified during the analysis of the state of the art, to determine the best potential solution. Figure 3.10 shows an excerpt of the NoP developed within this study.

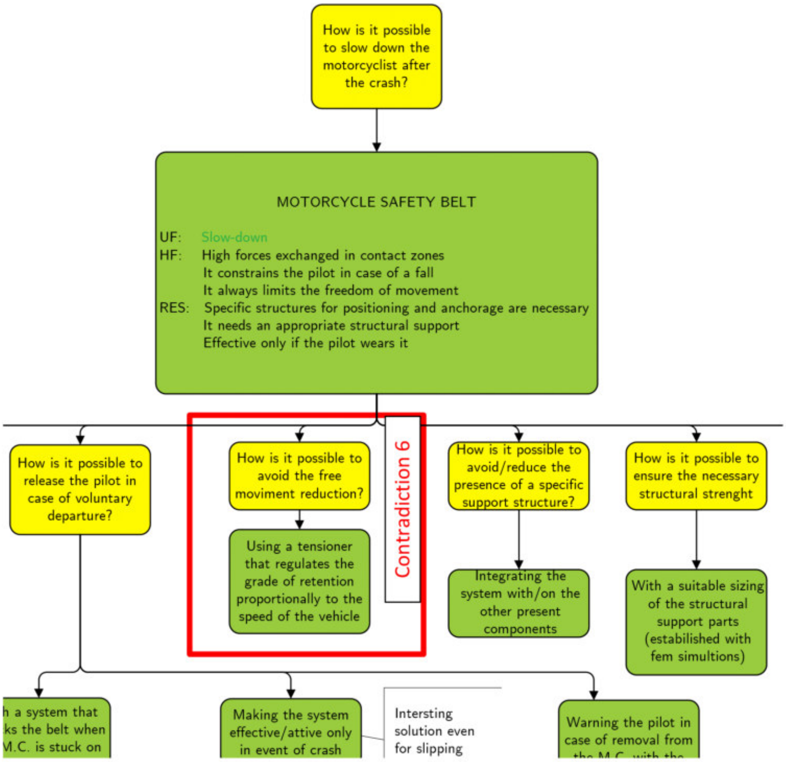

Figure 3.10: An excerpt of the NoP relative to the "slow-down the motorcyclist" problem.

This operation allowed to solve many contradictions, and the NoP was further refined. In figure 3.11 it is shown a OTSM-TRIZ model of contradiction, that can help to better understand a typical contradiction which may arise in the NoP development.

Here it is possible to see the characteristic scheme of one contradiction where are reported:

- the component/element object of the contradiction (in green);
- the control parameter/feature (in orange);
- the evaluation parameters (in blue).

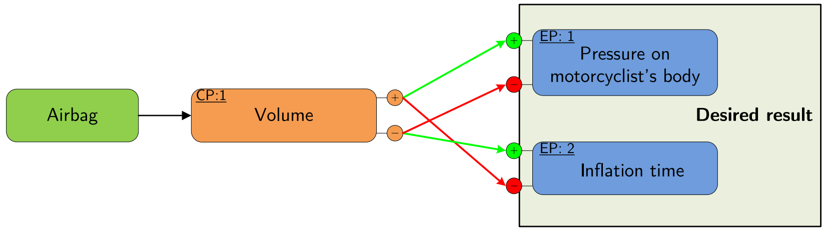

Figure 3.11: Example of contradiction model.

The control parameter (volume) of the component (airbag) should assume two values: (+) to improve the evaluation parameter on the top (Pressure on rider's body), but this increase worsens the evaluation parameter on the bottom (Inflation time). Contrary, if the control parameter (Volume) assumes a value (-) the pressure on rider's body increase, but then the inflation time improves (decrease). In figure 3.12, the functional model of the contradiction case is shown.

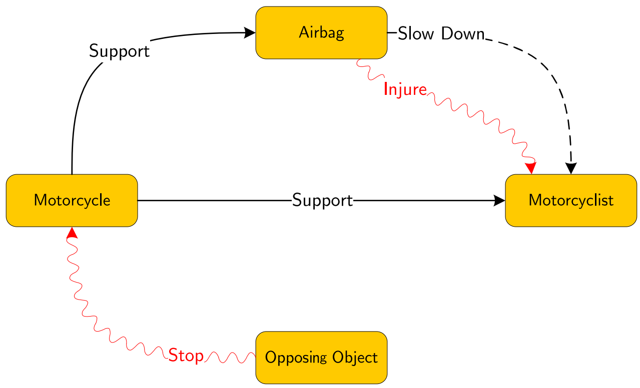

Figure 3.12: Example of contradiction: functional model.

In this case, the airbag is unable to sufficiently slow down the rider, and furthermore, during this action it injured the rider. Regarding the second harmful action, the opposite object that abruptly stops the motorcycle, it would not be in the interest of this analysis. The functional model must assess a specific case, indeed in this analysis, it was not considered, for example, the possible interaction between the motorcyclist and the opposing vehicle. The last step to resolve the contradiction is using the contradiction matrix (see figure 3.13).

In this case three principles are suggested (the number reported universally identify the TRIZ principle):

- 6 Universality,
- 35 Parameter changes and
- 4 Asymmetry

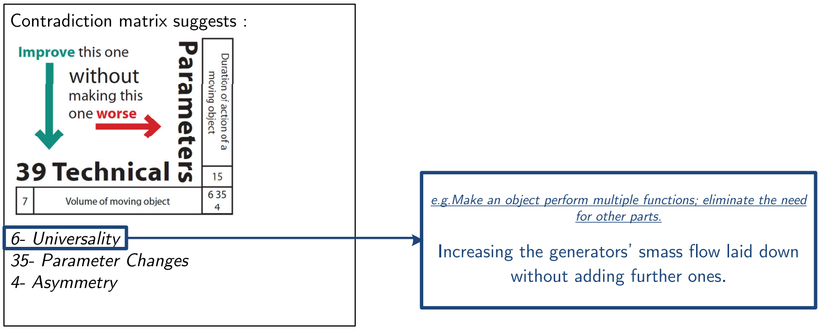

Figure 3.13: Contradiction matrix suggestions for the specific case.

The first principle results the best for this case, indeed, increasing the generators mass flow, without adding other generators, it could be a resolutive action for this problem. With the same process used for this contradiction, it was possible to resolve all contradictions found in the NoP development. It was comprised of 116 problems and 154 partial solutions. Thirteen solutions with different degree of development were identified:

- PTW airbag.
- Wearable airbag.
- PTW safety belt/jacket.
- Integrated structural restraint system.
- Increased viscosity of the fluid in the rider's surrounding volume.
- Air overpressure in the rider's opposite feed direction.
- Electromagnetic attraction / repulsion.
- Integration of safety systems on the O.V..
- Wrap-around protective structure.
- Electro-active polymers to contain rider's movements.
- Rider's ejection.
- Rider's locking/limiting with vacuum effect.
- Control of the seat movement with rider fixed on it.

Each of these alternatives was assessed according to the methodology outlined in the next section, and thanks to this, to establish which is the best potential one.

3.3 Choosing the best potential solution

The selection of the most promising solution was the last and most crucial phase of the problem-solving process. In this study, the assessment of the best potential solution was done using the Weighted Sum Method (WSM) (Pohekar and Ramachandran (2004); Borgianni et al. (2015)). This approach is based on the Decision Matrix (DM) and it consists in a set of criteria upon which the potential alternatives can be broken down, scored and summed to obtain a total score used to rank the solutions. The WSM states that, if there are M alternative solutions and N criteria then, the best alternative is the one that satisfies the equation 3.3:

$$\mathrm{A}^*_{WSM} = \max \sum_{N}^{j} a_{ij} w_j, \qquad for \quad i = 1, 2, 3, ...M \tag{3.3}$$

Where:

- A^*_{WSM} is the score of the best alternative;
- N is the number of decision criteria;
- M is the number of alternatives;
- a_{ij} is the actual value of the i^{th} alternative in terms of the j^{th} criterion;
- w_j is the weight of importance of the j^{th} criterion.

The total value of each alternative is equal to the sum of the products $a_{ij} w_j$. This method presents well known limits related to the subjectivity of the weights assignment, but it is still the most common approach. The decision criteria were defined according to identified features:

1. from the survey and the subsequent result analysis;
2. during the development of the NoP;
3. from the state of the art.

These criteria are reported in the first row on the top of Table 3.2. Regarding the criteria extracted from Kano's survey, a different weight will be assigned taking into consideration the importance of each category, i.e. for an indifferent category a weight value from one to five will be selected, while for an attractive feature/criterion (more important) the range will be from six to ten. The state of the art contributed to the definition of three decision criteria: the first one based on the effectiveness assessment of each solution (i.e. objective results emerged from previous studies), the second one on the possible integration with other safety device and the last one based on the ease of implementation. It is fundamental to translate the concept solutions into a real systems. Relatively to the second criterion, the possible device collaboration/integration with other safety devices, it was positively rated.

The assigned weights are reported on the second row, while in the third row there are the normalized criteria weights. In the first column of Table 3.2 all possible solutions able to solve the problem are listed. In this analysis the Decision Matrix is composed by eleven criteria and thirteen solutions (table 3.2).

In the DM implementation, a range of values from 1 to 10 was chosen to assign both the weight of criteria and to evaluate the performance of each solution

Table 3.2: Decision Matrix.

	Integrability (on the PTW)	Re-usability (after an accident)	Transferability (on other PTW)	Inexpensiveness (device cost)	Multimedia	Obligation to wear	Operation dependent from other devices	Handling influence	Ease of implementation	Effectiveness of the solution	Integration with other safety device	
Criteria weight	7	8	8	7	1	4	3	5	6	10	6	65
Normalized criteria weight	0.108	0.123	0.123	0.108	0.015	0.062	0.046	0.077	0.092	0.154	0.092	A^*_{WSM}
PTW airbag	10	1	1	3	1	10	1	9	6	6	10	**5,42**
Wearable airbag	3	7	10	8	4	1	6	5	10	7	5	**6,52**
PTW safety belt/jacket	5	8	7	7	4	3	5	6	9	6	9	**6,66**
Integrated structural restraint system	10	3	1	5	1	10	1	9	6	5	6	**5,35**
Increased viscosity of the fluid in the rider's surrounding volume	7	7	2	4	2	5	4	6	1	10	1	**5,00**
Air overpressure in the rider's opposite feed direction	8	7	2	4	1	5	4	6	3	6	8	**5,31**
Electromagnetic attraction / repulsion	6	10	3	4	1	4	1	5	1	3	7	**4,57**
Integration of safety systems on the O.V.	1	1	1	10	1	10	6	10	1	6	9	**4,95**
Wrap-around protective structure	10	3	1	1	10	10	10	2	5	8	9	**5,58**
Electroactive polymers to contain rider's movements	10	5	2	2	1	10	1	9	1	7	8	**5,43**
Rider's ejection	9	2	1	2	3	5	1	7	1	1	4	**3,11**
Rider's locking / limiting with vacuum effect	6	7	2	3	1	5	4	7	2	3	7	**4,42**
Control of the seat movement with rider fixed on it	6	4	2	4	1	5	4	1	6	3	7	**4,06**

with respect to the above metrics. The presented outcomes resulted from a final brainstorming session among the author and involved experts in passive safety field, in order to limit the method subjectivity in the value assignments process.

The A^*_{WSM} values are listed in the last column of Table 3.2. "Rider's ejection" or "Control of the seat movement with rider fixed on it" are lower A^*_{WSM} values than "Wearable airbag" or "Wrap-around protective structure". This means that, the first two solutions would be less pleasant for the customers and/or that these ones may present several uncertainties on their real effectiveness. Indeed, "Rider's ejection" and "Control of the seat movement with rider fixed on it" obtained a good evaluation: for "Integrability (on the PTW)" for the first one and "Integration with other safety device" for the second one, but in general, they present many criteria with low values. This fact could derive from the low level of the relative NoP branch development of these solutions. Indeed, some of them are conceptually very good and innovative, but during the development they presented many technological limits that reduced their evaluation.

In conclusion, the "PTW safety belt/jacket" resulted the best potential solution among those found with the NoP development, and for this reason it was chosen to be implemented. In its conceptual/functional definition, the chosen solution was designed as a system based on a safety belt/jacket, partly integrated into the PTW (structural and functional components) and partly worn by the rider. This choice derived from the preliminary interviews carried out before the survey creation. From these interviews, it emerged that the customers prefer safety systems directly integrated into the vehicle, which do not require any action/activity to be carried out by the rider. On the other hand, the wearability of a part of the device allows its partial transferability on other PTWs.

From the conceptual point of view (emerged from the analysis of the state of the art and the customer's needs analysis) and from the solutions found (emerged from the NoP), the new device should provide for the use of wide belts or a jacket (to increase the contact/action surface between the rider's body and the retention component, limiting the pressures acting on the rider's chest) and it should be realized with a strong fabric (but small thickness to limit the weight), very visible (to improve the rider's visibility in the traffic), and easy to store (and fold) when it is not used. In fact, one of the most important information, extracted from the preliminary interviews, was the discomfort associated to all wearable safety devices. Protective clothings and helmet are bulky, uncomfortable, and impossible to store in the PTW when they are not used, causing a discomfort for the users. The functional parts of the best solution are designed as typical components of a car seat belt device. To be noticed that the use of standard components limit the realization costs by ensuring a good performance. This is a fundamental point, indeed, the use of a restraint system (conceptually similar to car seat belt system) could ensure a cooperation with other safety devices (i.e.airbags), and its effectiveness is by now undisputed. Furthermore, this aspect ensures a high facility of implementation.

Starting from this preliminary conceptual configuration, the device will result in technical and geometrical components, in order to be modelled in a virtual environment and simulated in crash configurations.

Chapter 4

Preliminary assessment (first simulation) and first device development

4.1 Design of the new safety device

The solution, considered in the DM and previously mentioned, was directly derived from the partial solutions of the NoP and took into account, during the actualization process, the survey customer's needs. This section describes three different possible device configurations developed during the NoP creation. These are trying to translate, the NoP conceptual solutions in technical/real solutions. In order to understand the "translation" process, the three configurations designed will be briefly described. For each of the proposed device solutions (figure 4.1), a series of comments and observations will be reported, in order to make more comprehensible the design process.

The first solution designed, the most rudimentary (figure 4.1a), is comprised of a belt system, schematically characterized by:

1. a long belt that comes out the seat, doubles to permit the belt passage around the head and comes back together on the front side;
2. a short belt;
3. a tongue (male) connector placed on one of the long belt extremities;
4. a buckle (female) connector placed on one of the short belt extremities;
5. a seat with holes to allow the belts passage across the seat;
6. structural belt anchorages to the PTW frame under the seat (not visible in figure 4.1a).

This type of system, even if it is very simple from a technical point of view, is not very user-friendly. Indeed, for its use, the rider must wear one of the two belts (the long one around the head) and connect the tongue (at the long belt extremity) with the buckle at the end of the short belt. This latter is positioned between the rider's legs. Furthermore, the belts are not aesthetically pleasing when the PTW is parked. In addition to all these motivations, this solution is unable to improve two of the three typical harmful functions connected with the safety belt use:

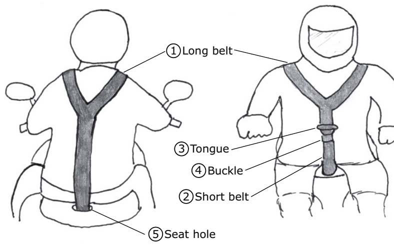

(a) First device solution sketch.

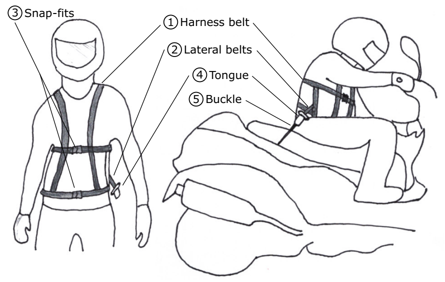

(b) Second device solution sketch.

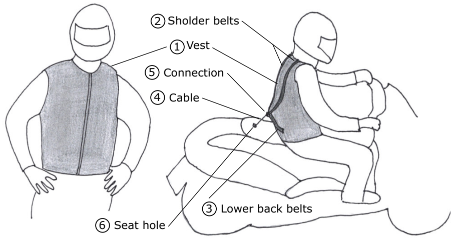

(c) Third device solution sketch.

Figure 4.1: Development of device based on safety belt .

- the limitation of free movement;
- the permanent pilot's constraint to the PTW.

Indeed, the poor extendibility of the system, due only to the belts elasticity, restricts the free longitudinal rider's displacement causing possible discomfort. Furthermore, the spatial position of the tongue-buckle connection makes it difficult to implement an automatic de-touching system, necessary when the retention is not required (this kind of device is always active). On the contrary, presenting two symmetric shoulder belts, this system could reduce the high pressures exchanged in belt contact zones; even if, part of the restraint force, acting on the genital region, could injure it. In view of these considerations, this first solution was not considered satisfactory.

In order to change the belt pressures position acting on the rider's body and to eliminate the two harmful functions just reported, another solution was created. The second solution (figure 4.1b) is characterized by:

1. a harness belt composed of two shoulder belts, one thoracic belt and one pelvic belt;
2. two lateral belts linked with the harness belt;
3. two snap-fits to link together the two sides of the thoracic belts;
4. two tongue (male) connectors, one for each lateral belt;

5. two buckle (female) connectors with cables, one for each side of the PTW seat;
6. two retractors (placed into the lateral fairing) to link the restraint cables with the PTW frame, however allowing a controlled cables extraction (not visible in figure 4.1b).

Analysing this solution, it is possible to see that this one is easier to wear than the previous one. Indeed, it is wearable as a vest and it is easy to lock, thanks to the two frontal snap-fits. Furthermore, the increased number of belts allows a better pressure distribution on the rider's body, not involving sensitive body parts. The harness belt is linked to the PTW with two tongue-buckle connectors, one for each side. In case of low speed rider's displacement, the retractors allow movements of the buckles and their cables and in turn of the rider. This should considerably increase the rider's comfort during driving.

Regarding the rider's constrain on the PTW, this solution results better than the previous one, because, when this action is not necessary, the retractor presence can ensure a major operating space. Indeed, it could be possible to exploit its presence, for example, to unlock the cables/belts allowing the rider's separation from the PTW.

Moreover, the harness belt could not be very handy due to its substantial number of belts. These ones could result aesthetically unpleasing for the final users. For all these reasons, also this solution was not considered satisfactory. Despite everything, these two device models highlighted findings and gave useful technical information for the NoP development.

In the last solution presented, a new component was introduced: the retractor. The retractor is a standard component of a car seat belt system. It uses a spool as its central element. The spool (or spindle) is attached to one end of the webbing. Inside the retractor, a spring applies a rotation force. This works to rotate the spool so it winds up any loose webbing. When you pull the webbing out, the spool rotates counter-clockwise, which turns the attached spring in the same direction. Effectively, the rotating spool works to untwist the spring. The spring wants to return to its original shape, so it resists this twisting motion. If you release the webbing, the spring will tighten up, rotating the spool clockwise until there is no more slack in the belt. In figure 4.2 a realistic view of a spring retractor is reported while, in figure 4.3 is shown the lock functioning of a ball sensor retractor.

The third model of the device represents the final development. Even if, some of the technical solutions proposed are only at conceptual level, it represents the best solution of the conceptual study. Its sketch is reported in figure 4.1c and it consists of:

1. a wearable vest with a front zipper;
2. two belts embedded or partial embedded in the vest and link to it at the shoulders;
3. two belts embedded or partially embedded in the vest and link to it at the lower back;

Figure 4.2: A view of a spring retractor.

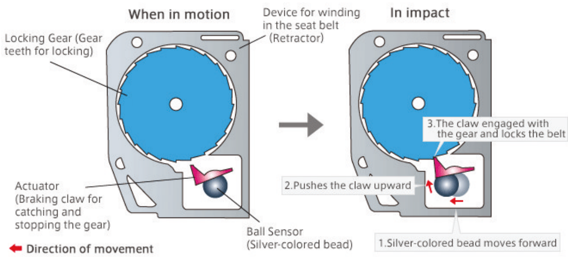

Figure 4.3: Schematic lock functioning of a ball sensor retractor.

4. a cable;
5. a connection between the cable and the vest belts;
6. a seat with a hole to allow the belt passage across the seat;
7. a slip-ring (not visible in figure 4.1c);
8. one retractor with pretensioner placed under the seat (not visible in figure 4.1c).

The use of a vest, in place of one or more belts (seen in the first two solutions), ensures the largest contact surface between the wearable component and the rider's body. This significantly limits the pressure acting on the body. The vest, especially with embedded belts, is handy to wear and store (for example under the seat) when it is not used. Furthermore, it could have customizable colour (one attractive feature for customers), or reflective parts to improve the rider's visibility in the traffic jam. In the vest two couples of belts are present; the first one acting on the shoulders and the second one acting on the lower back part of the vest, in order to obtain a better force distribution. On the basis of the knowledge on the use of a car seat belt retractor, a pretensioner was included to pre-load the system. Its effectiveness, in this type of application, is not proven, but its use results fundamental in a car accident, to guarantee the correct driver's position in the first moments after the crash. For this reason, it was taken into account in this first design stage. The pretensioner efficiency, for PTW applications, will be subsequently verified. On the market many types of pretensioner (piston, spheres etc) are present, but the final effect is the same. In figure 4.4 is shown a balls pretensioner functioning. Here, when the sensors detect an impact, a pyrotechnic gas generator pulls the gas, at high pressure, into a pipe moving the spheres stored inside of it. These rotates the spool pre-loading the webbing.

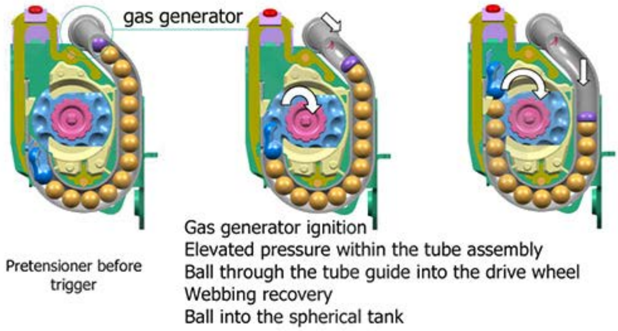

Figure 4.4: Functioning of a pyrotechnic spheres pretensioner.

The pretensioner operation is characterized by a following sequence of events:

- anyone of up to four sensors must be triggered;
- then a user-defined time delay occurs and
- then the pretensioner acts.

Regarding the retractor, a load limiter will be considered in the modelling process. This because, it is typically integrated with the retractor and it can prevent damages due to the pressure overload. Indeed, during the tensioning action, when the force from the webbing reaches a pre-set level, the device regulates the force limiting the load on the rider's chest.

The link between the vest belts and the cable was positioned in a central position on the vest back. The cable was preferred to the belt, in order to reduce the encumbrance, ensuring a higher mechanical resistance. The car D-ring or slip-ring, shown in 4.5, is a simple component that allows continuous sliding of a belt through a sharp change of angle. In car application, it is fitted in correspondence of the inner B pillar. In this preliminary phase, it was considered placed under the seat behind the rider's back. For its positioning, as well as for the retractor, it will be necessary a further and proper design of the structural parts, where these components will be fixed. In this study, the design is focused only on a functional/safe device effectiveness because methods to ensure an adequate resistance of a PTW frame are already known. Regarding the hole in the seat, it is necessary to allow the cable movement through the seat. From a practical point of view, a correct hole design could make it directly usable as slip-ring.

A fundamental component/element is represented by the type of connection used to link the vest belts with the restraint cable. The connection may be the key to control the selective rider's restraining. The solution from the NoP suggests to

Figure 4.5: Seat belt slip-ring.

link the rider with the active restraint system part (cable, retractor, pretensioner), only if required by the configuration. In all other cases, he is completely free to move respect to the PTW. This would ensure a perfect comfort and a safer device behaviour. As already discussed for the structural components, a specific design of this component is not the focus of this research.

However, the NoP suggests, for example, the use of a small backrest which could include a magnetic system. With this backrest it could be possible to attract and hold, in a correct position, a ferromagnetic component placed on the vest belt ends. In specific crash cases, discriminated by sensors and an electronic control unit, the system activates a very fast device that, locking a connection, integrates the vest belts with the cable. Furthermore, the backrest could integrate a slip-ring component, allowing its correct height from the seat. The component/element here introduced was considered only at conceptual/functional level, and it was not implemented in the FE model because, in this first part of the device development, the focus was to establish the device effective.

4.2 FE models

In this section the activities required to set up a complete and representative FE crash test are presented. The steps performed are in accordance with the guidelines of the ISO 13232 (ISO (2005)). All simulations were performed using LS-DYNA® software of the LSTC (Livermore Software Technology Corporation)(Halquist (2007)).

4.2.1 Belted Safety Jacket

The Belted Safety Jacket represents the best solution emerged from the Decision Matrix and from the conceptual design process described in the previous section. As shown below (figure 4.6), it consists of a sleeveless jacket (vest), four belts connected with the vest, a cable as restraint component, a slip-ring, a retractor, and a pretensioner. In figure 4.6 a general view of the FE model of the device, is shown.

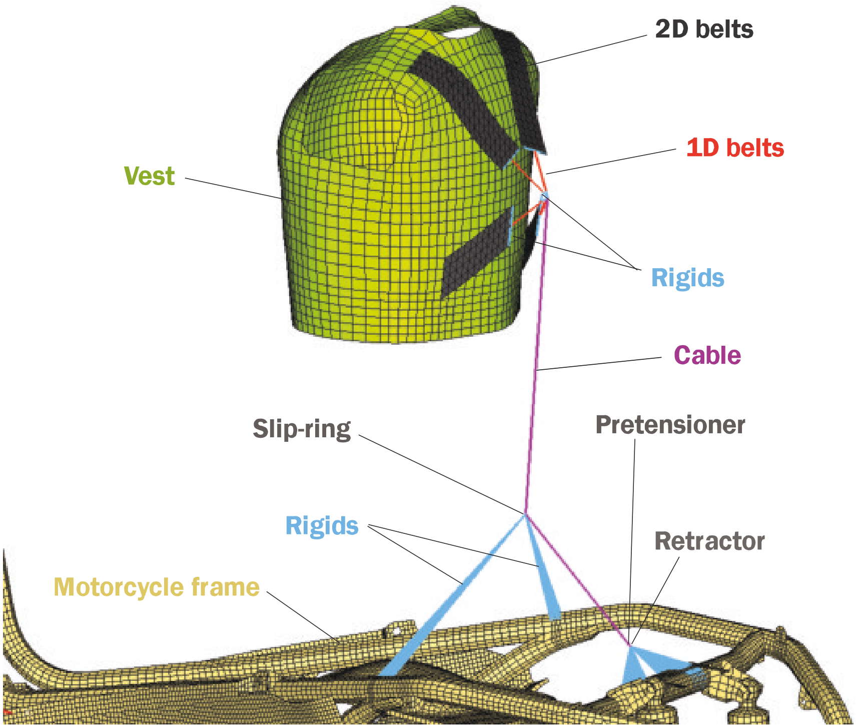

Figure 4.6: General view of F.E. device model.

The vest was modelled with *Quad4* (99% of elements) and *Tria3* shell elements (in yellow). The vest geometry was created modelling a skin element around the dummy model. The material used is fabric (polyamide) with mechanical characteristics commonly used for car seat belts. The thickness of the fabric combined with its geometry, makes it lighter and easier to wear.

- **VEST MATERIAL PROPERTIES**

- RO (Mass density) = 1.0x10^2 Kg/m^3
- EA (Young's modulus - longitudinal direction) = 2.0x10^4 N/m^2;
- EB (Young's modulus - transverse direction) = 2.0x10^4 N/m^2;

- EC (Young's modulus - normal direction) = 2.0x10^4 N/m^2;
- PRBA (ν_{ba}, Poisson's ratio ba direction) = 3.0x10^{-1};
- PRCA (ν_{ca}, Poisson's ratio ca direction) = 3.0x10^{-1};
- PRCB (ν_{cb}, Poisson's ratio cb direction) = 3.0x10^{-1};
- GAB (G_{ba}, shear modulus ab direction) = 7.69x10^3 N/m^2;
- GBC (G_{bc}, shear modulus ab direction) = 7.69x10^3 N/m^2;
- GCA (G_{ca}, shear modulus ab direction) = 7.69x10^3 N/m^2;
- CSE (Compressive stress elimination) = 0.0;
- DAMP (Rayleigh damping coefficient) = 1.0x10^{-1};
- FORM (membrane formulation) = 4.0.

• **VEST MODEL PROPERTIES**

- ELFORM (Element formulation) = 9;
- SHRF (Shear correction factor) = 1.0;
- NIP (Number of through thickness integration points) = 2;
- ICOMP (Flag for orthotropic/anisotropic layered composite material model) = 1;
- T1 (Shell thickness) = 5.0x10^{-4} m;
- B(1) (β_1, material angle at first integration point) = 90.0;
- B(2) (β_2, material angle at second integration point) = 0.0.

As shown in figure 4.6, on the back side of the vest four belts are present. Belts were modelled with *Tria3* shell elements (in grey). Shell elements were used only for the elements which are or potentially might be in contact with the dummy, because, they shall ensure a better contact behaviour with other components. The material used is polyamide, the same used for the vest. Also the mechanical characteristics are the same but the thickness is different (1.20 mm). On one side, the belts were linked to the vest with a node *equivalence*, while, on the other side, the edge nodes were linked with a 1D *rigid* element. Edges not in contact with the vest were parallel, in order to fix the width of the belt in the link points equal to 55 mm.

The 1D belts (modelled as *seatbelt* elements) are connected to the centre node of the *rigids*, on the free edge of the 2D belts (on the opposite side of the vest). These are single degree of freedom elements connecting two nodes (rods). When the strain in an element is positive (i.e. the current length is greater than the unstretched length), a tension force is calculated from the material characteristics and is applied along the current axis of the element to oppose further stretching. The unstretched length of the belt is the initial distance between the two nodes defining the position of the element plus the initial slack length. These components were modelled as *seatbelt* elements. They are characterized by the material following reported (in the list), but their property is a *SectSeatbelt*, which does not require additional information. The length of *seatbelt* elements was set to 10 mm.

- **1D BELTS MATERIAL PROPERTIES**

  - MPUL (Mass density) = 8.0x10^4 Kg/m^3;
  - LLCID (Load curve identification for loading);
  - ULCID (Load curve identification for unloading);
  - LMIN (Minimum length for elements connected to slip rings and retractors) = 3.0x10^{-3} m.

To allow proper cable operation with slip-ring and retractor this component was modelled as *Seatbelt* elements. 50 elements (not visible in figure 4.6) were virtually created inside the retractor, to simulate the presence of a cable spool. Material and load curve identification for loading/unloading (force vs. engineering strain) were directly extracted from LSTC model available online.

The slip-ring was modelled as a 0 dimension element. Two elements meet at the slip-ring. Node B in the belt material remains attached to the slip-ring node, but belt material (in the form of unstretched length) is passed from element 1 to element 2 to achieve slip (see figure 4.7). To define a slip-ring, it is necessary to identify the two belt elements which meet at the slip-ring: the friction coefficient and the slip-ring node. The two elements must have a common node coincident with the slip-ring node. Typically, the slip-ring node is part of the vehicle body structure and, therefore, belt elements should not be connected to this node directly. In the created model the slip-ring was positioned just under the seat and it was linked to PTW frame with *Rigids* elements.

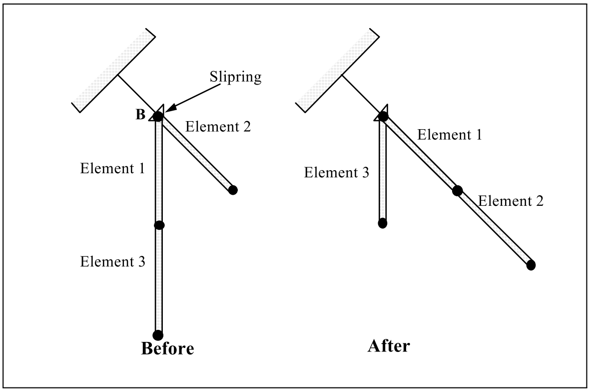

Figure 4.7: Elements passing through slip-ring (*Source:* Halquist (2007)).

Retractor is the device core. As described above, it manages the retention force applied to the cable. The load curve and the max value imposed, shown in figure 4.8, were directly derived from literature data (Foret-Bruno et al. (1998),(2001); Kent et al. (2003)).

From the conceptual analysis carried out, its position was planned under the seat and near the frame, where, a free volume was available and the main structural components are located. It was linked with the PTW frame through *Rigid*

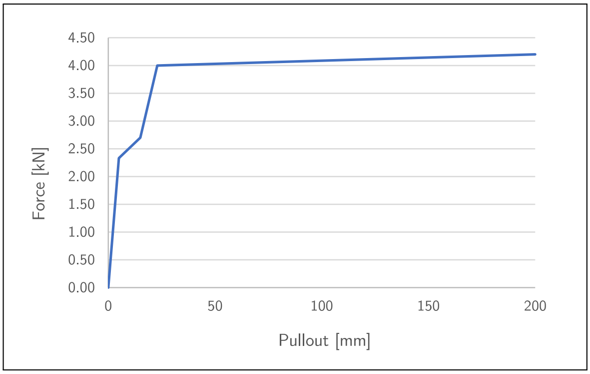

Figure 4.8: Retractor characteristic load curve.

elements, in order to ensure a good stiffness and to avoid stability problem for the model.

For this study it was chosen a type 5 pretensioner among those provided in LS-DYNA®. This type represents a pyrotechnic device which spins the spool of a retractor, stowing the belt inside it. The user defines a pull-in versus time curve which applies once the pretensioner activates. In figure 4.9 it is reported the load curve used.

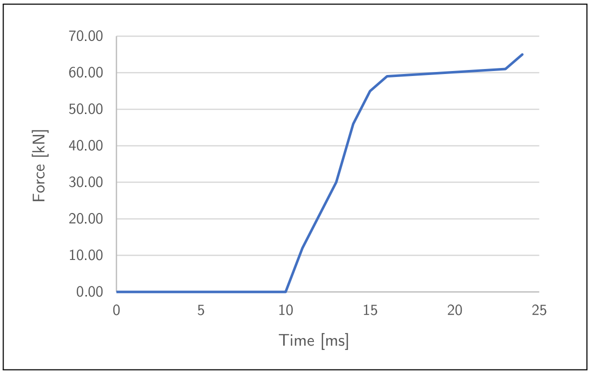

Figure 4.9: Pretensioner characteristic load curve.

For this model it was created a pretensioner with a sensor activation time delay equal to 23 ms. Indeed, it were considered 13 ms, as time between the simulation start and the PTW first contact (with the car), and 10 ms as delay in the device activation.

4.2.2 Motorcycle

Although the purpose of this study is to provide a safety device that can be adapted to as many vehicles as possible, at this early stage, tests focused on one three-wheeler scooter. In the specific the PTW model used to conduct the simulations was a Piaggio MP3. The virtual model was already validated in previous studies conducted by the Department of Industrial Engineering (DIEF), at the University of Florence (Barbani et al. (2012a)(2012b)(2014a)(2014b)). The Piaggio MP3 model is shown in figure 4.10.

Figure 4.10: Piaggio MP3 FE model.

4.2.3 Car

In order to comply with the specifications listed in the section 6 of ISO 13232 (ISO (2005)), the FE model of a Ford Taurus was used as OV (Opposing Vehicle). This choice was made for the easy availability of the model that had already been made available by the NCAC (National Crash Analysis Center). In figure 4.11 the representation of the FE model of the Ford Taurus is shown.

Figure 4.11: Ford Taurus FE model.

4.2.4 Dummy

In chapter 2 some considerations regarding the dummy to be used during the crash test were presented. ISO 13232 part 3 (ISO (2005)) would recommend the use of a dummy MATD with frangible bones in the lower limbs. The use of such a dummy has advantages from the point of view of the accuracy of results, but unfortunately it is really expensive. For this reason, in the majority of experimental crash tests MATD dummy is replaced by dummy Hybrid III 50th percentile. It has no frangible parts and thus, it can be used several times. The FE dummy model was a numerical reproduction of Hybrid III 50th percentile. The model was developed and distributed by LSTC (Livermore Software Technology Corporation). Its specifications are reported in Guha (2014). Figure 4.12 shows the FE model of the dummy.

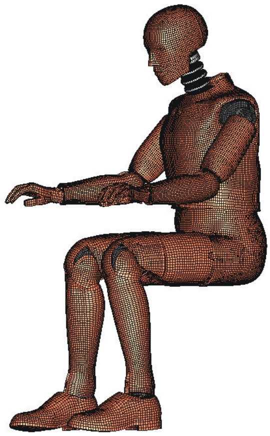

Figure 4.12: Dummy FE model.

4.2.5 Helmet

The FE helmet model used in the simulations was created by the DIEF. The model reproduces a full-size helmet and it was validated by Pratellesi et al. (2011) reproducing a drop test according to ECE/UN 22 R4 regulations (United Nations (2000)).The results obtained are within the regulatory limits. In figure 4.13 the FE helmet model is shown.

4.3 FE configuration test and assessment

The virtual testing environment is the result of the assembly of the models described in the previous paragraphs. Obviously, every impact configuration requires some changes that are the characteristic parameters of MC and OV (e.g. speed and RHA). Another essential step in assembling the full model is the definition and handling of contacts between the device and the various surfaces with which it can come into contact during the simulation. Clearly, there must be no compenetration between the components of the models: for example the dummy, during its longitudinal translation, does not have to go through the jacket, and vice

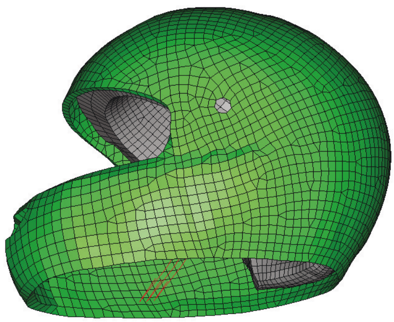

Figure 4.13: Full-size helmet FE model.

versa. To ensure this behaviour, it was necessary to manage interactions among the different surfaces.

Similarly, a specific contact was modelled to prevent the wrong interaction between the cable and the rest of the model. For the preliminary efficiency assessment of the safety device, one of the seven basic impact configurations described in the ISO standard 13232 (ISO (2005)) was reproduced. Configuration 413 6.7/13.4 was chosen, because it represents one of the most dangerous configuration as highlighted by Barbani et al. (2012a). In figure 4.14 it is shown the complete FE simulation model.

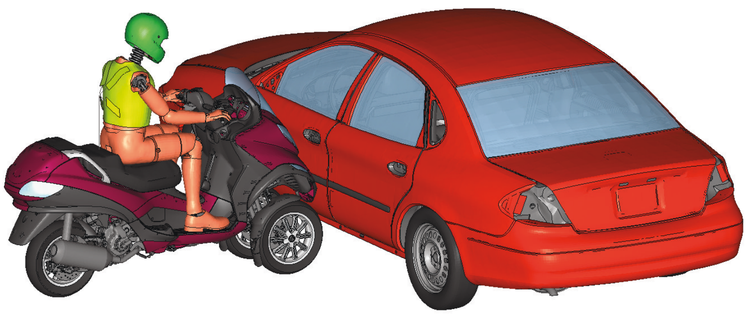

Figure 4.14: Configuration 413 6.7/13.4 FE model.

The protective performance of the device was evaluated comparing the biomechanical injury indexes with and without the device. Four indexes were considered: Head Injury Criterion (HIC) (Versace (1971); Hutchinson et al. (1998)) (equation 1.1 on page 28), Nij (Biomechanical Neck Injury Predictor) (IIHS (2009)) (equation 1.2 on page 30), *Chest Deflection* (Backaitis and St-Laurent (1986)) and Viscous Criterion (V^*C) (Lau and Viano (1986)) (equation 1.5 on page 31). In table 4.1 the values of the bio-mechanical injury indexes, derived from the configuration 413 6.7/13.4 (configuration test), are listed.

HIC and N_{ij} percentage reductions are very high while V^*C reduction is lower, but still remarkable. As expected, *Chest Deflection* undergoes a moderate increase, since the jacket acts mainly on the dummy thorax. It is important to note that, although increased, the $ChestDeflection$ value is still under the limit (50 mm) defined in the Directive 96/79/EC (1996).

Table 4.1: Comparison: bio-mechanical injury indexes (with and W/O the device) and relative variation.

Biomechanical Index	W/O	With	Limit	Δ value
HIC	2459	148	1000	−93.96%
$\boldsymbol{N_{ij}}$	0.68	0.19	1.00	−71.20%
Chest Deflection [mm]	10.20	11.96	50.00	+17.26%
V*C [m/s]	0.13	0.08	1.00	−37.60%

Figure 4.15 shows a visual comparison of the numerical simulations with and without the device. Since the second frame (4.15(a)), a restraint effect of the safety jacket is already visible. The cable under the dummy is in tension, and the vest belts start to retain the jacket (no influence on the dummy position is visible). The frames of figure 4.15(b) and 4.15(c) clearly show that the device is able to avoid the dummy head and shoulder collision against the car. It is important to note the following: the reduction of the longitudinal movement of the dummy (towards the car) and the different neck angles before and after the head impact against the car. Indeed, with the device, the neck suffers more hyperflexion due to the restraint system acting on the thorax; but this effect turns out to be much less harmful compared to the violent impact against the OV. The last frame (4.15(d)) reports an increase of the motorcycle pitch due to the dummy inertia. Quantitative (bio-mechanical indexes) and qualitative evaluation (video frames), confirm the effectiveness of the device to reduce rider's injuries.

4.4 Design Of Experiment

After an initial assessment, a parametrical study was performed to evaluate the effect of design parameters on the restraint performance of the device. In literature, it is possible to find much information about the belt anchorage points (three or four) (Rouhana et al. (2003), and about innovative seat belts with independent control of the shoulder and lap portions (Pipkorn et al. (2016); López-Valdés and Juste-Lorente (2015)). These sources highlight the great influence of the geometrical characteristics on the system behaviour; thus geometrical parameters were included as variable in the study. In addition, since the general objective of the research was to develop a safety device installable on all PTWs, changes in the device layout will be necessary to adapt it to the frame of different models. For this reason, the assessment of the device performance with different geometrical

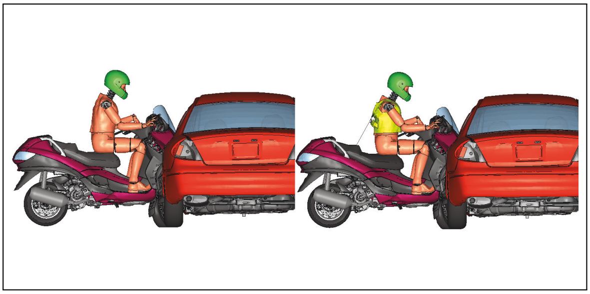

(a) Comparison at 50 *ms*.

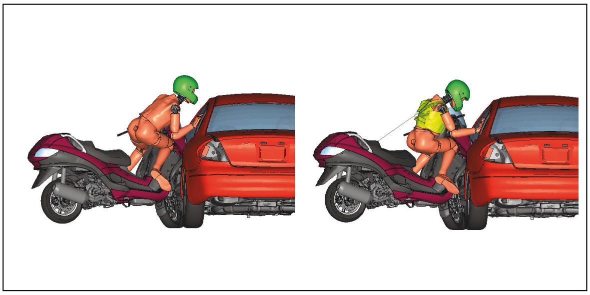

(b) Comparison at 100 *ms*.

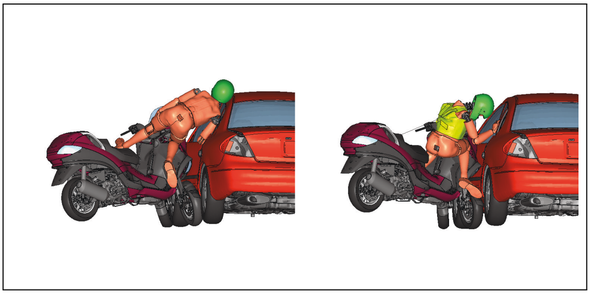

(c) Comparison at 150 *ms*.

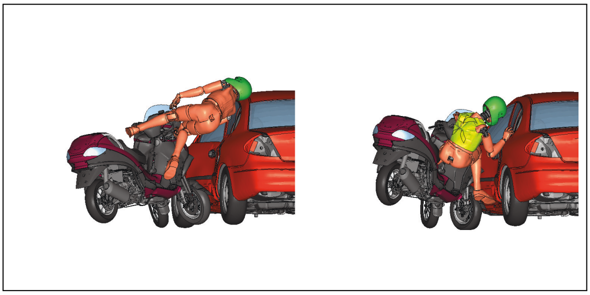

(d) Comparison at 200 *ms*.

Figure 4.15: Comparison: video simulation W/O and with device.

parameters is crucial. A full factorial Design Of Experiment (DOE) was chosen since no information about factorial interactions was available. Five factors and two levels were considered. Three out of the five factors are linked to geometrical dimensions of the device:

- Longitudinal slip-ring position;
- Vertical slip-ring position and
- Belts/restraint cable vertical link position.

The remaining variables are binary and represent alternative options of the system configuration:

- Pretensioner presence;
- Vest-belts link position.

Although the problem was evidently non-linear, two levels were selected since: 1) the range of the geometrical variables was narrow; 2) the computational time of the finite elements model was high, and a linear approximation was accepted for a preliminary study. The limits of the variability range were determined considering the dimensions of a typical seat. Setting the initial configuration as reference (figure 4.16a), the changes for each variable were considered (4.2). Their schematic representation can be found in clockwise order in figure 4.16, starting from configuration (a).

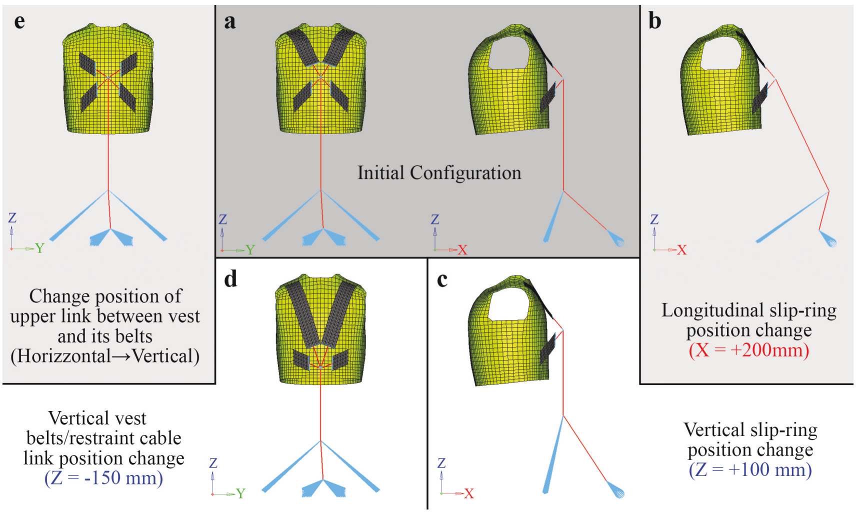

Figure 4.16: Configuration 413 6.7/13.4 F.E. model.

The full factorial design, with 5 factors (3 numerical, 2 categorical) and 2 levels, consists of 32 experiments (i.e. FE simulations). Replications of the 32 configurations were not considered since the experiment was a finite element calculation and there were no external factors that may influence the tests. The backward

Table 4.2: DOE: variables/factors considered and their values.

Variable/ Factor	Figure 4.16, reference letter	Factor type	Nomenclature	Min value [mm]	Max value [mm]
Pretensioner presence or not	Not showed	Text	Pretensioner	No	Yes
Longitudinal slip-ring position	b	Numerical	Slip X	0	200
Vertical slip-ring position	c	Numerical	Slip Z	0	100
Belts/ restraint cable vertical link position	d	Numerical	Belts/Cable Z	270	420
Vest-belts	e	Text	Belt/Jacket orientation	Horizzontal	Vertical

elimination strategy was used to derive an explanatory model of the results. This strategy starts considering all the potential terms of the model and subsequently, removing the least significant terms at every step. The elimination stops when all the variables of the model have p-values, that are less than or equal to the specified α *to-remove* value. A default α *to-remove* value of 0.10 was considered. This automatic procedure had two main weak points:

1. If two independent variables were highly correlated, only one of the two could be taken into account within the model, even if both were statistically significant.
2. Special knowledge of the analyst could not be included in automatic procedures. This might result in a model not optimized from a practical point of view.

To solve these two issues, authors reviewed the model at the end of the automatic variable inclusion procedure, to be sure that it fits the qualitative requirement. The acceptability threshold of each model was specified in terms of $R^2{}_{adjt}$ and a minimum value was set at 0.70. The review procedure included the following steps:

- Automatically fit a hierarchical model with a backward elimination procedure;
- Add a level of interaction until the $R^2{}_{adjt}$ index increases.
- If the highest possible level of interaction was reached and the $R^2{}_{adjt}$ threshold was not reached, increase the α *to-remove* value.

In the present study, the $R^2{}_{adjt}$ threshold was always reached at the first iteration, as shown in the results. In table 4.3 the input values of the factors and the relative bio-mechanical injury indexes, calculated from the FE simulations are reported. Comparing the values of HIC and N_{ij} indexes, it is possible to see that all the values resulted from the 32 DOE simulations are lower than the simulation without the device fitted on the motorcycle (identified as run 0) (figure 4.17a and 4.17b).

Table 4.3: DOE: Input factor values - Output biomechanical injury index values. The row highlighted in grey identifies the simulation relative to the initial configuration. Run 0 identify the simulation W/O device.

INPUT						OUTPUT			
Run order	**Pretensioner**	**Slip X position**	**Slip Z position**	**Belts/Cable Z position**	**Belts/upper link position**	***HIC***	***N_{ij} Max***	***Chest deflection [mm]***	***V*C [m/s]***
0	-	-	-	-	-	2459	0.677	10.2	0.125
1	No	0	0	270	Horizontal	117	0.238	14.2	0.186
2	No	200	0	420	Horizontal	140	0.186	18.7	0.141
3	No	0	100	420	Vertical	132	0.209	14.5	0.141
4	No	200	100	270	Horizontal	123	0.154	4.1	0.022
5	No	0	100	270	Horizontal	124	0.182	13.4	0.194
6	No	200	100	270	Vertical	158	0.181	7.6	0.289
7	Yes	200	100	420	Vertical	244	0.246	10.5	0.064
8	Yes	0	100	270	Vertical	288	0.239	13.9	0.112
9	Yes	0	100	270	Horizontal	293	0.240	14	0.106
0	Yes	200	0	420	Horizontal	139	0.239	18.2	0.136
11	Yes	0	100	420	Horizontal	399	0.168	12.7	0.084
12	Yes	0	0	420	Horizontal	148	0.190	11.9	0.078
13	Yes	0	0	270	Vertical	182	0.197	19	0.164
14	Yes	200	100	270	Vertical	258	0.201	18.2	0.143
15	Yes	0	100	420	Vertical	104	0.157	13.7	0.145
16	No	0	0	420	Vertical	169	0.277	11.2	0.087
17	No	200	100	420	Horizontal	270	0.201	9.5	0.057
18	Yes	0	0	270	Horizontal	173	0.200	17.7	0.122
19	No	0	0	420	Horizontal	113	0.263	16.2	0.152
20	Yes	200	0	420	Vertical	150	0.202	19.3	0.125
21	No	0	0	270	Vertical	147	0.235	12.6	0.113
22	No	0	100	420	Horizontal	160	0.221	13.3	0.080
23	No	200	0	270	Vertical	252	0.157	9.5	0.062
24	Yes	200	0	270	Vertical	260	0.243	8.7	0.052
25	Yes	200	0	270	Horizontal	266	0.253	8.1	0.052
26	Yes	200	100	420	Horizontal	242	0.245	7.8	0.045
27	No	200	100	420	Vertical	160	0.175	11.6	0.077
28	No	0	100	270	Vertical	107	0.184	13.3	0.155
29	No	200	0	270	Horizontal	183	0.133	9.7	0.067
30	Yes	200	100	270	Horizontal	181	0.255	4.5	0.021
31	No	200	0	420	Vertical	165	0.159	12.5	0.100
32	Yes	0	0	420	Vertical	141	0.214	13.0	0.102

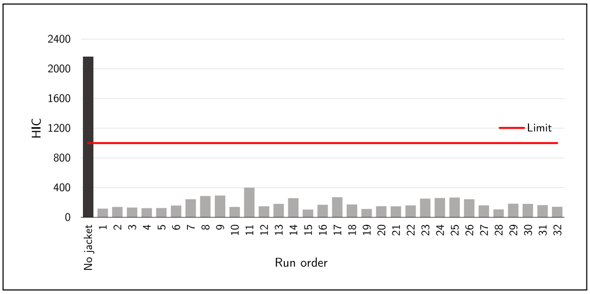

(a) DOE results: Head Injury Criterion.

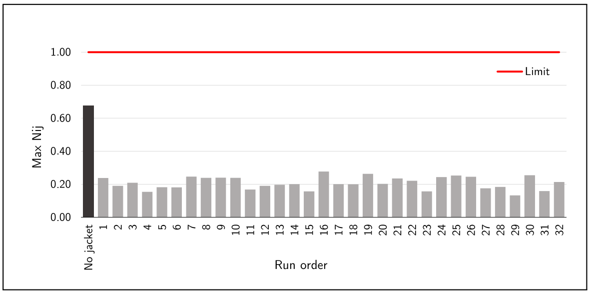

(b) DOE results: Neck Injury Index.

(c) DOE results: Chest deflection.

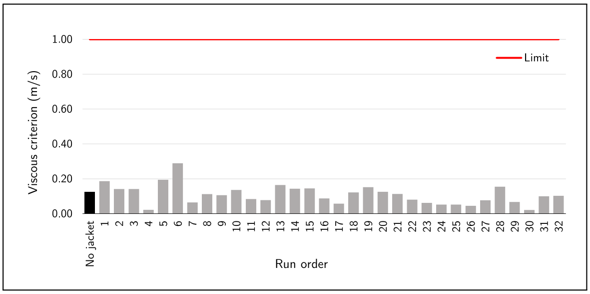

(d) DOE results: Viscous Criterion.

Figure 4.17: Bio-mechanical injury indexes results.

Results demonstrate that, whatever the device geometrical configuration, the head impact against the car is avoided. Thus, these data suggest that the device may be effective also in other geometric configurations and therefore for other PTW models, although vehicle characteristics will influence the initial rider's position and the global inertia, with consequences on the accident dynamics. Results of the chest deflection show an increase in 71% of the configurations, with reference to the configuration without the device (figure 4.17c), while for the viscous criterion in only 34% of the cases (figure 4.17d). Nonetheless the maximum values of both indexes are below the respective acceptability limits.

In Table 4.4 the ${R^2}_{adjt}$ value is reported for each of the response variables, together with the model order and the used α *to-remove* value. Table 4.4 shows that a high interaction level was necessary to explain the variability of the crash event, and that the models are highly representative of the simulations (i.e. high ${R^2}_{adjt}$ values). Implications are twofold: the model well fits reality, which is partially described by the main effect of the independent variables and mostly by their interactions and, the model complexity increases and the model could be difficulty used to assess the device behaviour not in correspondence of the variable imposed values. For such a use of the model further simulations or experiments are required.

Table 4.4: DOE: ${R^2}_{adjt}$ value, factorial terms order and α used for each output variables.

Response variable	$\mathbf{R^2}_{\mathbf{adjt}}$	Terms order	α to-remove
Head Injury Criterion	82.6%	4^{th}	0.10
Neck Injury Max	80.9%	4^{th}	0.10
Chest Deflection [mm]	70.3%	4^{th}	0.13
Viscous Criterion [m/s]	89.1%	4^{th}	0.10

4.5 Response optimization

With the information obtained from the Design Of Experiment, it was possible to establish the best combination of the factors analyzed, to obtain the maximum device effectiveness. Indeed, the response optimization -a DOE factorial tool of Minitab program- is able to identify the combination of variable settings that jointly optimize a single response or a set of responses. This is useful when the evaluation of the impact of multiple variables on multiple responses is required. Before starting to use the response optimizer to optimize multiple responses, it was mandatory to fit a model for each response separately. These information were already available from regression analysis carried out during the DOE. In the specific, terms of fourth order, for all bio-mechanical indexes (responses) analyzed, were considered. In this study, in order to search for optimal responses based on the requirements it was necessary to minimize all responses, as the purpose is to reduce the rider's injuries. The analysis calculates an individual desirability for each response. It is possible to assign a specific weight to it, depending on its importance. Figure 4.18 shows how various weights affect the shape of the desirability function. Desirability is on the y-axis and the response is on the x-axis.

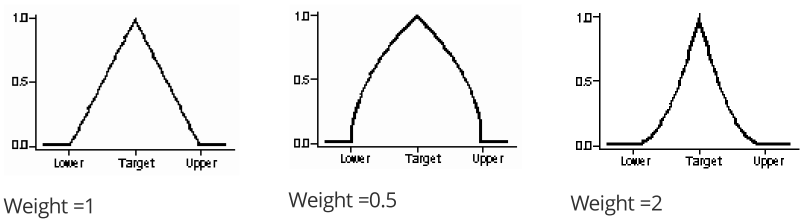

Figure 4.18: Response optimization plot.

Where:

- A weight = 1 gives the same importance both to the target and the bounds. This is a neutral setting.
- A weight > 1 lays more emphasis on the target. Increasing the weight requires the response to move closer to the target to achieve a specified desirability.
- A weight < 1 lays less emphasis on the target. Decreasing the weight does not require that the response to move so close to the target.

In this study, the same value equal to one, was assigned to all responses. These values are combined to determine the composite, or overall, desirability of the multi-response system. An optimal solution occurs when composite desirability obtains its maximum. The obtained results are shown in figure 4.19.

Here, highlighted in red on the top side (between the two extremes values defined in the factorial design), the factors values that maximize the composite desirability[1], are visible. The best device set-up takes in to account:

- No pretensioner presence.
- Longitudinal slip-ring position setted on the value 1447 mm.
- Vertical slip-ring position setted on the value 700 mm.
- Belts restraint cable vertical link position setted on the value 869 mm.
- Horizontal Belt/Jacket orientation.

The desirability (D) value reached is very high, over 90%. From a first assessment is evident the negative influence of the N_{ij} individual desirability on the

[1] Individual and composite desirabilities assess how well a combination of variables satisfies the goals defined for the responses. Individual desirability (d) evaluates how the settings optimize a single response; composite desirability (D) evaluates how the settings optimize a set of responses overall. Desirability has a range from zero to one. One represents the ideal case; zero indicates that one or more responses are outside their acceptable limits.

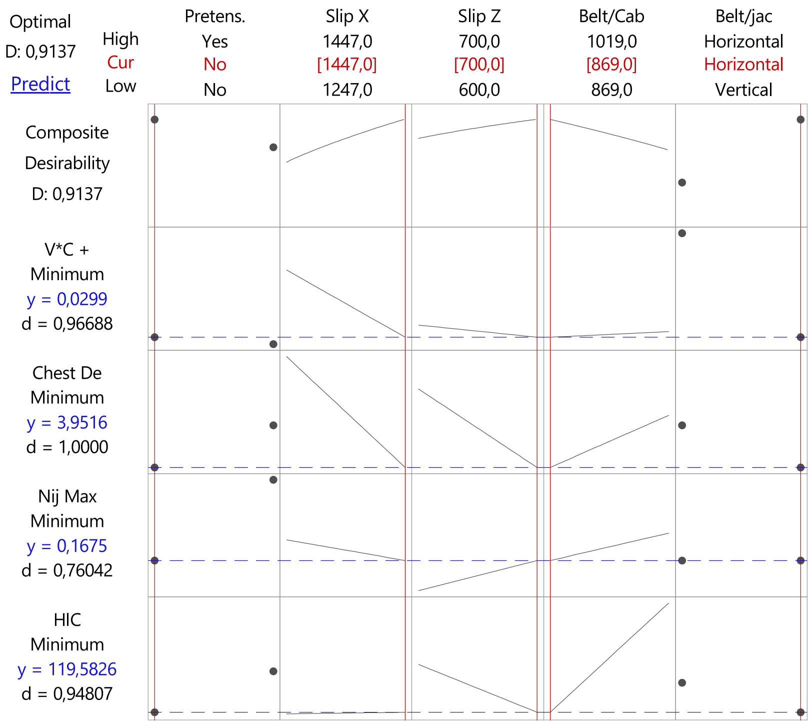

Figure 4.19: Response optimization plot.

total value. Indeed, the composite desirability is simply the weighted geometric mean of the individual desirabilities (equation 4.1).

$$D = (n(d_i^{w_i}))^{\frac{1}{W}} \tag{4.1}$$

Where:

- d_i is the individual desirability for the i^{th} response.
- w_i importance of the i^{th} response.
- W is the $\sum w_i$
- n is the number of responses.

In the specific, an analysis of the best factors values shows that, the presence of the pretensioner is not important for bio-mechanical injury reduction. The Z position of the slip-ring has a reverse influence on N_{ij} individual desirability. The straight line relative to the interaction between slip-ring Z position and N_{ij}, indeed, has positive slope (backwards compared to the direction of the other ones), and the value of 700.0 (the highest and the best for composite desirability) defines the worst scenario. Contrary, the best value for slip-ring X position (the highest) results strongly and positively influential on N_{ij}, *Chest defletion* and *V*C* desirability. While, it results irrelevant on *HIC* desirability. The belts/restraint cable vertical link position was set on lower value, and its influence results positive for all output. Same behavior is visible for the vest-belts link horizontal position. Setting the device in this geometrical configuration (appropriate to the fourth run in table 4.3), enables to obtain excellent bio-mechanical injury indexes. From the assessment of the PTW encumbrance of this device's set-up, it is clear that the presence of a passenger on the PTW is excluded. Indeed, the slip-ring X position, results placed under the passenger' seat portion, as visible in figure 4.20.

Figure 4.20: Optimized slip-ring position.

In figure 4.21 it is shown the response optimization plot with slip-ring X set up at the lowest value (1247.0). This analysis was carried out to compare the results of different starting variables set-up and to assess the responses in the configuration which does not adversely affect the presence of the passenger. The results show meaningful differences. The composite desirability decreases considerably (-32%), while the bio-mechanical indexes are increasing by around 37% for *HIC*, 20% for N_{ij}, 208% for *Chest deflection* and 185% for *V*C*. However, these values are in all cases considerably below their limits.

In view of the results emerged from the geometrical device optimization process, it was decided to consider the geometrical set-up first relative to the first response optimization (without constrains). This device configuration ensured better injury index values, and for this reason, it will be adopted to test the device effectiveness in the other impact configurations defined in the following chapter.

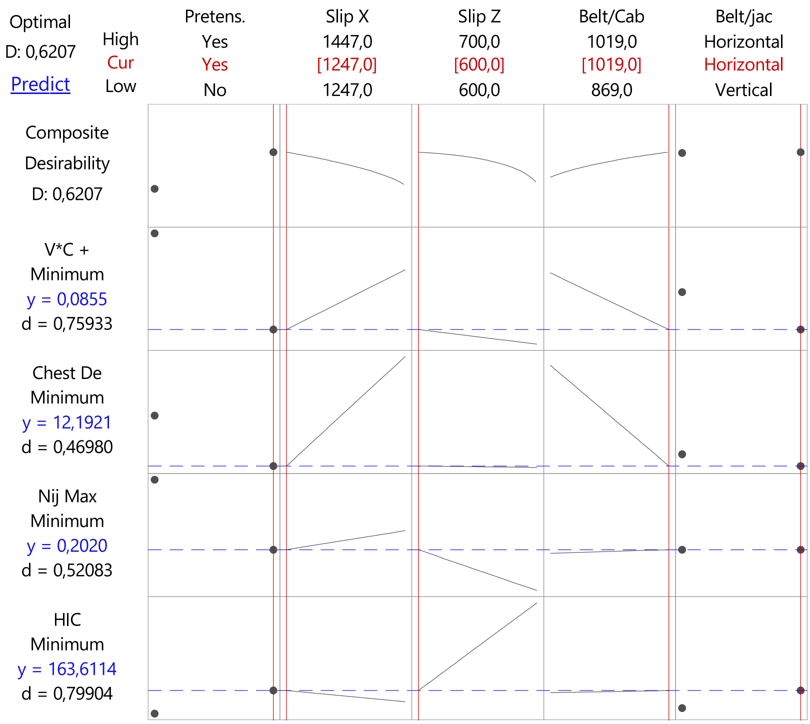

Figure 4.21: Response optimization plot with slip-ring X set up at the lowest value.

Chapter 5

Definition of the most representative PTW-car impact scenarios

In this chapter the ISO 13232 (ISO (2005)) methodology will be applied to an European Powered Two-Wheelers (PTWs) accidentological database, in order to verify if the set of the seven most relevant configurations, proposed by the ISO standard, does correspond to the most representative European accident scenarios. This information is essential to assess the effectiveness of the Safety Belt Jacket in representative accident scenarios.

5.1 ISO 13232

Since the early 1970s, passive safety of Powered Two-Wheelers (PTWs) was a research topic to increase rider's safety. Several research institutes investigated rider's injuries and proposed new solutions for rider's protection (Bothwell et al. (1973), Hirsch and Bothwell (1974), Happian-Smith et al. (1987), Happian-Smith and Chinn (1990), Nieboer et al. (1993), Yettram et al. (1994), Chinn et al. (1996)).

Nonetheless it was clear that without standardized procedures and methods it was impossible to compare the results of these studies. For this reason, the United Nations, the Inland Transport Committee and the Economic Commission for Europe developed the first release of the ISO 13232 standard in 1996 - updated in 2005 - (ISO (2005), Van Driessche (1994)). The methodology defined in ISO 13232 (ISO (2005)) standard was promptly adopted by the research community (Ibitoye et al. (2006), Yamazaki et al. (2001), Withnall et al. (2003), Deguchi (2005), Van Auken et al. (2005), Barbani et al. (2014b), Aikyo et al. (2015)).

Using a database of real world accident cases, the standard ISO 13232 (ISO (2005)) defined impact scenarios, variables to be measured, crash tests methods and risk/benefit calculation. Nowadays it represents the only standard framework to perform analyses on protection devices fitted on motorcycles. In the ISO 13232 (ISO (2005)) two hundred MC-car scenarios were defined. Each scenario was identified by a three-digit code: the first and the second digits indicate respectively the contact points of the OV and of the MC, while the third one is the Relative Heading Angle (RHA). This code was followed by the speed values at impact (in m/s) of the OV and the MC (respectively OVS and MCS).

The selection of the seven required impact configurations, for the preliminary assessment of safety devices, and overall, the method used to identify this subset were highly valuable outcomes of the ISO 13232 (ISO (2005)) standard. The method was based on a combination of accidentological data and prior experimental test experience. Over twenty years from its first release, the results of a comparative study, to investigate if the ISO 13232 (ISO (2005)) most relevant scenarios are representative of the European context, could support future research activities and before using the seven configurations for the assessment of the BSJ.

In this respect, Berg (Berg et al. (1998)) had already highlighted discrepancies with the ISO 13232 (ISO (2005)) results. For these reasons in this study an in-depth analysis on the ISO13232 database (ISO (2005)), the application of the ISO 13232 (ISO (2005)) methodology to the more recent MAIDS database (MAIDS (2009)), and a comparison of the seven most important accident configurations, derived from the two data sets, was performed in order to highlight possible differences.

In this work the ISO 13232 method, for the definition of the seven most relevant impact scenarios (i.e. geometries and vehicle velocities), was applied to the MAIDS database (MAIDS (2009)) to evaluate if the ISO13232 configurations are still up-to-date and representative of the European accident scenarios. In order to test the correct application of the ISO standard, in the initial stage of the work, the ISO 13232 accidentological database was rebuilt from the tables included in the standard. The successful completion of this process allowed also to identify some minimal differences in global descriptive data of specific impact configurations (i.e. 711, 414, 115, 313, 513, 131, 514 and 241 configurations, figure 5.1).

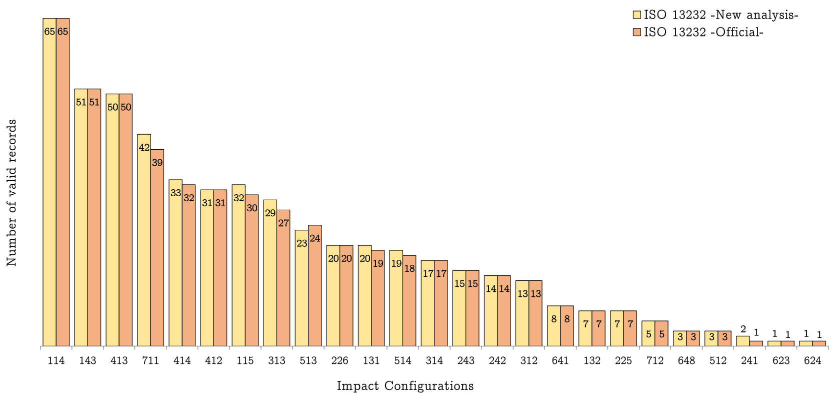

Figure 5.1: Comparison of valid impact configurations in ISO 13232 database.

After a double procedural check, differences were ascribed to the ISO 13232 data processing. However, the intermediate processing steps were not reported in the ISO 13232, but only the initial raw data and the final results were included. It was thus impossible to understand the origin of the differences. Since the new processing of the ISO 13232 database does not show a systematic processing error and the results are globally in line with those of the standard, they were adopted as the ISO 13232 reference during the following analyses.

Subsequently MAIDS data (MAIDS (2009)) were processed to become comparable to the ISO 13232 data (ISO (2005)). Records were filtered to retain only the ones with the following features: car as opposing vehicle; PTW without pillion rider, and rider in seating position at impact. Afterwards each accident was assigned a scenario code number and nominal values for the OV and MC speeds, according to the ISO 13232 coding procedure, and all the physically unrealisable configurations were discarded. The process returned 279 valid impact cases.

Subsequently injuries in MAIDS database were recoded in compliance with the ISO 13232 part 2 - table A.1 and A.2), because the original data were coded according to the AIS 1998/2005. For 213 injuries of MAIDS database no match was found with AIS coding, thus the related injury information was not used. As a consequence, 40 valid cases have zero injuries associated, similarly to Los Angeles and Hannover databases of the ISO 13232, where some injuries were neglected because they present invalid body region and injury type coding number.

At the end of these preliminary operations, homogeneous and comparable datasets were available to carry out a frequency analysis. A further analysis was performed using the 25 geometries reported in table B.1 part 2 of the ISO 13232 standard, followed by a frequency analysis on injuries. All thirteen body regions of table C.1 part 2 of the ISO 13232 were considered. In addition, body regions were grouped into three main body areas (i.e. upper, central and lower) to better understand injury distribution. All analyses, if not differently specified, were performed on injuries of moderate or high level of severity, corresponding to AIS2+ levels.

In the ISO 13232 (ISO (2005)) injuries analysis, significant differences between the claimed concussion analysis and the effective data, were reported. Last part of annex F specified that head concussive injuries were limited to helmeted records, while it was evident that all concussive injuries were included in data processing (e.g. in configuration 114, in table D.1 of ISO 13232, 16 records were reported, but in raw data the helmeted cases were 5, 1 case was without helmet and 10 cases with no information on helmet). Thus, for the sake of comparability with the ISO 13232 data, the analyses performed on MAIDS (MAIDS (2009)) data took into account all injuries, with or without helmet.

In order to perform a comparison on the dangerousness of each impact configuration both in terms of accident occurrences and of injury severity, a synthetic index named Configuration Risk Index (C.R.I.) was proposed. In equation 5.1 the C.R.I. definition is reported: accident occurrences and injuries of specific configuration are combined and weighted with the number of total accidents and injuries.

$$C.R.I._{(x)} = \left(\frac{A_{(x)}}{A_{(t)}} \cdot \frac{\sum_{i=2}^{n} (I_{(x,AISi)}) \cdot i}{I_{(t)} \cdot (\sum_{i=2}^{n} i/n - 1)} \right) \cdot S.F. \qquad \text{n=6,} \tag{5.1}$$

Where:

- x the configuration code,
- $A_{(x)}$ is the number of accidents for configuration x,

- $A_{(t)}$ is the total number of accidents for all configurations,
- i is the considered AIS level (from 2 to 6),
- $I_{(x,AISi)}$ is the number of injuries for configuration x and for AISi level,
- $I_{(t)}$ is the total number of injuries for all configurations,
- $S.F.$ (= 100) is a scale factor.

5.2 Results

5.2.1 Impact configurations

As previously stated, a new analysis on the ISO 13232 (ISO (2005)) data was carried out to check the capability to reproduce its methodology. Raw data was completely digitalized, starting from data reported in the standard, and then processed according to the procedures described in part 2 of the ISO 13232. Comparing the results with the ISO 13232 ones a few differences were identified in configuration counting. The most relevant difference consists in two accidents of configuration 115, which in turn would increase its relevance and ranking, overcoming configuration 412.

The application of the ISO 13232 to the MAIDS (MAIDS (2009)) database triggered some additional considerations about removed or neglected impact configurations in the standard. Three impact configurations were eliminated in the ISO 13232. In the specific:

- 214,
- 227 and
- 718.

Configuration 214 was removed because of the difficulty to implement an experimental test procedure capable to ensure accuracy and repeatability. This motivation appears questionable because the vehicles reciprocal position is very similar to 314, 414 e 514 configurations, all included in the standard. In terms of occurrence frequency, configuration 214 was relevant in MAIDS database, where it ranked seventh.

Considerations are necessary also for configurations 227 and 718, both of them present with valid records only in MAIDS (MAIDS (2009)) database. Configuration 227 was reported, as reclassified geometry, in table 5 of part 2 of the ISO 13232 (ISO (2005)), but it was not included neither among final valid or removed configurations. While, configuration 718 was not listed neither among the reclassified or removed configurations, but it should be among the reclassified ones being very similar to 711 (valid configuration).

Finally, a great number of sideswipe impact configurations were removed, even if in real life they are very common, and in order to have homogeneous comparison data between the two databases, results regarding 214, 227 and 718 configurations were ignored in this analysis. However, the authors suggest that these configurations should be re-considered in a future review of the standard.

Focusing on the results of the frequency analysis performed on the ISO 13232 and MAIDS data, configurations 412, 413 and 414, in MAIDS derived results, represent a smaller share of the dataset compared to the ISO database while, 312, 313 and 314 a larger one (figure 5.2). These differences may result from a possible different interpretation of car contact points since car models were not provided in MAIDS database. Consequently, the OVs (Opposite Vehicles) lengths were unknown, and the contact points were codified only on the basis of the contact point description (available information), considering these points located on a sedan car. This coding activity represents a current limitation of the work, and it should be improved in future analyses.

The frequency analysis of the impact configurations highlighted differences between databases (figure 5.2). In the ISO 13232 data configuration 114 is the most frequent one with 12.7%, followed in descending order by configurations 143 (10.0%), 413 (9.8%), 711 (8.2%), 414 (6.5%), 115 (6.3%), and 412 (6.1%). In the ranking derived from MAIDS data, configuration 313 is the most frequent one with 15.8%, followed in descending order by configurations 312 (11.1%), 114 (9.0%), 115 (9.0%), 711 (8.6%), 143 (6.1%), and 413 (6.1%). The full set of configurations is reported in figure 5.2. No accidents were recorded for 641, 648, 241, 623 and 624 impact configurations in the MAIDS (MAIDS (2009)) database. The same configurations are of limited importance also in the ISO 13232 (ISO (2005)) analysis.

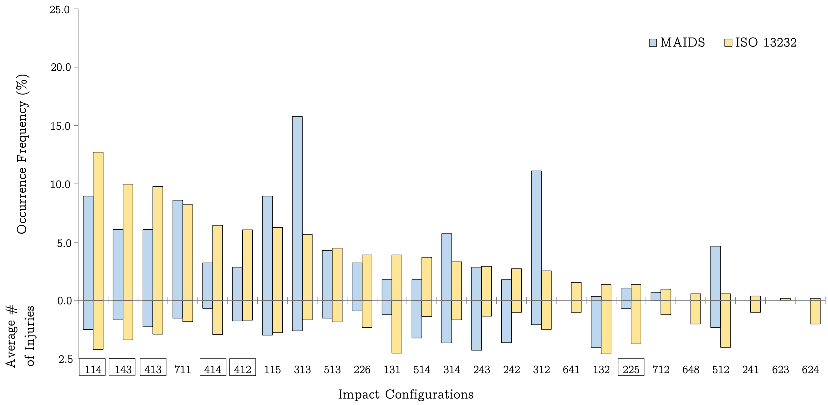

Figure 5.2: Comparison MAIDS - ISO13232: Configuration occurrence frequency (Upper); Average number of injuries for configuration (Lower). Ranked according to the ISO 13232. The boxed numbers identify the seven-impact configurations chosen by the ISO 13232.

Focusing the attention on the most important seven rankings, configurations 114, 143, 413, 711 and 115 are present in both sets and differ only in terms of relevance. Differently configurations 414 and 412 (fifth and seventh position in the ISO 13232) are not present among the seven MAIDS configurations, and they are replaced by configurations 313 and 312, having a higher ranking (first and second position respectively).

Interestingly the same type of results can be observed in Berg's work (Berg et al. (1998)), where the positions from one to seven are occupied by 114, 226, 413, 313, 412, 115 and 314 respectively. Five configurations are in common between the ISO and MAIDS databases, while 226 and 314 are more important in MAIDS and replace 143 and 711.

The preliminary work on the ISO 13232 (ISO (2005)) database allowed a separate analysis of the Los Angeles and Hanover data. In figure 5.3 the number of valid records for each of the two databases is reported. Interestingly Hannover data are concentrated on the first seven configurations emerged by the ISO 13232 analysis plus configurations 131, 132 and 712. On the contrary, Los Angeles data are evenly distributed among all configurations. The distribution of Hannover data impacted the final outcome of the ISO 13232 required configurations.

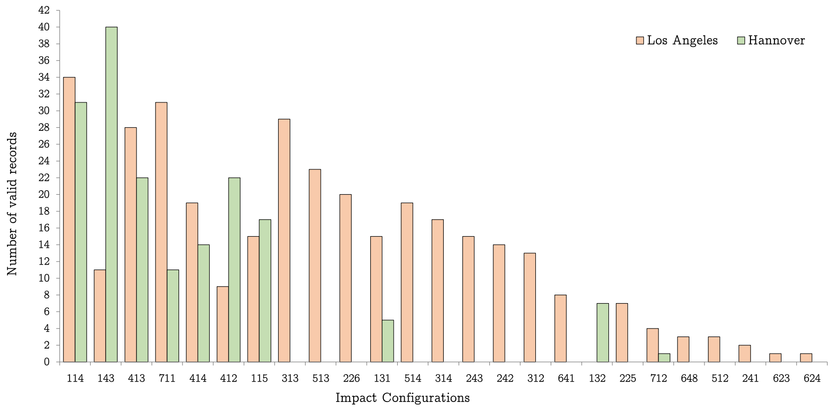

Figure 5.3: ISO13232: Comparison of valid impact configurations between Los Angeles and Hannover databases.

5.2.2 Injury analyses

In the bottom of figure 5.2 the ratios between the total injuries recorded for each configuration are shown together with the total number of accidents for each configuration. Inside each database, the ranking of the configurations, based on the average injuries, is different compared to the one based on frequency. This result suggests that the most probable accident scenario is not necessarily the most dangerous. Comparing the average number of injuries between databases, different rankings can be found: e.g. configuration 131 is the second one in the ISO 13232 database (2.3 avg. injuries) and the sixteenth one in MAIDS database (0.6 avg. injuries), while in terms of occurrence frequency it is ranked in the eleventh and fifteenth position respectively.

In figure 5.4 the injury distribution of each of the thirteen body regions listed in ISO 13232 is reported (only AIS2+ injuries). In both databases, the three most injured body regions correspond but they are differently ranked: in ISO 13232 they are head, lower leg and upper extremities respectively with 6.6%, 5.1% and 3.9%, while in MAIDS data they are upper extremities, lower leg and head respectively with 8.6%, 7.1% and 6.4%.

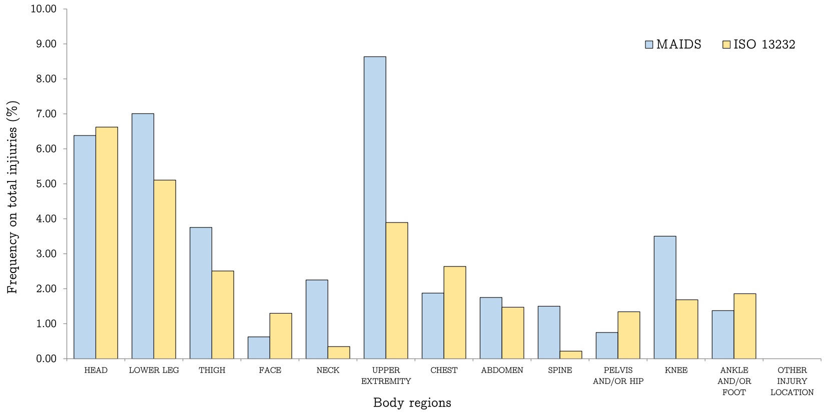

Figure 5.4: Comparison MAIDS-ISO13232: Distribution (%) of generic injuries (AIS2+) per Body region.

An interesting point of view can be found grouping the body regions in three main areas: upper, central and lower. In the upper area head, face and neck regions are included; central area consists of upper extremity, chest, abdomen and spine; pelvis and hips, thigh, knee, lower leg, ankle and foot form the lower area. The ISO 13232 (ISO (2005)) body region "*other injury location*" was not included in this analysis since in both databases (MAIDS and ISO 13232) all its injuries were AIS1+. This grouping allows to identify the macro area most affected by the injuries (figure 5.5). In both databases, the most injured body macro area was the lower one (12.5%, ISO13232, and 16.4%, MAIDS). Differently, the second most injured macro area was the upper one for ISO 13232 (8.3%) and the central one for MAIDS data (13.8%) (MAIDS (2009)).

The lower body area is always the most injured one, while the upper and central region have reversed positions (in ISO 13232 upper region ranked second). This difference could derive from a significant presence of un-helmeted rider records in the ISO 13232 database (57%) while in MAIDS the percentage is minor (7%). Considering only "helmeted" cases for both databases, a significant reduction of injury percentage in upper body region can be observed in the ISO 13232 (from 8.3% to 5.7%) (figure 5.6). With this data subset the ISO 13232 injuries distribution is similar to MAIDS, confirming the helmet efficiency in injury mitigation (Evans and Frick (1988), Rodgers (1990), Servadei et al. (2003), Deutermann (2004)).

Considering all (helmeted and not) severe injuries (AIS4+), their distribution shows an interesting reverse trend compared with the previous one (figure 5.7).

In this case, the upper area represents the highest injury share in both data sources with 1.9% (ISO (2005)) and 1.6% (MAIDS). The central and lower regions are respectively second and third, with 1.5% and 0.2% for the ISO 13232 data,

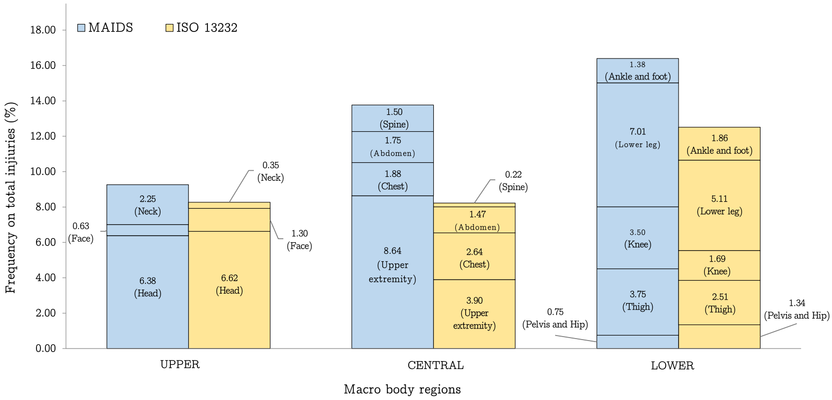

Figure 5.5: Comparison MAIDS-ISO13232: Distribution (%) of generic injuries with AIS2+ for Macro body region.

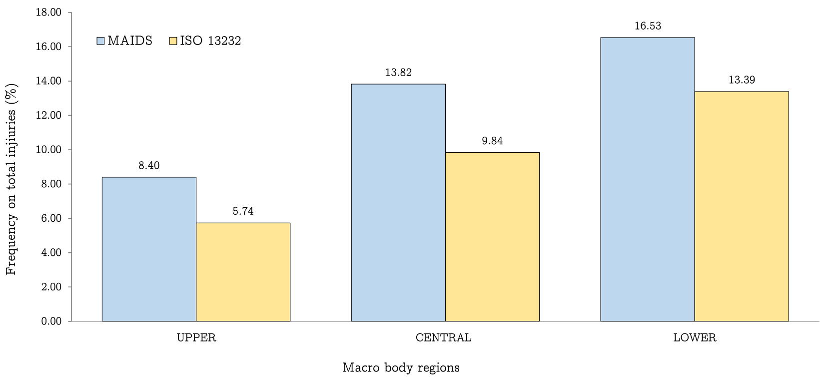

Figure 5.6: Comparison MAIDS-ISO13232: Distribution (%) of generic injuries with AIS2+ (only helmeted cases) per Macro body region.

and 0.8% and 0.3% for MAIDS (MAIDS (2009)). Similar results can be found in literature (Sporner et al. (1990), MAIDS (2009)) and they show the tendency to have an injury shift from lower to upper body area with an increase of AIS value.

5.2.3 Configuration risk analyses

In addition to the ISO 13232 procedure, C.R.I. was proposed in this research to perform an objective assessment of the overall dangerousness of each scenario (equation 5.1). The results of a C.R.I., based ranking of the scenarios, were compared with the frequency based method used in ISO 13232 to select the most relevant scenarios. The results are reported in figure 5.8 and 5.9, where relevant changes in the ranking can be observed.

The first ten positions of the frequency occurrence (yellow and cyan columns in

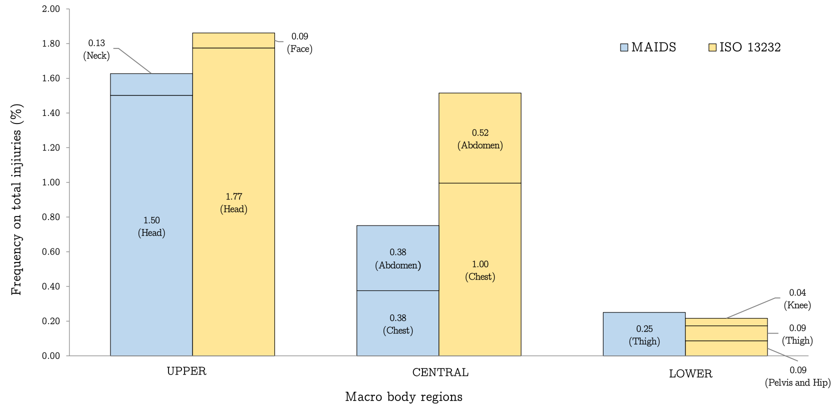

Figure 5.7: Comparison MAIDS-ISO13232: Distribution (%) of generic injuries with AIS4+ for Macro body region.

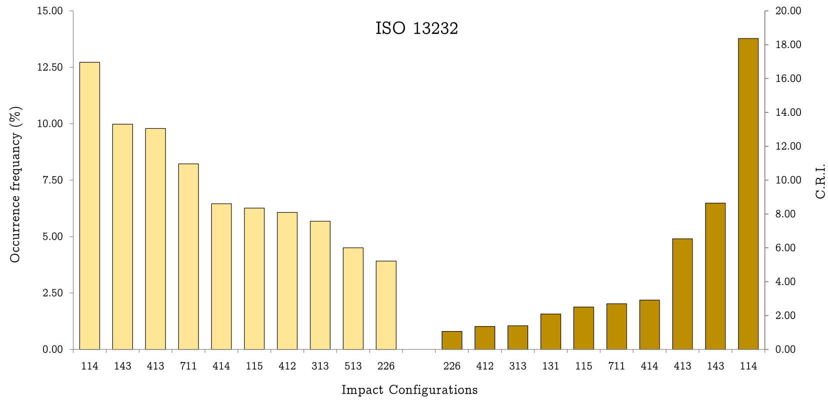

Figure 5.8: Configuration order comparison: occurrence frequency (%) and C.R.I.: ISO 13232.

decreasing order from left to right) and the C.R.I. method (ocher and blue columns in decreasing order from right to left) for each database are reported. In both databases, a different configuration ranking is obtained upon usage of a different method. This predictable result is due to a different distribution of average severity injuries compared to the configuration occurrence. In the ISO 13232 data (figure 5.8) the first three positions are occupied in both cases and in the same order, by 114, 143 and 413, but C.R.I. highlights the higher dangerousness of 114 respect to the other two scenarios. Differently configuration 711 presents lower C.R.I. value than in occurrence frequency, and it is swapped with 414. Finally, configuration 131 was included in the seven most relevant scenarios replacing configuration 412, although with a different relevance level.

Globally C.R.I. highlights that the dangerousness of the first three scenarios

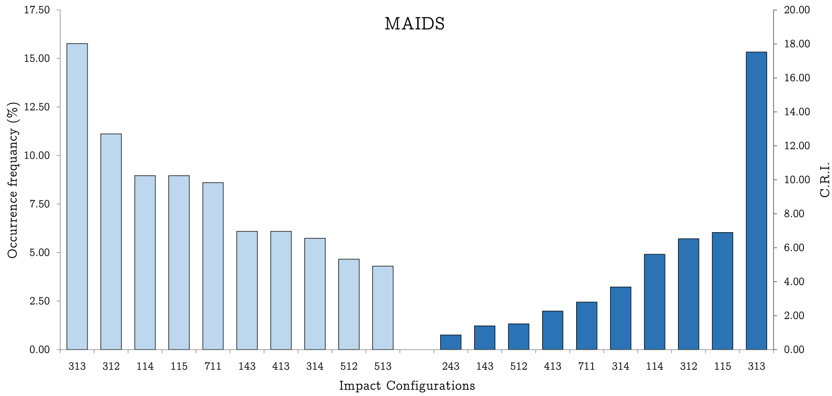

Figure 5.9: Configuration order comparison: occurrence frequency (%) and C.R.I.: MAIDS.

is at least double compared to the fourth ranking scenario. Similar results were obtained with MAIDS (MAIDS (2009)) data (figure 5.9). The most relevant configuration (313) was confirmed in both rankings, but with an amplified importance when C.R.I. was used. In this dataset, more ranking changes were generated with the two methods, but only one difference was reported in the seven most relevant scenarios: configuration 143, included with the occurrence frequency method, was replaced by configuration 314 in the C.R.I. based ranking. Data in figure 5.2 and figure 5.10 show that C.R.I. is able to highlight the main configuration and reduce the importance of the secondary ones achieving simpler and clearer data.

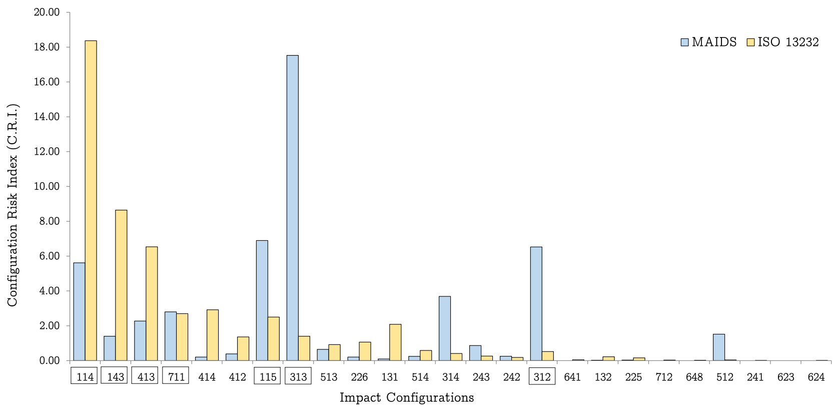

Figure 5.10: Comparison MAIDS-ISO13232: Configuration Risk Index (C.R.I.) distribution. The boxed numbers identify the seven most representative impact configuration based on MAIDS data and C.R.I. index.

A comparison of C.R.I. based ranking among databases (figure 5.10) identifies configurations 114, 143, 413, 414, 711, 115 and 131 as the seven most relevant ones for ISO 13232, and configurations 313, 115, 312, 114, 711, 314, and 413 for MAIDS. Once again, results underline differences not only in the order of the seven highly recommended scenarios defined in the standard but in the identification of the impact configurations.

The comparison, performed on the basis of two different criteria (occurrence frequency and C.R.I.) showed that the seven most relevant configurations proposed by ISO 13232 (ISO (2005)) are not completely representative of the European context. Therefore, to develop passive safety devices in the European area, the use of the ISO 13232 standard may not be appropriate. The Los Angeles and Hannover data (ISO 13232 databases) were considered to be representative of a worldwide context but, probably, they are too specific of those areas. On the contrary, MAIDS (MAIDS (2009)) database was created collecting data from five different European countries and several cities.

In ISO 13232 six configurations were selected based on occurrence frequencies (114, 143, 413, 414, 412 -configuration 413 was considered twice with different impact speeds-); configuration 711 (ranked fourth according to frequency) was discarded without a clear motivation; the seventh configuration, 225, was chosen based on considerations related to previous research on leg protectors, and on the physical exposure of the lower leg in the scenario. In figure 5.2 the seven-impact configurations chosen by ISO 13232 are boxed. The analyses performed in this work supported the definition of a new set of impact configurations, representative of the European area and based on C.R.I. ranking. The initial proposal was: 313, 115, 312, 114, 314, 711, and 413 in descending order of relevance. Three out of seven configurations are very similar (313, 312 and 314), differing only for the RHA.

The fifth and eighth configurations (314 and 512 respectively) were discarded in favour of the configuration 143 (ninth). This choice was made on the basis of the following considerations. Since configurations 312 and 314 are mirrored configuration to the normal of the OVs side (same MC and OV contact points but different RHA), configuration 314 was considered too close at 312 and 313. Furthermore, the presence of the configuration 114, among those selected, can ensure a good evaluation of the rider's impacts against the car bonnet and the wind-shield. Regarding the configuration 512, also in this case it is very similar to the another configuration presents in the set. Indeed, between 512 and 312 only the OV impact point changes, and furthermore, the difference in CRI values with configuration 143 is practically negligible. For this reason it was preferred to consider, seen the vehicles layout, the configuration 143.

Taking into account the appropriate considerations expressed by the ISO 13232 on the importance of configuration 225 to test leg protection devices, in the newly proposed set of configurations 115, 711 (not present in the ISO 13232 set) and 314 were included, and they were reputed a suitable replacement for this scope. Configuration 225, not significant based on C.R.I. processing of MAIDSdata, may be employed as a preferential configuration for further testing specific leg protector devices. Previous considerations led to the following proposed set of most relevant configurations for initial development and testing of protective devices: 313, 115, 312, 114, 711, 413 and 143. The latter impact configurations are boxed in figure 5.10. In conclusion, only three out of seven configurations are in common between the ISO 13232 set and the new set of configurations defined in this study. The new set is reputed more representative than the one proposed by the ISO 13232, because it considers all five possible RHAs (ranging from 0° and 180°) and it takes into account configurations 711 and 115. The latter configurations were discarded by ISO 13232, but the MAIDS data had proven their relevance as accident scenarios.

5.3 Definition of the impact configurations speed pairs

To thoroughly define impact configurations as done in the ISO 13232 (ISO (2005)), speed pairs need to be specified. The ISO 13232 considered some practical limiting factors to define its selection criteria, which should be revised based on the technological progress. In the specific, ISO 13232 (ISO (2005)) based the choice of OV and MC speeds on a combination of statistical and practical factors. Among the practical factors the facts are:

- some test facilities can only perform moving-moving tests where there is an integer speed ratio between MC and OV speeds (e.g., 2:1, 1:2, etc.);
- in the absence of active rider's control impacts involving low MC speeds (6,7 m/s or less), are very difficult to do, because of large variations in MC roll angle at these speeds. These variations tend to reduce repeatability.

For these reasons, the selected speed combinations were limited to those ones with integer OV/MC speed ratios, and MC speeds either equal to zero or greater than 6,7 m/s. After 21 years since the first release of ISO 13232 (the 2005 update did not matter the speed pairs definition), it is reasonable to consider that the practical limiting factors considered by the standard can be neglected. For this reason, the approach used to define the speed pairs, was based only on statistical factors. The difficulty of this activity was to define a consistent criterion, which would allow to order the physically possible speed pairs (for each impact configuration), on the basis of their dangerousness. With this rationale an index (*SDI* - Speed Damage Index -) was proposed (equation 5.2).

$$Speed\ Damage\ Index_{(x,y)} = \left(\frac{\sum_{i=1}^{n} \left(I_{(x,y,AISi)} \right) \cdot i}{I_{(x,y)}} \right) \qquad \text{n=6}, \qquad (5.2)$$

Where:

- x: configuration code,
- y: speed pair code (i.e. 0-9.8, 6.7-13.4),
- i: AIS level (from 1 to 6),
- $I_{(x,y,AISi)}$: number of injuries for configuration x, speed pair y and for AISi level,

- $I_{(x,y)}$: total number of injuries for a specific impact configuration and speed pair.

To better understand equation 5.2, in table 5.1 is listed an example for impact configuration 114 and speed pair equal to 0-6.7 m/s.

Table 5.1: Example of *SDI* computation.

Impact configuration (x)	Speed pair (y)	Injuries with AIS=1	Injuries with AIS=2	Injuries with AIS=3	Injuries with AIS=4	Injuries with AIS=5	Injuries with AIS=6	Total Injury ($I_{(x,y)}$)	*Speed Damage Index*
114	0-6.7	5	6	0	0	0	0	11	1.545

Extending the *Speed Damage Index* calculation at each speed pair, it was possible to define a table for each impact configuration (table 5.2). In the first column, it is reported the number of events for each speed pair (second column). In the third column the corresponding value of the *SDI* is shown. To select a single speed pair for each impact configuration, an objective procedure generally applicable to any database and based on four steps was defined:

1. for each impact configuration: sort the *SDI* in descending order (and their respective speed pairs),
2. identify the *SDI* median value,
    - if the *SDI* median value is unique (odd number of valid speed pairs or no combination of more than one speed pair with the same *SDI*), the corresponding speed pair is considered valid.
    - if the *SDI* median value is not unique, it is necessary to pass to step (3).
3. multiply the ambiguous *SDIs* for the number of events occurred for each specific speed pair. This defines another index (for the sake of convenience, it was called Combined index given that it considers injury and frequency),
    - if the Combined index value is unique, the corresponding speed pair is considered valid.
    - if the Combined index value is not unique, it is necessary to consider step (4).
4. select the speed pair with the highest PTW speed.

In table 5.2 the data related to the 114 impact configuration are shown: the cells with at least one valid event for the specific speed pair are highlighted (in light green). In this case, the *SDI* median value is unique, and the relative row is coloured in dark green. As it is possible to note, in the *SDI* median value determination, the speed pairs with no valid records were neglected.

In the other tables (5.3 to 5.8), the results are reported for the other six relevant impact configurations determined on the basis of the C.R.I. and the subsequent considerations. The rows highlighted in pink identify the impact speed pairs discarded by the ISO 13232 (impossible configurations).

Table 5.2: 114 speed pair decision table.

114 impact configuration			
Number of events	Speed pair	*Speed Damage Index*	Combined Index
1	9,8-9,8	4.000	
1	0-13,4	2.000	
1	0-20,1	2.000	
1	9,8-20,1	2.000	
1	6,7-20,1	1.846	
4	0-9,8	1.667	
5	0-6,7	1.545	
2	6,7-13,4	1.333	
4	6,7-9,8	1.182	
3	6,7-6,7	1.000	
1	9,8-6,7	1.000	
0	6,7-0	0.000	
0	9,8-0	0.000	
1	9,8-13,4	0.000	
0	13,4-0	0.000	
0	13,4-6,7	0.000	
0	13,4-9,8	0.000	
0	13,4-13,4	0.000	
0	13,4-20,1	0.000	
0	20,1-0	0.000	
0	20,1-6,7	0.000	
0	20,1-9,8	0.000	
0	20,1-13,4	0.000	
0	20,1-20,1	0.000	

Table 5.3: 143 speed pair decision table.

143 impact configuration			
Number of events	Speed pair	*Speed Damage Index*	Combined Index
1	13,4-0	2.000	
2	9,8-0	1.667	
1	6,7-9,8	1.375	
2	9,8-13,4	1.375	
2	13,4-6,7	1.333	
2	6,7-13,4	1.250	
3	20,1-9,8	1.167	
1	9,8-9,8	1.125	
2	6,7-6,7	1.000	
0	0-6,7	0.000	
0	0-9,8	0.000	
0	0-13,4	0.000	
0	0-20,1	0.000	
0	6,7-0	0.000	
0	6,7-20,1	0.000	
0	9,8-6,7	0.000	
0	9,8-20,1	0.000	
0	13,4-9,8	0.000	
0	13,4-13,4	0.000	
0	13,4-20,1	0.000	
0	20,1-0	0.000	
1	20,1-6,7	0.000	
0	20,1-13,4	0.000	
0	20,1-20,1	0.000	

Table 5.4: 115 speed pair decision table.

115 impact configuration			
Number of events	Speed pair	*Speed Damage Index*	Combined Index
2	9,8-9,8	3.250	
5	20,1-20,1	2.700	
1	13,4-9,8	2.200	
1	0-6,7	2.000	
3	6,7-6,7	2.000	
3	6,7-20,1	1.750	
1	0-9,8	1.667	
1	0-20,1	1.600	
1	9,8-13,4	1.500	
1	9,8-20,1	1.500	
2	6,7-13,4	1.250	
3	9,8-6,7	1.071	
1	6,7-9,8	1.000	
0	0-13,4	0.000	
0	6,7-0	0.000	
0	9,8-0	0.000	
0	13,4-0	0.000	
0	13,4-6,7	0.000	
0	13,4-13,4	0.000	
0	13,4-20,1	0.000	
0	20,1-0	0.000	
0	20,1-6,7	0.000	
0	20,1-9,8	0.000	
0	20,1-13,4	0.000	

Table 5.5: 711 speed pair decision table.

711 impact configuration			
Number of events	Speed pair	*Speed Damage Index*	Combined Index
1	0-20,1	3.000	
1	9,8-13,4	3.000	
1	6,7-20,1	2.375	
3.000	0-13,4	1.400	4.200
9.000	0-6,7	1.273	11.455
3	6,7-13,4	1.250	
2	0-9,8	1.000	
4	6,7-9,8	1.000	
0	6,7-0	0.000	
0	6,7-6,7	0.000	
0	9,8-0	0.000	
0	9,8-6,7	0.000	
0	9,8-9,8	0.000	
0	9,8-20,1	0.000	
0	13,4-0	0.000	
0	13,4-6,7	0.000	
0	13,4-9,8	0.000	
0	13,4-13,4	0.000	
0	13,4-20,1	0.000	
0	20,1-0	0.000	
0	20,1-6,7	0.000	
0	20,1-9,8	0.000	
0	20,1-13,4	0.000	
0	20,1-20,1	0.000	

Table 5.6: 413 speed pair decision table.

413 impact configuration

Number of events	Speed pair	*Speed Damage Index*	Combined Index
1	0-13,4	2.000	
1	0-20,1	1.800	
2	6,7-20,1	1.778	
1	6,7-13,4	1.750	
2	9,8-6,7	1.600	
4	0-9,8	1.333	
2	9,8-9,8	1.250	
2	0-6,7	1.200	
2	6,7-9,8	1.167	
0	6,7-0	0.000	
0	6,7-6,7	0.000	
0	9,8-0	0.000	
0	9,8-13,4	0.000	
0	9,8-20,1	0.000	
0	13,4-0	0.000	
0	13,4-6,7	0.000	
0	13,4-9,8	0.000	
0	13,4-13,4	0.000	
0	13,4-20,1	0.000	
0	20,1-0	0.000	
0	20,1-6,7	0.000	
0	20,1-9,8	0.000	
0	20,1-13,4	0.000	
0	20,1-20,1	0.000	

Table 5.7: 313 speed pair decision table.

313 impact configuration

Number of events	Speed pair	*Speed Damage Index*	Combined Index
2	20,1-13,4	2.500	
2	13,4-6,7	2.375	
4	6,7-13,4	2.000	
10	0-9,8	1.758	
2	6,7-20,1	1.692	
1	0-20,1	1.667	
2	20,1-6,7	1.500	
8	0-6,7	1.400	
7	6,7-9,8	1.333	
3	6,7-6,7	1.250	
2	9,8-6,7	1.143	
0	0-13,4	0.000	
0	6,7-0	0.000	
0	9,8-0	0.000	
1	9,8-9,8	0.000	
0	9,8-13,4	0.000	
0	9,8-20,1	0.000	
0	13,4-0	0.000	
0	13,4-9,8	0.000	
0	13,4-13,4	0.000	
0	13,4-20,1	0.000	
0	20,1-0	0.000	
0	20,1-9,8	0.000	
0	20,1-20,1	0.000	

Table 5.8: 312 speed pair decision table.

312 impact configuration

Number of events	Speed pair	*Speed Damage Index*	Combined Index
5	6,7-6,7	2.000	
1	6,7-20,1	2.000	
1	13,4-13,4	2.000	
3	0-13,4	1.917	
1.000	0-20,1	1.833	1.833
4.000	6,7-9,8	1.429	5.714
6	0-9,8	1.313	
6	6,7-13,4	1.286	
3	0-6,7	1.000	
1	20,1-6,7	1.000	
0	6,7-0	0.000	
0	9,8-0	0.000	
0	9,8-6,7	0.000	
0	9,8-9,8	0.000	
0	9,8-13,4	0.000	
0	9,8-20,1	0.000	
0	13,4-0	0.000	
0	13,4-6,7	0.000	
0	13,4-9,8	0.000	
0	13,4-20,1	0.000	
0	20,1-0	0.000	
0	20,1-9,8	0.000	
0	20,1-13,4	0.000	
0	20,1-20,1	0.000	

Regarding the seven impact configurations just reported, only in 711 and 312 configurations the use of the second selection criterion, reported in the previous procedure, was necessary. Indeed, in both cases there is an ambiguity between two pairs (highlighted in yellow). In this cases the simplicity of the definition of the speed pair as combination of number of events and *SDI* (Combined Index) is evident.

The speed pair, considered for these impact configurations, is relative to the highest combined index value and is highlighted in dark green. In table 5.9 the final impact configurations and their relative speed pairs are listed. These ones will be the seven configurations in which the new device (BSJ) will be tested.

Table 5.9: Final impact configurations and their relative speed pairs.

Impact configuration	**OV impact speed** *[m/s]*	**MC impact speed** *[m/s]*
114	0.0	9.8
143	13.4	6.7
413	9.8	6.7
711	0.0	6.7
115	0.0	9.8
313	0.0	20.1
312	6.7	9.8

Chapter 6

Assessment of BSJ effectiveness

For a more complete assessment of the new device (Belted Safety Jacket), six new impact scenarios and one already proposed, but with different vehicle speeds, were simulated. For each of these new configurations, a comparison of biomechanical indexes with and without the device fitted on the PTW-rider system, will be presented. Furthermore, a brief critical analysis of results and simulation frames will be carried out. In appendix A, for each configuration, all graphs relative to head acceleration, neck forces and moment, *Chest Deflection* and $V{*}C$, are reported.

6.1 Impact configuration 114 0/9.8

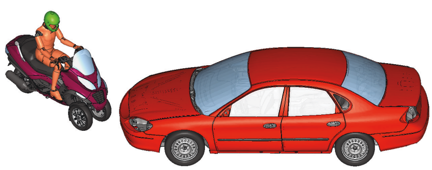

Figure 6.1: 114 vehicles relative position.

The first configuration analyzed was the 114 with stationary O.V. and moving PTW at 9.8 m/s. The frontal of the PTW impacts the frontal center of the car with a RHA of 135° (figure 6.1). In figure 6.2 the comparison of the first 200 ms simulation frames, are shown. It is possible to note that, during the initial 100 ms, the device is irrelevant on the dummy position, but the restraint cable (rear of rider) and the vest are already stretched.

At 150 ms the first effects of the device presence are visible. The dummy position begins to be different especially in terms of neck inclination and vertical location of the pelvis. The device slowing down action, combined with the head/helmet inertia causes the neck flexion, while without the device the neck was extended. This behaviour is clearly visible in figure A.20 in appendix A.

In the last frames of figure 6.2 this effect is even more evident. Figure 6.3 shows the final dummy position. Without the device, the rotation of the upper body is noticeable; head and feet are almost at the same height and furthermore, the dummy is completely out of the PTW shape. On the contrary, with the device,

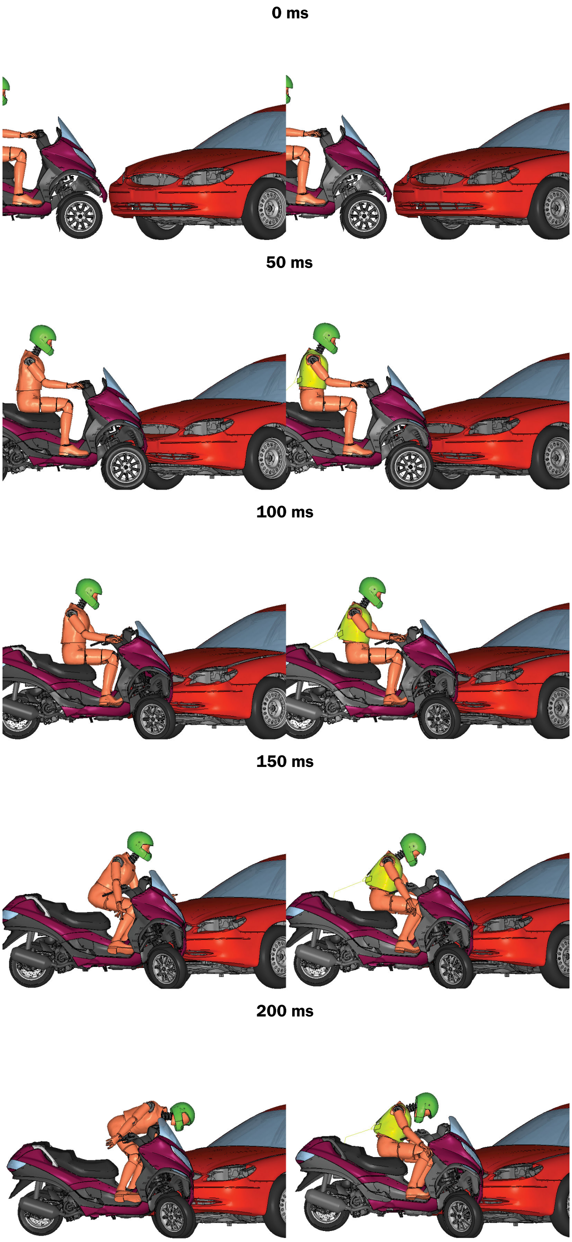

Figure 6.2: 114 simulation frames (W/O device on the left, with device on the right): 0-200 *ms*.

the dummy is still sitting, and its lateral displacement is very small. The latter result is very important because, in case of accident without BSJ, the rider would be exposed at secondary impact against the car bonnet or the ground. Furthermore, the final configuration exposes principally the head to further impacts, with possibility of serious injuries.

In table 6.1 the bio-mechanical injury indexes (with and W/O the device) are reported together with their relative variations compared to the configuration without the device. Although the configuration does not present particular problems also without the device (all values registered are lower than the limits), the BSJ is able to further reduce values of the bio-mechanical indexes (table 6.1). The head collision with the O.V. is also listed in the bottom part of the table. In both cases (W/O and with the device) no direct head impact against the car occurred. In appendix A subsection A.2.1, the graphs relative to dynamic actions acting on head and neck, and the *Chest Deflection* and *V*C* trends, are reported.

Table 6.1: Comparison of 114 0/9.8 impact configuration: bio-mechanical injury indexes (with and W/O the device), their relative variations and head impact event.

Biomechanical Index	W/O	With	Limit	Δ value
HIC	111	64	1000	−42.3%
$\boldsymbol{N_{ij}}$	0.30	0.11	1.00	−63.3%
Chest Deflection [mm]	4.83	3.14	50.00	−35.0%
V*C [m/s]	0.02	0.01	1.00	−50.0%

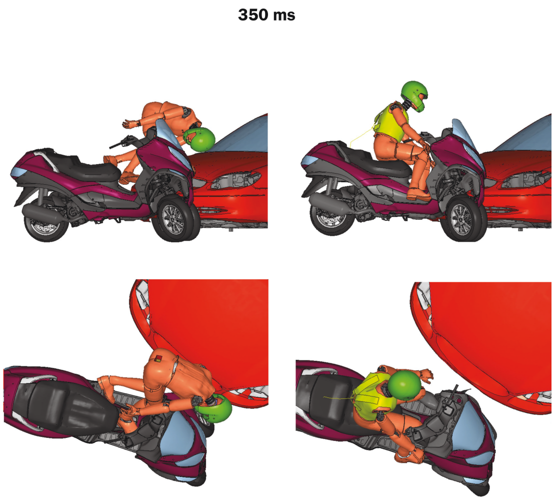

Figure 6.3: 114 simulation frames: final dummy position (W/O device on the left, with device on the right).

6.2 Impact configuration 143 13.4/6.7

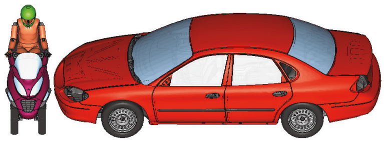

Figure 6.4: 143 vehicles relative position.

This impact configuration represents: moving O.V. at 13.4 m/s and a moving PTW at 9.8 m/s. The Opposing Vehicle impacts the centre of the left lateral side of the PTW with a RHA of 90° (figure 6.4).

Figure 6.5 shows the initial 200 ms of the simulation frames. As already seen in the previous impact configuration, in the first 100 ms the device does not influence the dummy position. On the contrary, starting from 150 ms, some differences, especially in the upper part of the dummy body are evident: without the device, the head and the thorax are rotated compared to the legs, which are locked by the car. At 200 ms the dummy position results completely different. In this phase, the device seems to be able to limit the body lateral rotation. This effect results more visible in the last frames, where the dummy on the left is practically parallel to the ground.

On the other hand, in presence of the device, the dummy body is in contact with the bonnet, even if the motorcycle displacement seems to drag the dummy. For this type of impact the prolonged presence of the cable could be harmful in the second part of the impact. The final positions of the dummies are shown in figure 6.6. The frames on the left highlight a body position completely exposed to secondary head and shoulders impact against the ground. With the device other impacts with the car bonnet may probably occur.

In table 6.2 the bio-mechanical injury indexes are listed. *HIC* experiences the most sharp decrease: the value passes from 845 to 263 with a reduction of 68.87%. This decrease is particularly important because the *HIC* value without the device is very close to the limit. Regarding the other indexes the changes are hardly significant especially for the Viscous Criterion, which is very far from the limit.

Table 6.2: Comparison of 143 13.4/6.7 impact configuration: bio-mechanical injury indexes (with and W/O the device), their relative variations and head impact event.

Biomechanical Index	W/O	With	Limit	Δ value
HIC	845	263	1000	−68.9%
N_{ij}	0.30	0.27	1.00	−10.0%
Chest Deflection [mm]	5.49	2.57	50.00	−53.2%
V*C [m/s]	0.018	0.024	1.00	+33.3%

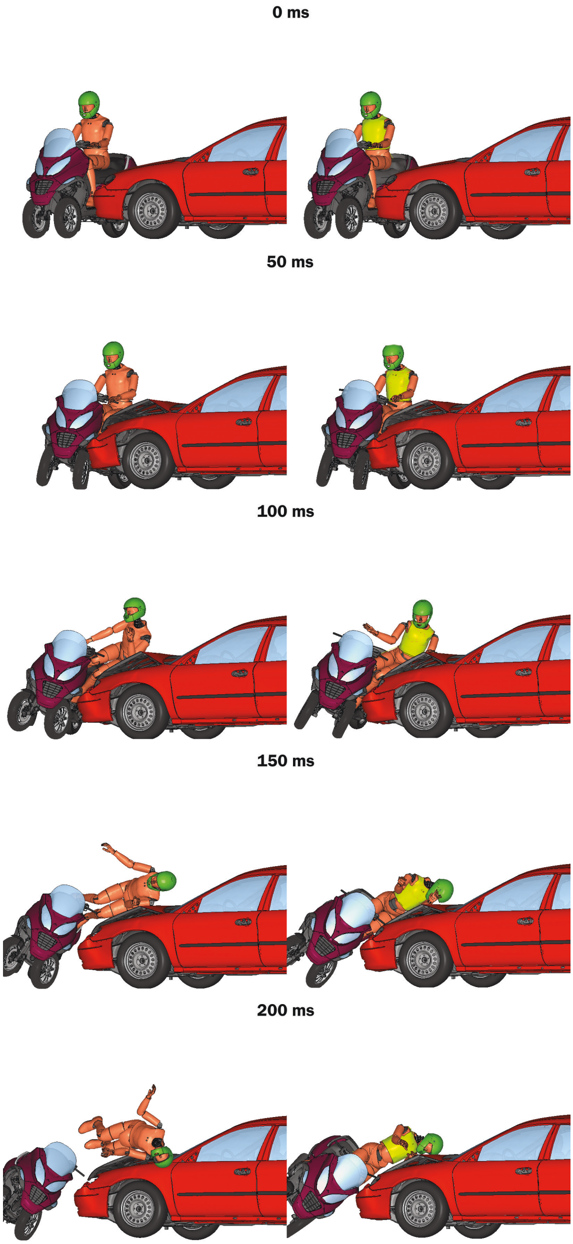

Figure 6.5: 143 simulation frames (W/O device on the left, with device on the right): 0-200 *ms*.

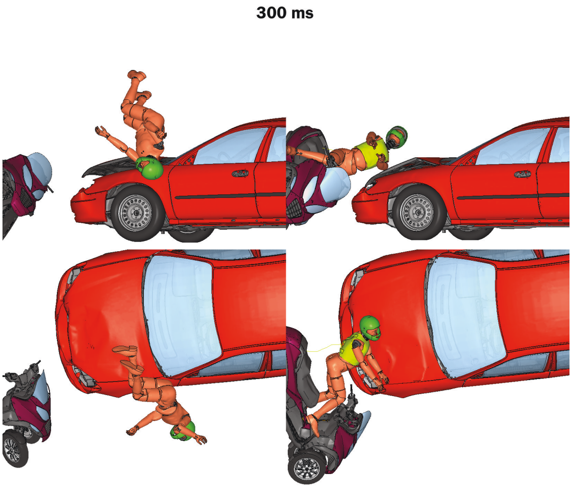

Figure 6.6: 143 simulation frames: final dummy position (W/O device on the left, with device on the right).

6.3 Impact configuration 413 9.8/6.7

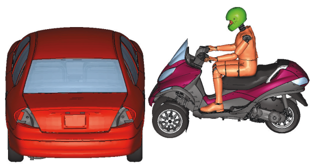

Figure 6.7: 413 vehicles relative position.

The configuration 413, shown in figure 6.7, was already described in chapter 4. In this analysis both impact speeds are changed. In the specific, the O.V. speed was increased from 6.7 *ms* to 9.8 *ms*, while the MC speed was halved. Analysing the simulation frames of figure 6.8, it is possible to see big differences in dummy displacements. Without the device the rider's model loses the contact with the PTW, and it is projected towards the car.

On the contrary, with the device fitted on the motorcycle, the dummy keeps a good position for the duration of the simulation. As in the previous configurations, the device presence and its retentive action increase the neck flexion. Despite this behavior, the N_{ij} is reduced by over 31% (table 6.3). From figure 6.9, it is possible to understand that in this specific vehicles configuration, the dummy head impact against the car is avoided (without device), only because the car speed is higher that the PTW speed. Otherwise, as seen in chapter 4, the dummy would hit the car.

Although the head impact was avoided, the tables 6.3 shows that the *HIC* index is substantially higher without the device. The Belted Safety Jacket reduces the *HIC* by 71%, even if the *HIC* value registered without the device is too far from its limit. Probably, in presence of another type of OV (e.g. a minivan), without device, the bio-mechanical indexes would be higher than in this case. Indeed, in presence of a higher and longer vehicle, probably the dummy would impact against its rear part. Regarding the *Chest Deflection* and *V*C*, the decrease and the increase respectively are quite insignificant, if they are compared to the limits. However it is noticeable the absence of negative effects linked to the device use. For an in-depth analysis of the simulation, in appendix A subsection A.2.3, graphs of dynamic actions acting on neck and head are reported.

Table 6.3: Comparison of 413 9.8/6.7 impact configuration: bio-mechanical injury indexes (with and W/O the device), their relative variations and head impact event.

Biomechanical Index	W/O	With	Limit	Δ value
HIC	90	26	1000	−71.1%
N_{ij}	0.16	0.11	1.00	−31.3%
Chest Deflection [mm]	2.40	1.39	50.00	−42.1%
V*C [m/s]	0.005	0.013	1.00	+160.0%

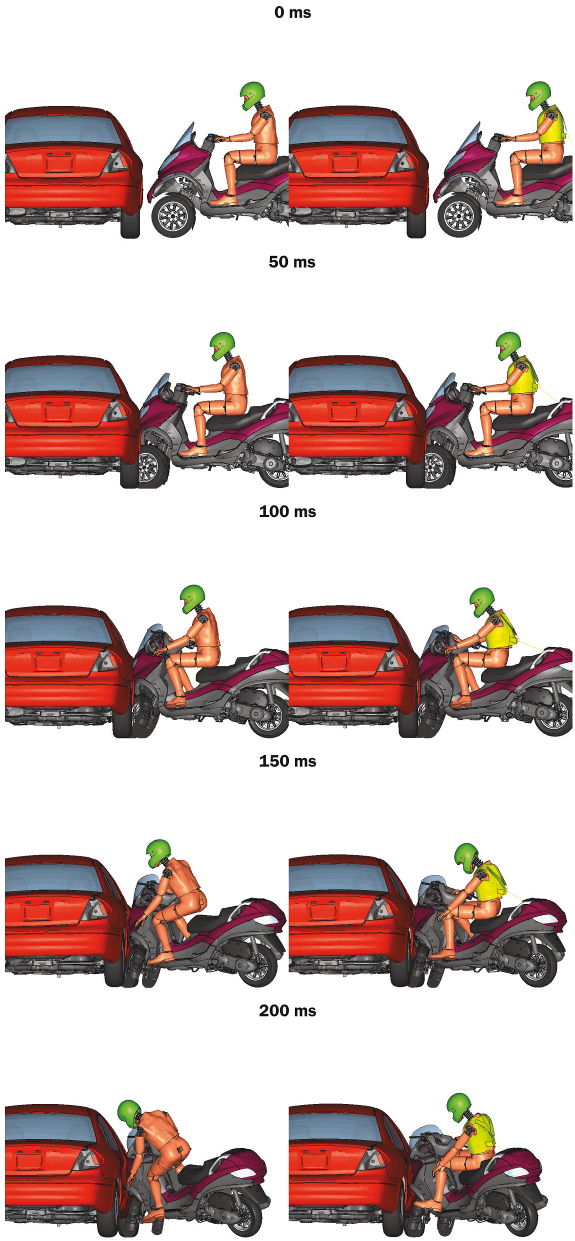

Figure 6.8: 413 simulation frames (W/O device on the left, with device on the right): 0-200 *ms*.

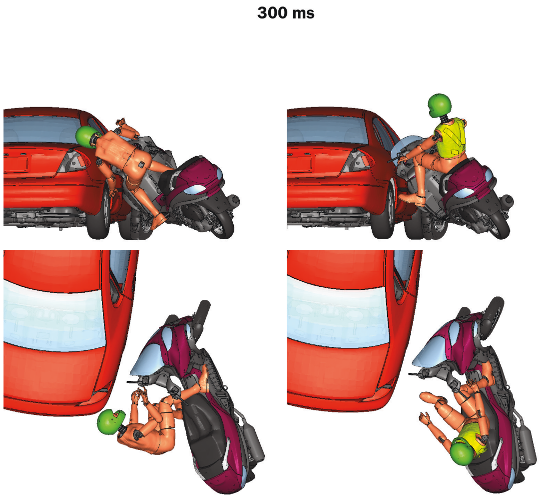

Figure 6.9: 413 simulation frames: final dummy position (W/O device on the left, with device on the right).

6.4 Impact configuration 711 0/6.7

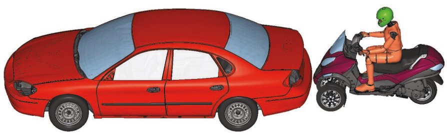

Figure 6.10: 711 vehicles relative position.

This is an impact configuration that was not present among those proposed by ISO 13232. It reproduces a classic rear-end collision, where the PTW hits against the car. In this particular case the vehicle speeds are very low, and the PTW proceeds at 6.7 m/s, while the car is stationary. This scenario is very common in real life. It represents an incomplete PTW stopping manoeuvre, where the PTW hits perpendicularly the OV rear bumper (figure 6.10).

In figure 6.11 it is possible to see, as already noted in other configurations that at 100 ms, even if the device stretches the restraint cable and the vest, this does not affect the dummy position. On the contrary at 150 ms the effect of the device presence is evident. In the configuration without the device, the dummy starts the typical frontal rotation in the sagittal plane, while, in presence of BJS this effect is avoided. On the other hand, the dummy experiences a more pronounced neck flexion due to the restraint force and this effect results more evident at 200 ms.

Another important difference is the lack of the thorax impact against the handlebar. In figure 6.12 the final position of the dummy is shown. Also in this case, where the relative impact speed is very low, the dummy loses the contact with the seat and its hands lose the contact with the handlebar, if it is not slowed down by the device. For this reason it is foreseeable that further injuries due to secondary impacts may occur. As previously announced, the bio-mechanical injury index variations (with and W/O the device), listed in table 6.4, are extremely limited, and also the largest changes, relative to *Chest Deflection* and *V*C*, are negligible if compared with the limits (the index values are a very long way from the limits).

Table 6.4: Comparison of 711 0/6.7 impact configuration: bio-mechanical injury indexes (with and W/O the device), their relative variations and head impact event.

Biomechanical Index	W/O	With	Limit	Δ value
HIC	48	45	1000	−6.3%
N_{ij}	0.11	0.12	1.00	+9.1%
Chest Deflection [mm]	4.68	3.44	50.00	−26.5%
V*C [m/s]	0.025	0.011	1.00	−56.0%

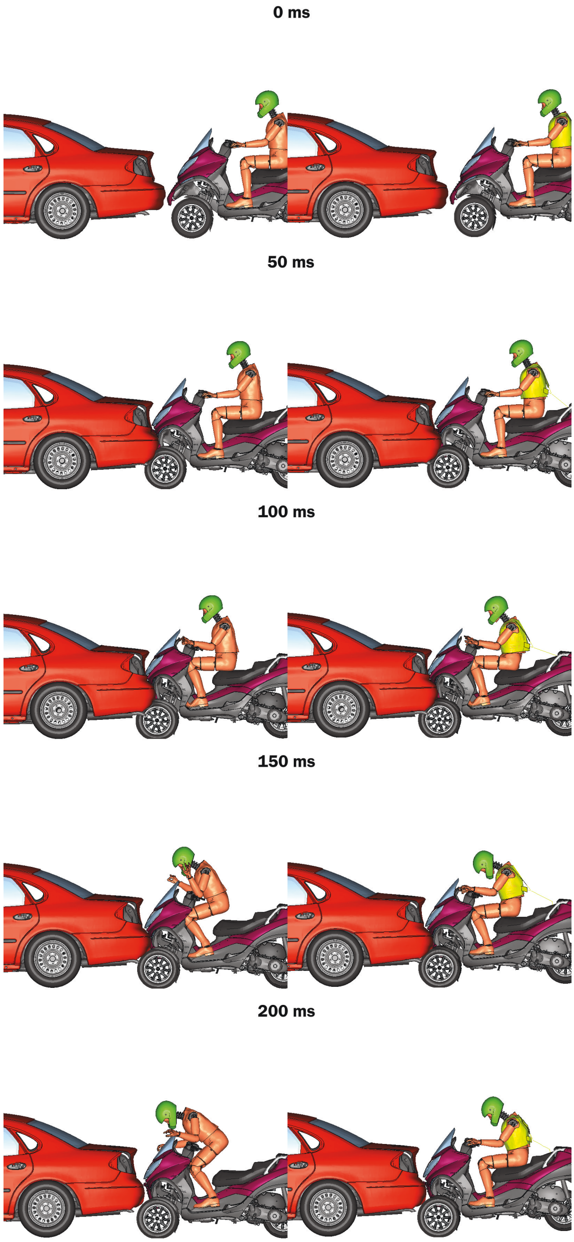

Figure 6.11: 711 simulation frames (W/O device on the left, with device on the right): 0-200 ms.

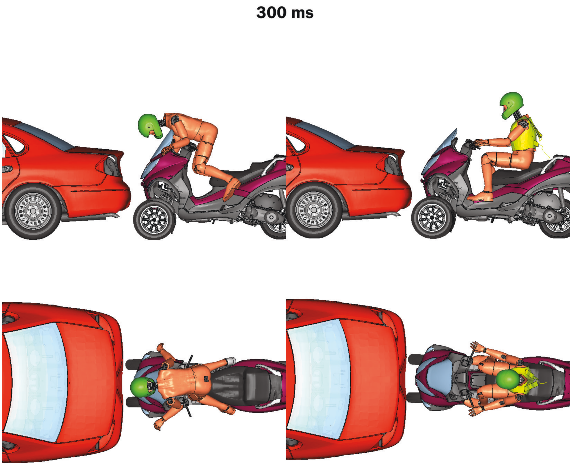

Figure 6.12: 711 simulation frames: final dummy position (W/O device on the left, with device on the right).

6.5 Impact configuration 115 0/9.8

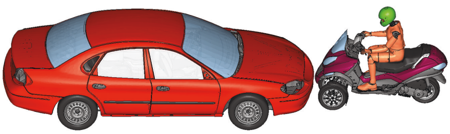

Figure 6.13: 115 vehicles relative position.

The 115 impact configuration represents a front end impact between the vehicles. Also this configuration is not present in the ones proposed by ISO 13232. In the simulation the PTW hits the car at 9.8 m/s while the car is in stationary position (figure 6.13). As it is possible to see in figure 6.14, the dummy behaviors (with and without the device) results very similar to that seen for the configuration 711. Indeed, the device presence avoids the chest impact against the handlebar, but it increases the neck flexion.

These qualitative considerations are supported by the graphs in section A.2.5. Even if, the head acceleration peak is higher in case of accident without the device, the *HIC* (listed in table 6.5) results increased of approximately 50%. The *HIC* registered value is still abundantly under the limit. Also the N_{ij} is increased of about 30%, due to the major dynamic actions like: shear force and bending moment acting on the neck.

On the other hand, a significant reduction of *Chest Deflection* and *V*C* (84.52 and 90.10 respectively) are registered. Furthermore, as already seen in other configurations, the final position of the dummy is considerably better in presence of the device (figure 6.15). Despite the limited impact speed, the dummy completely loses the initial seating position; it moves and turns forward, crossing over the handlebar and exposing the head to other impacts. With the device the final position is very similar to the initial.

Table 6.5: Comparison of 115 0/9.8 impact configuration: bio-mechanical injury indexes (with and W/O the device), their relative variations and head impact event.

Biomechanical Index	W/O	With	Limit	Δ value
HIC	60	92	1000	+53.3%
N_{ij}	0.12	0.16	1.00	+33.3%
Chest Deflection [mm]	18.35	2.84	50.00	−84.5%
V*C [m/s]	0.15	0.014	1.00	−90.1%

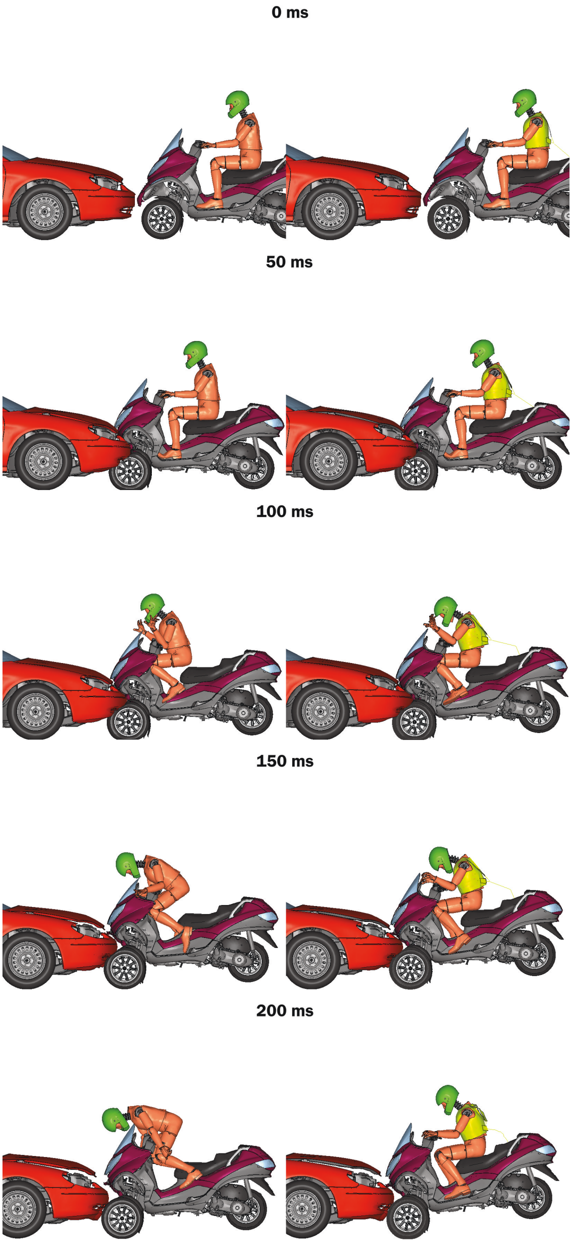

Figure 6.14: 115 simulation frames (W/O device on the left, with device on the right): 0-200 ms.

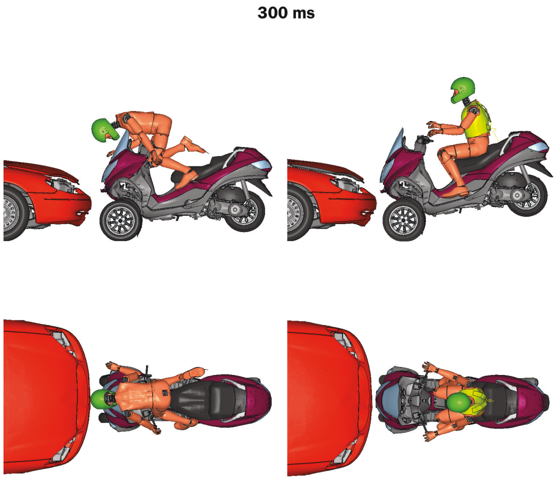

Figure 6.15: 115 simulation frames: final dummy positions (W/O device on the left, with device on the right).

6.6 Impact configuration 313 0/20.1

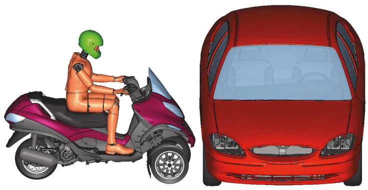

Figure 6.16: 313 vehicles relative position.

Configuration 313 provides a perpendicular front MC impact, at 20.1 *m/s*, on the frontal wheel of the stationary car (figure 6.16). The MC impact speed is the highest within the set of configurations and the impact is very severe. In figure 6.17 the first 150 *ms* of the simulation frames are shown.

In both configurations of the scenario the upper part of the dummy violently hits against the motorcycle wind-shield. In the simulation without the device, the neck crashes almost perpendicularly against the wind-shield. In this case the dynamic actions on the neck are very high (figure A.48, figure A.49 and figure A.20 in appendix A). This entails big deformations of neck mesh and the simulation was stopped by the solver during the detachment phase between the dummy and the PTW. Even if the simulation was not completed, the graphs extracted show that the fundamental part of the simulation impact occurred and its relative information are available. Naturally, looking at the frames, at the impact point and at the *HIC* value, it is clear that any other subsequent values, relative to the neck, could be affected by errors. Furthermore, the extracted data are complete to carry out a correct indexes evaluation. In this case, the *HIC* and the N_{ij} are higher than 7000 and 1.3 respectively. Also in the simulation with the device fitted on the motorcycle, the dummy hits against the wind-shield, but in this case the face is the body part involved. Indeed, during the frontal displacement and the subsequent retention action, the helmet spins to the rear, exposing the face to the impact (figure 6.17). As listed in table 6.6, in this case the *HIC* was greatly reduced compared to the case without the device (more than 50%), but it remains largely above the limit. Differently, the N_{ij}, *Chest Deflection* and *V*C* were significantly reduced, and N_{ij}, thanks to the device, remains below the limit.

Regarding the final position of the dummy, the comparable information are limited to the initial 150 *ms* (just before the simulation without the device was stopped). However the configuration with the device was completed and at 150 *ms* no substantial differences between the two simulations were noticed. It is reasonable to think that the final motorcycle behaviours are comparable. In the final part of the impact, the motorcycle pitch was very high, and the motorcycle was almost perpendicular to the ground. With the device fitted on the PTW, the rider is still on the motorcycle, but it is no possible to predict what would happen later (figure 6.19).

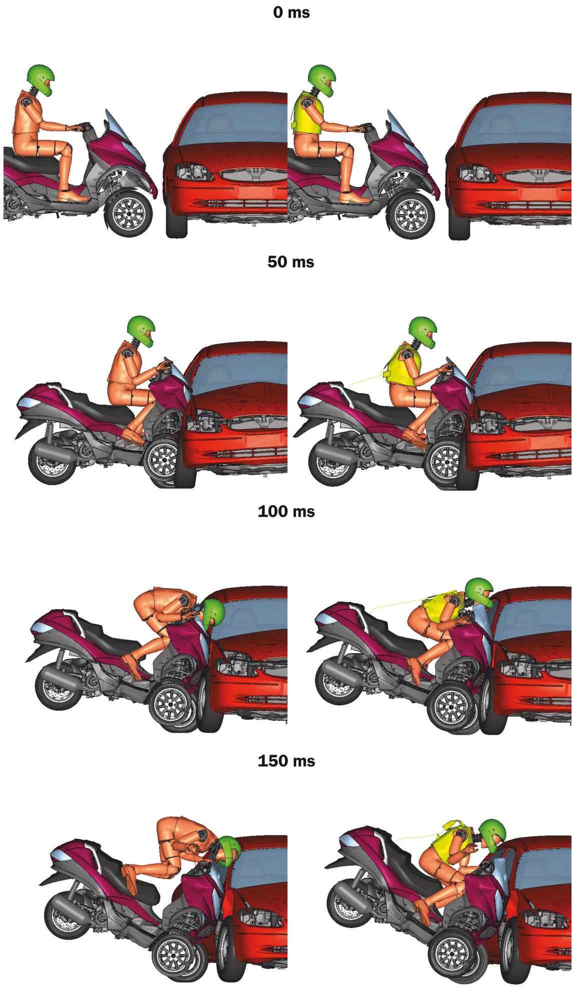

Figure 6.17: 313 simulation frames (W/O device on the left, with device on the right): 0-150 ms.

Table 6.6: Comparison of 313 0/20.1 impact configuration: bio-mechanical injury indexes (with and W/O the device), their relative variations and head impact event.

Biomechanical Index	W/O	With	Limit	Δ value
HIC	7753	3156	1000	−59.3%
N_{ij}	1.35	0.70	1.00	−48.2%
Chest Deflection [mm]	27.3	25.2	50.00	−7.7%
V*C [m/s]	0.41	0.39	1.00	−4.9%

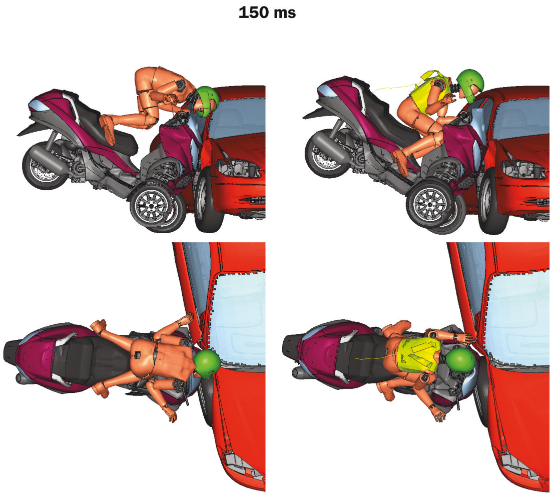

Figure 6.18: 313 simulation frames: final dummy position (W/O device on the left, with device on the right).

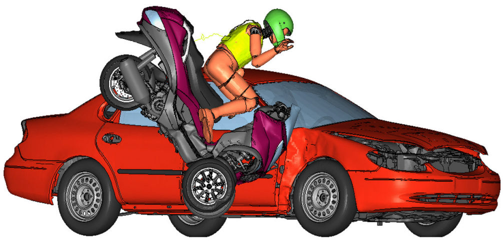

Figure 6.19: 313 simulation frames (300 ms): final dummy position with device.

6.7 Impact configuration 312 6.7/9.8

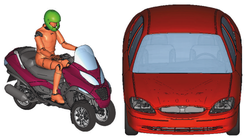

Figure 6.20: 312 vehicles relative position.

Impact configuration 312 is represented in figure 6.20. In this scenario, the PTW impacts at 9.8 m/s against the frontal right wheel of the car that travels at 6.7 m/s with an angle of 45° (figure 6.20). As it is possible to see from the frames of figure 6.21 (and confirmed by the injury indexes listed in table 6.7 and by the graphs in section A.2.7), the effectiveness of the device is almost negligible.

In this particular speeds configuration, the dummy lateral displacement without the device, is limited by the presence of the car. For this reason the performance of the device results limited. Regarding the injury indexes (table 6.7), *HIC* and *Chest Deflection* are practically unchanged with or without the device, while N_{ij} undergoes a substantial increase in presence of BSJ. Naturally, this effect is due to the device presence that restraints the rider after its impact with the car. Although the device presence results less significant, the final rider's position is certainly safer than without it (figure 6.22). Indeed, with the retention effect ensured by the device, both dummy lower limbs are within the PTW silhouette, ensuring a major protection of the rider's legs.

Table 6.7: Comparison of 312 6.7/9.8 impact configuration: bio-mechanical injury indexes (with and W/O the device), their relative variations and head impact event.

Biomechanical Index	W/O	With	Limit	Δ value
HIC	92	94	1000	+2.2%
N_{ij}	0.09	0.22	1.00	+144.4%
Chest Deflection [mm]	2.25	2.00	50.00	−11.1%
V*C [m/s]	0.018	0.004	1.00	−77.8%

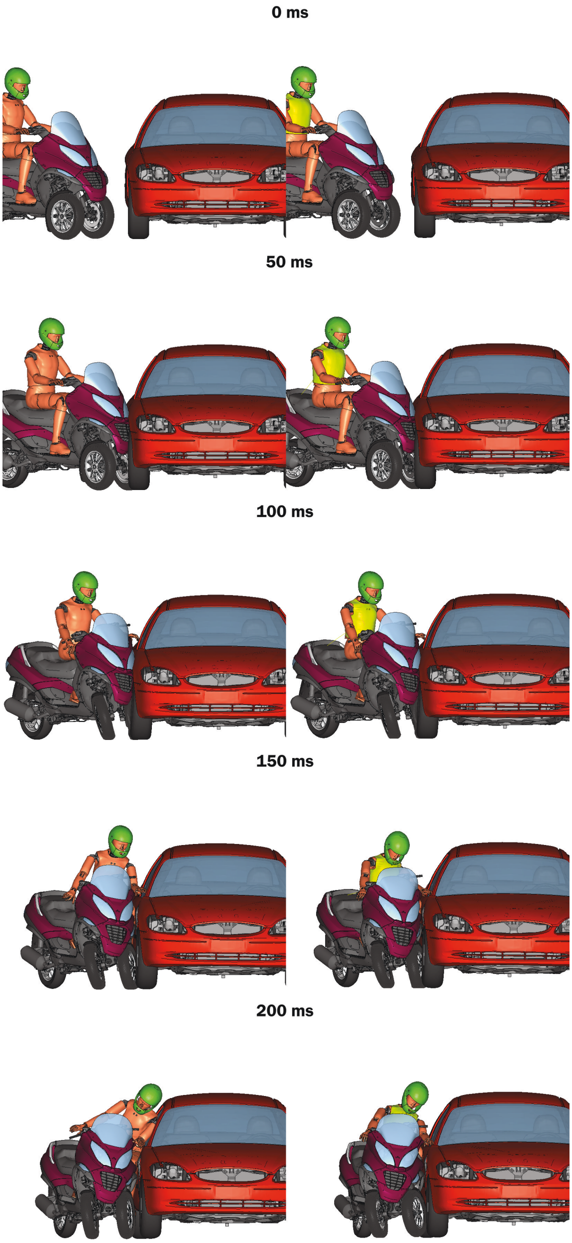

Figure 6.21: 312 simulation frames (W/O device on the left, with device on the right): 0-200 *ms*.

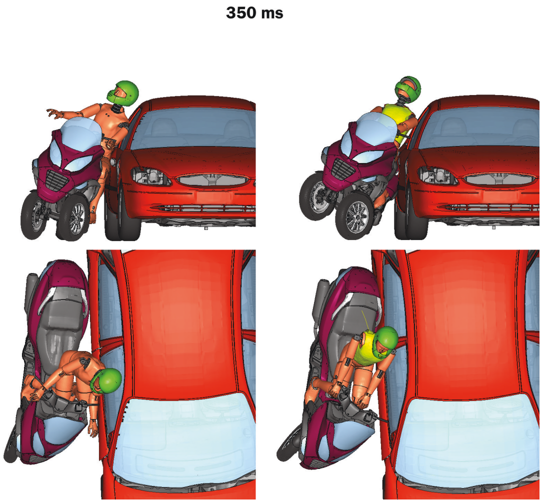

Figure 6.22: 312 simulation frames: final dummy position (W/O device on the left, with device on the right).

Conclusion

This research applied a structured design method to develop new solutions for riders' passive safety protection. In this regard, a map (Network of Problem) of possible answers to the problem, based on a problem-solving process, was realized: thirteen possible alternative solutions were identified. To assess all of them and to choose the best potential solution to be engineered, an on-line survey based on Kano's theory was created. Its results and the information from the state of the art on passive safety devices/systems allowed to extrapolate the product features to be implemented in order to increase the customer level of satisfaction.

By a combination of product features and other assessment criteria, the Weighted Sum Method established the order of the importance of the candidate solutions, from those, the Belted Safety Jacket was thus selected. The design, the characterization and the effectiveness of this solution was evaluated in a virtual environmental.

Based on previous studies the 413 6.7/13.4 ISO 13232 configuration was used for the initial assessment of the device. Bio-mechanical indexes derived from simulation results, demonstrated a good protective performance of the device; specifically, a significant mitigation of the bio-mechanical injury indexes relating to head and neck was reported. Differently, the chest was more loaded, although both chest deflection and Viscous Criterion results showed that no major trauma were reported by the dummy.

As a further step of the device development, a full factorial Design Of Experiment was implemented to understand possible correlations among the device characteristics and their interactions, and its retentive behaviour. The results show that the main effects of the independent variables of the response are less relevant than the ones of their interactions. Thus, high order terms are necessary to fit reality with a model (high ${R^2}_{adjt}$), that cannot be applied outside the variable ranges.

In addition, DOE results highlighted that the device was able, in any configuration, to avoid the dummy head impact against the car, and thus it reduced the head and neck injury indexes. The increase of the Chest Deflection and Viscous Criterion indexes was referred to the configuration without the safety device, although each value was always below the limits of acceptability. The device behaviour was robust enough to be insensitive to the change of the geometrical parameters. Thus its portability to other vehicles seems feasible. In conclusion, although the assessment was limited to a single impact configuration, the device significantly reduced the motorcyclist crash injuries. In order to confirm these results, the device was tested in other impact configurations.

This new set of seven accident configurations was defined by applying the procedure provided by the standard ISO 13232 to another motorcycle accident database (MAIDS). Integrating the results with a new proposed ranking method, the final set had only three configurations in common with those defined in the ISO 13232, testifying the importance of the research to define an updated and more representative set of configurations for the European context. Furthermore, in order to completely define the new set of configurations, a new objective speed pairs selection criterion was proposed. It was based exclusively on the statistical MAIDS data, and it allowed to overcome the practical constraints implemented in ISO 13232. The last part of the research focused on the device effectiveness assessment in the new set of scenarios

In general, even if, the seven impact configurations tested were not particularly inconclusive for the device testing, the Belted Safety Jacket was able to decrease the bio-mechanical injury indexes taken into account, especially the *HIC* and N_{ij} for the configurations 114, 143, 413 and 313. Contrary for the rear-end and head-on collisions (configuration 711 and 115 respectively), the device presence let to an increase of these indexes due to the restraint force. On the other hand, for these configurations, the device was able to avoid the chest impact against the handlebar, decreasing the *Chest Deflection* and *V*C* indexes. Except for the configurations 143 and 312, the device presence was able to ensure a more correct and safer final dummy position.

In all the assessed impact scenarios, except for 143 and 312, without the device, the dummy lost completely the contact with the seat, and its body frontal rotation, due to the legs impact against the handlebar, exposed the head, the neck and the shoulders to eventually secondary impact against the car or the ground. In configuration 313 the high MC speed made impossible to completely mitigate the impact consequences: indeed in both cases, with and without the device, the *HIC* value was far above the limit, while other indexes, with the BSJ were below the respective limits, especially N_{ij} which dropped below its limit. Regarding configuration 312, the very low relative speed between the vehicles made the presence of the device negligible; furthermore, the device resulted ineffective for the final dummy position, because the car side limits the free dummy displacement.

In conclusion the new device has shown a good behaviour for MC speeds ranging from 9.8 m/s to 13.4 m/s, while for lower speed in rear-end and head-on collisions, the restraint force is excessive and this creates forces and moment on the neck bigger than without the device. Even in these cases the device ensures a safer final dummy position avoiding the chest impact against handlebar.

To conclude, the impact configurations tested were a good base for a preliminary assessment of the device, but in view of the results obtained, only seven impact configurations are not sufficient to definitively establish its effectiveness. The two tests carried out for the configuration 413, with different impact speeds, showed substantial differences in the device behaviour and efficiency. Anyway, the results obtained so far are quite interesting and for this reason, further tests with different impact speeds and configurations are necessary to completely define its effectiveness. From the technological point of view, the definition of the de-touchable system between the vest and the restraint part of the device (seen during the device design activity) represents a fundamental step for the future device development. Finally, it could be interesting to evaluate the device possible integration with other safety systems, to ensure a greater safety level of protection.

Appendix A

Graphs

A.1 Survey outcomes: Device features

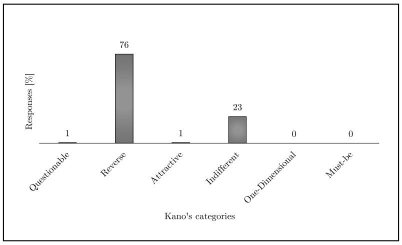

Figure A.1: Influence on motorcycle aesthetic.

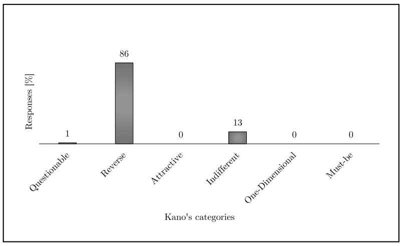

Figure A.2: Comfort limitation.

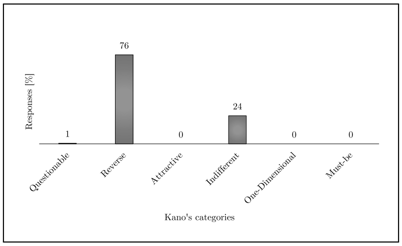

Figure A.3: Influence on PTW cost increase.

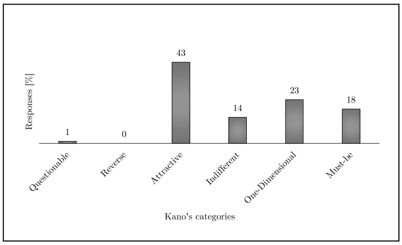

Figure A.4: Inexpensiveness (device cost).

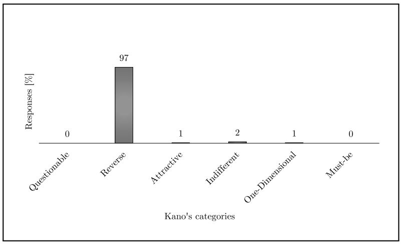

Figure A.5: Handling influence.

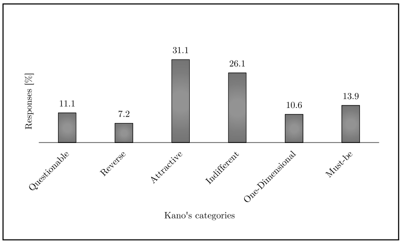

Figure A.6: Integrability on the PTW.

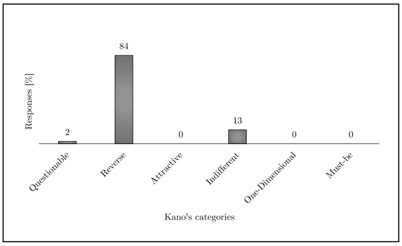

Figure A.7: Movements restriction.

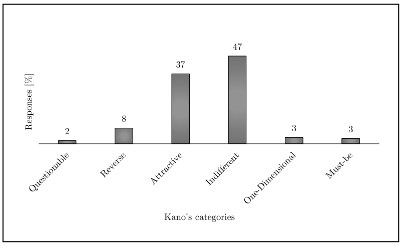

Figure A.8: Multimedia.

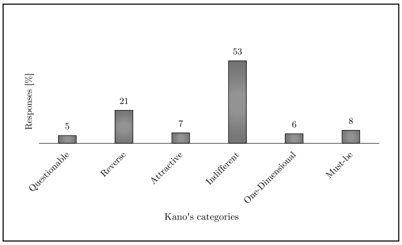

Figure A.9: Operation dependent on other devices.

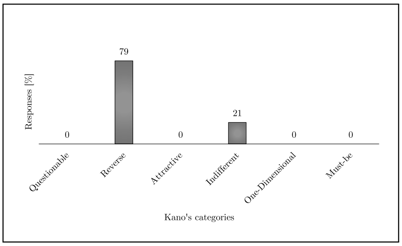

Figure A.10: Influence on performances.

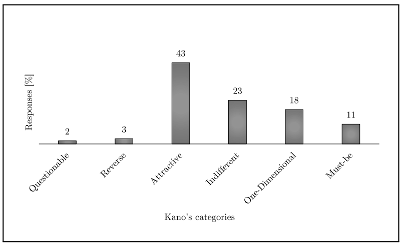

Figure A.11: Device Re-usability (after crash).

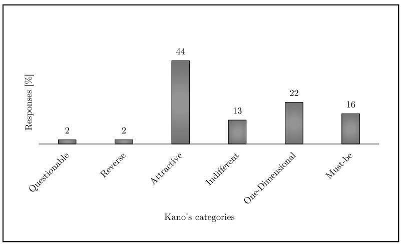

Figure A.12: Transferability on other PTWs.

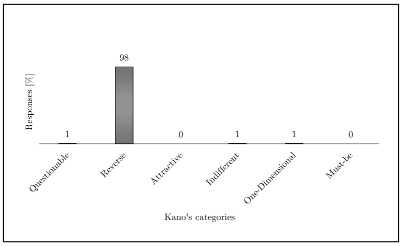

Figure A.13: Visibility limitation.

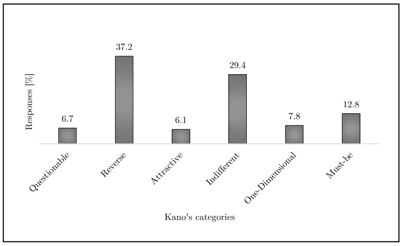

Figure A.14: Obligation to wear.

A.2 Impact configuration

A.2.1 Configuration 114 0/9.8

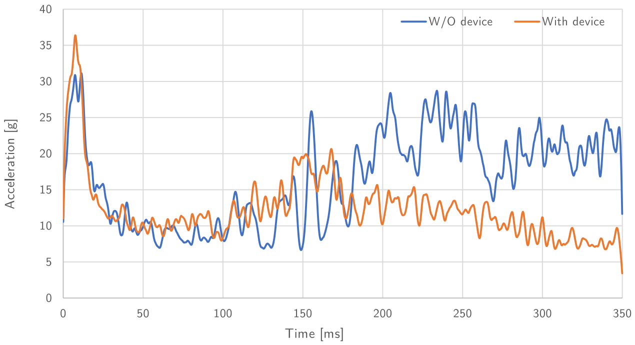

Figure A.15: Head acceleration.

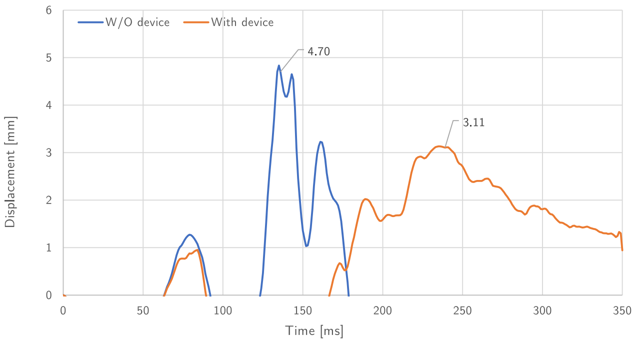

Figure A.16: Chest Deflection.

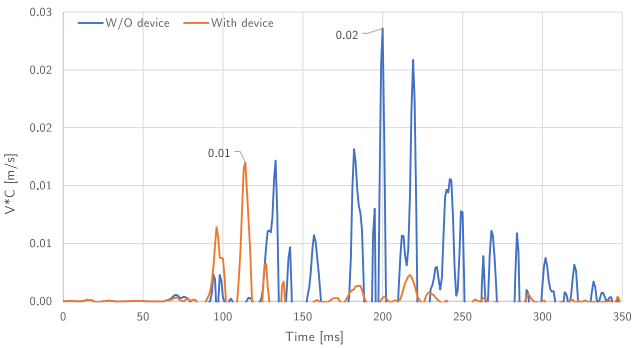

Figure A.17: Viscous Criterion.

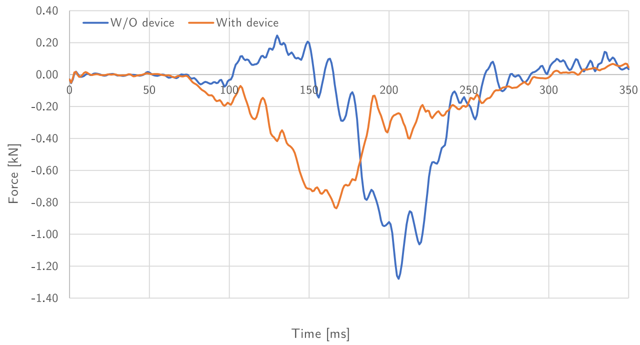

Figure A.18: Neck (X) Shear Force.

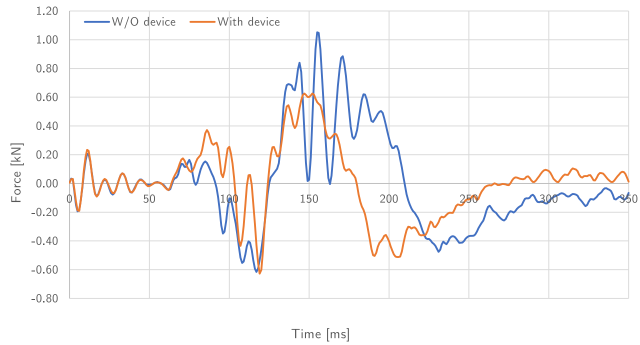

Figure A.19: Neck (Z) Axial Force.

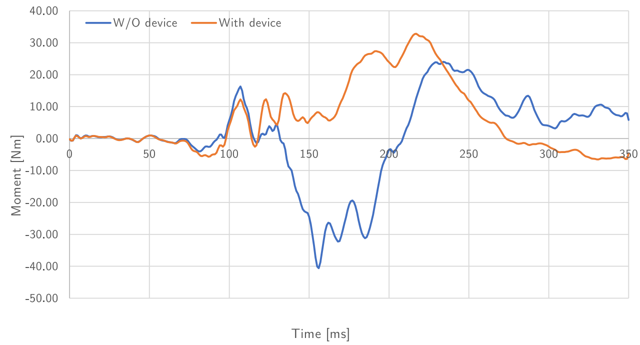

Figure A.20: Neck (Y) bending moment.

A.2.2 Configuration 143 13.4/6.7

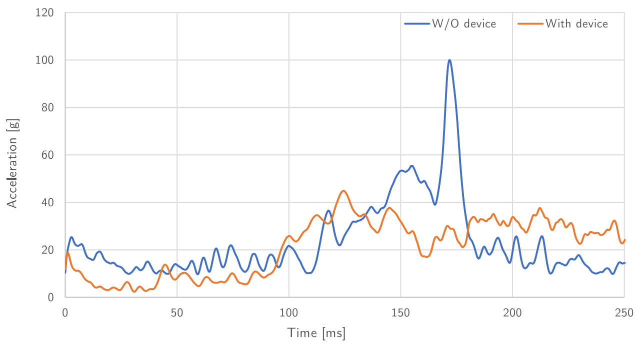

Figure A.21: Head acceleration.

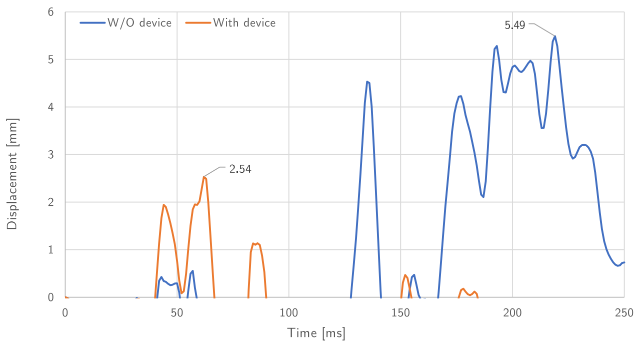

Figure A.22: Chest Deflection.

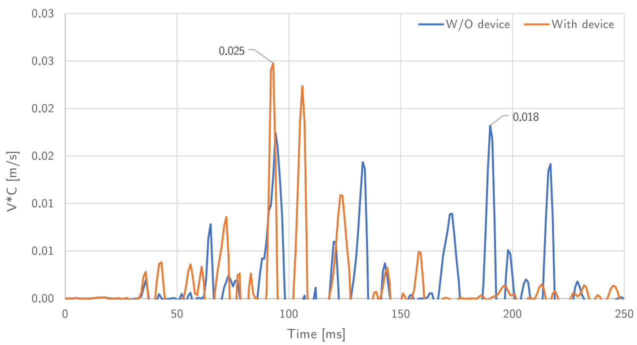

Figure A.23: Viscous Criterion.

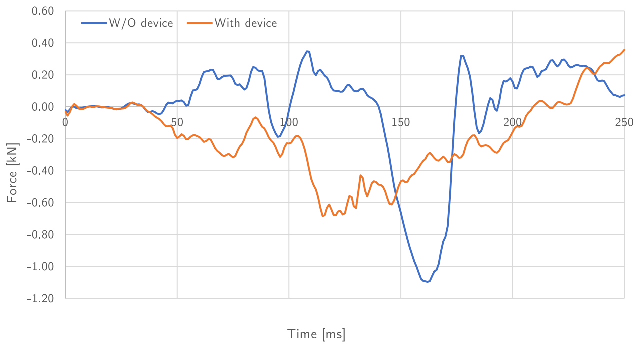

Figure A.24: Neck (X) Shear Force.

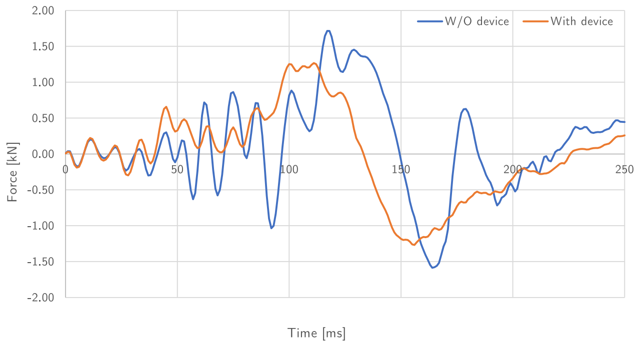

Figure A.25: Neck (Z) Axial Force.

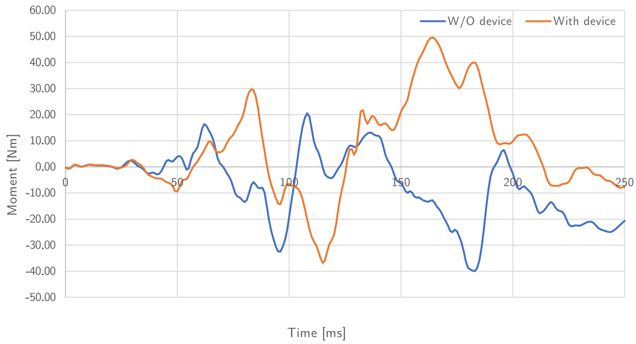

Figure A.26: Neck (Y) bending moment.

A.2.3 Configuration 413 9.8/6.7

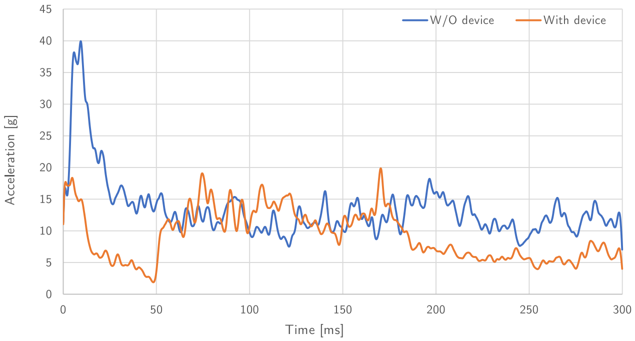

Figure A.27: Head acceleration.

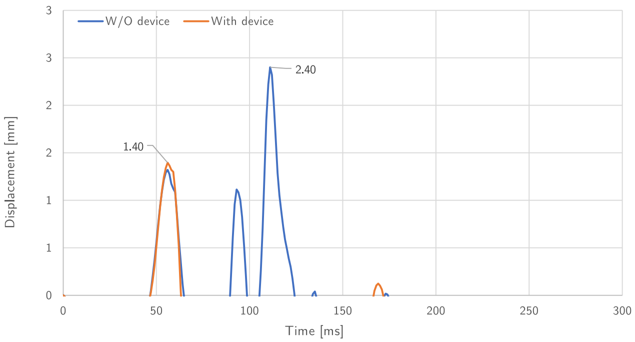

Figure A.28: Chest Deflection.

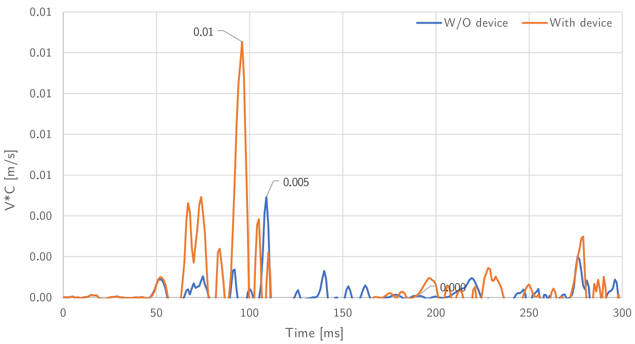

Figure A.29: Viscous Criterion.

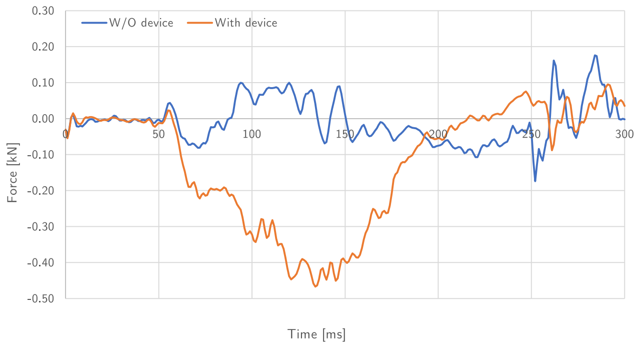

Figure A.30: Neck (X) Shear Force.

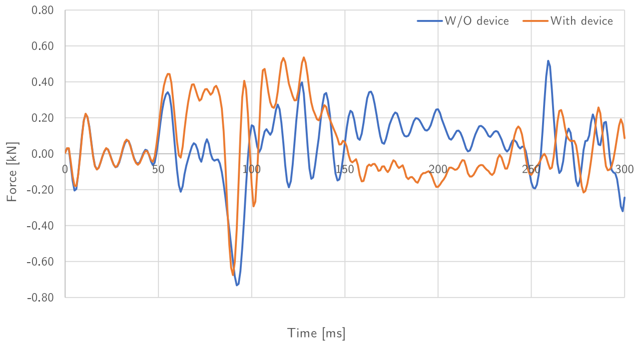

Figure A.31: Neck (Z) Axial Force.

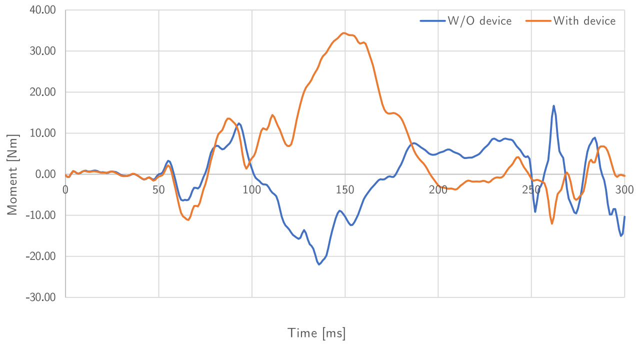

Figure A.32: Neck (Y) bending moment.

A.2.4 Configuration 711 0/6.7

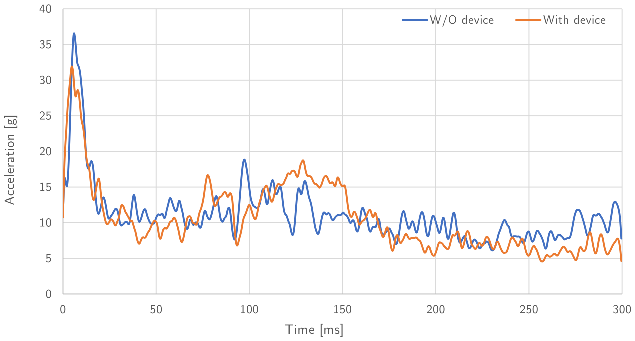

Figure A.33: Head acceleration.

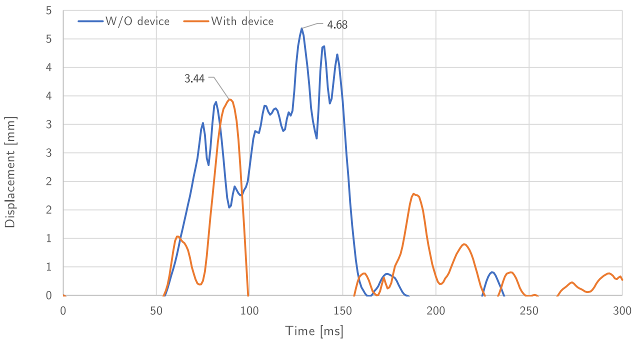

Figure A.34: Chest Deflection.

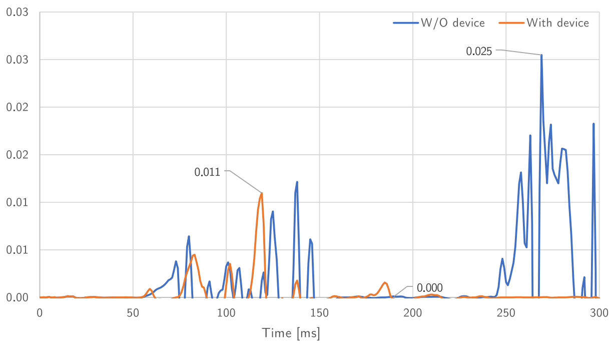

Figure A.35: Viscous Criterion.

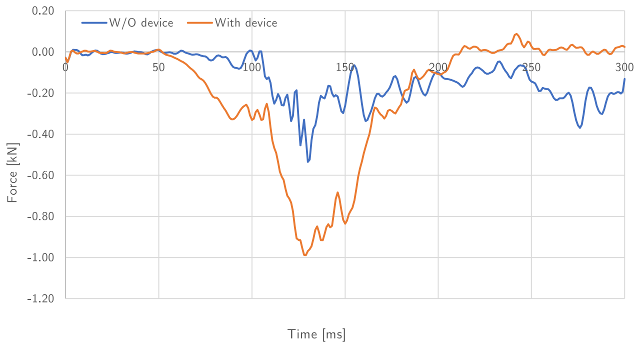

Figure A.36: Neck (X) Shear Force.

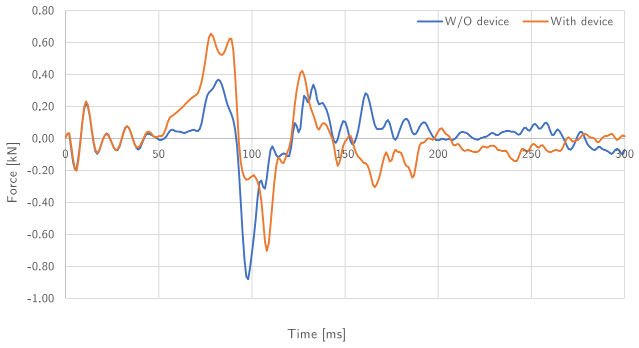

Figure A.37: Neck (Z) Axial Force.

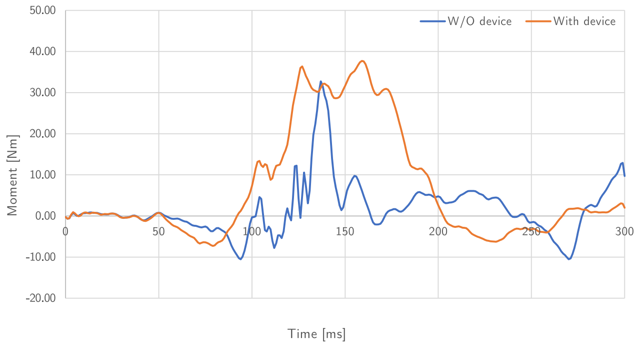

Figure A.38: Neck (Y) bending moment.

A.2.5 Configuration 115 0/9.8

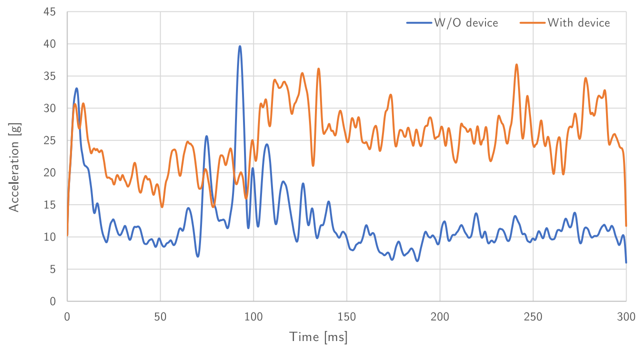

Figure A.39: Head acceleration.

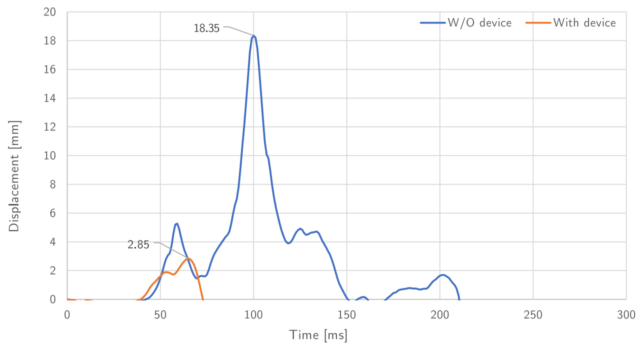

Figure A.40: Chest Deflection.

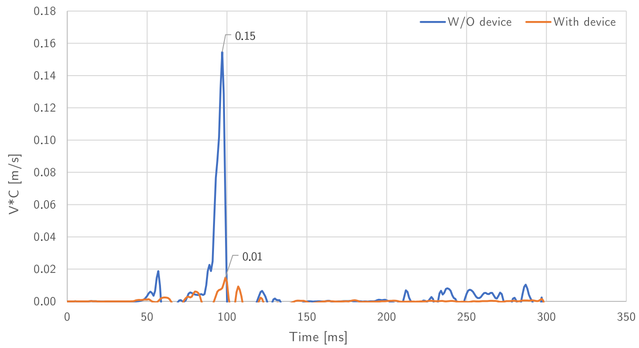

Figure A.41: Viscous Criterion.

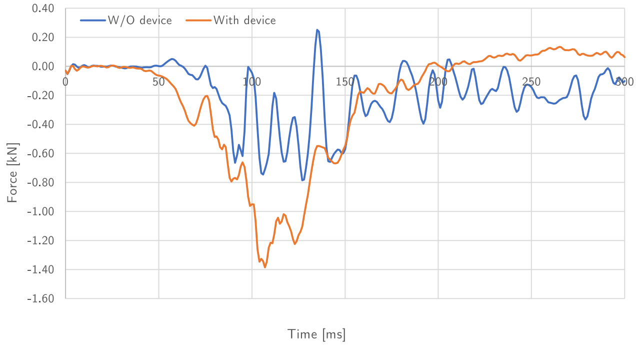

Figure A.42: Neck (X) Shear Force.

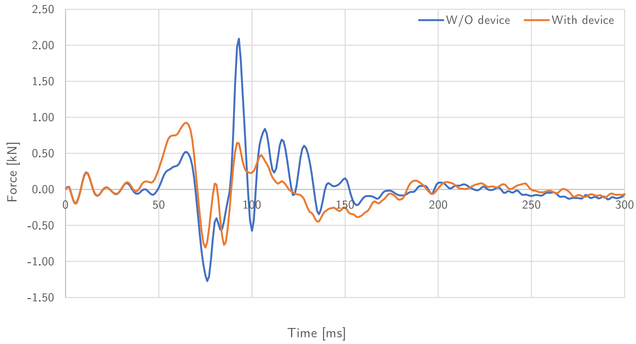

Figure A.43: Neck (Z) Axial Force.

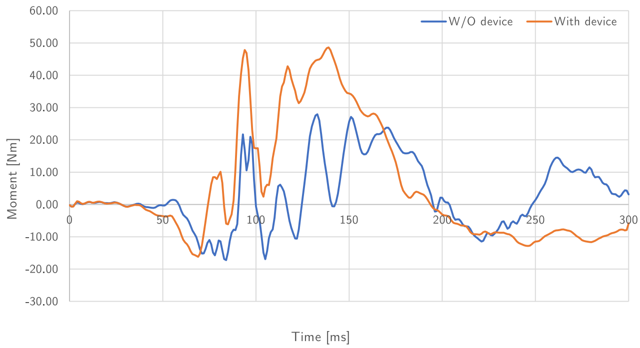

Figure A.44: Neck (Y) bending moment.

A.2.6 Configuration 313 0/20.1

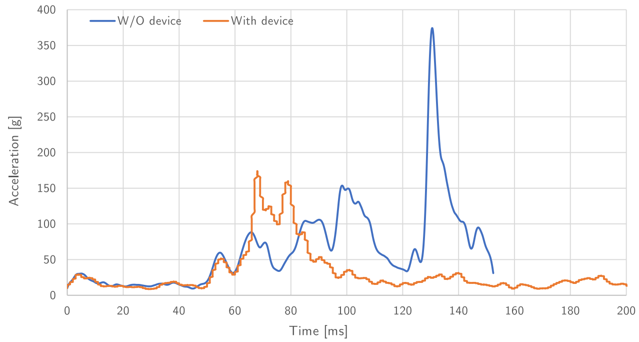

Figure A.45: Head acceleration.

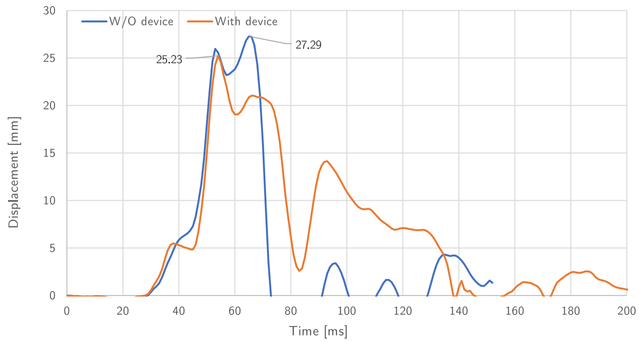

Figure A.46: Chest Deflection.

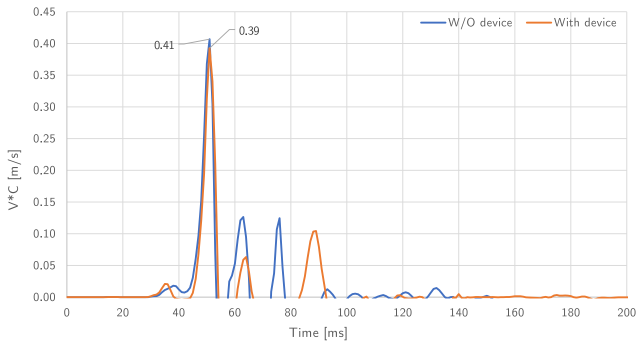

Figure A.47: Viscous Criterion.

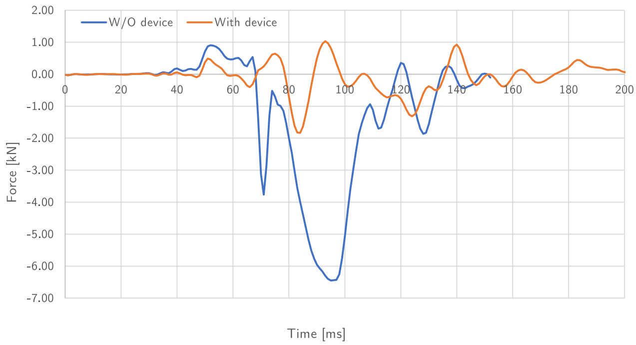

Figure A.48: Neck (X) Shear Force.

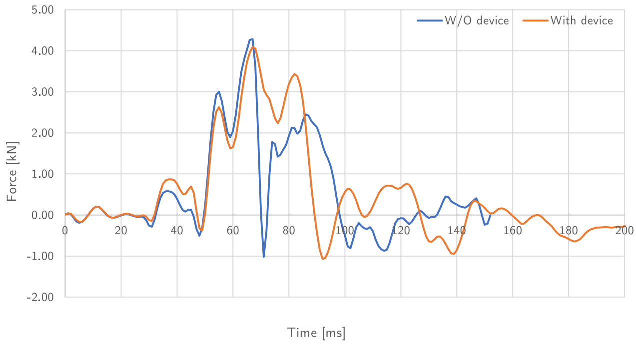

Figure A.49: Neck (Z) Axial Force.

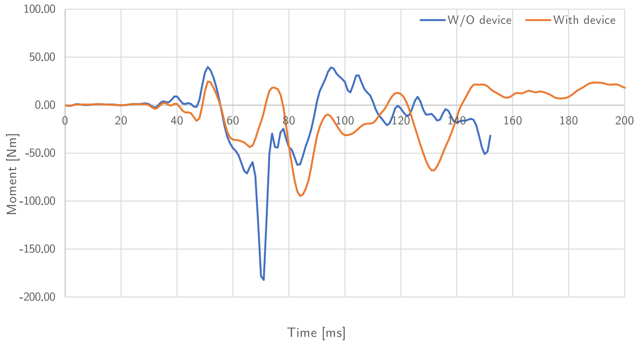

Figure A.50: Neck (Y) bending moment.

A.2.7 Configuration 312 6.7/9.8

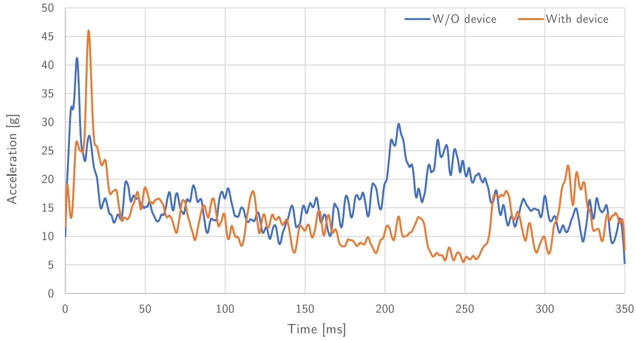

Figure A.51: Head acceleration.

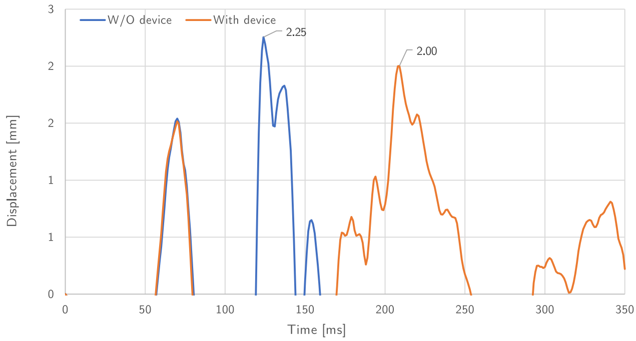

Figure A.52: Chest Deflection.

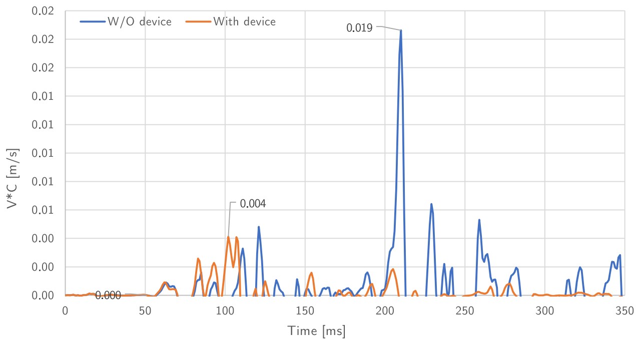

Figure A.53: Viscous Criterion.

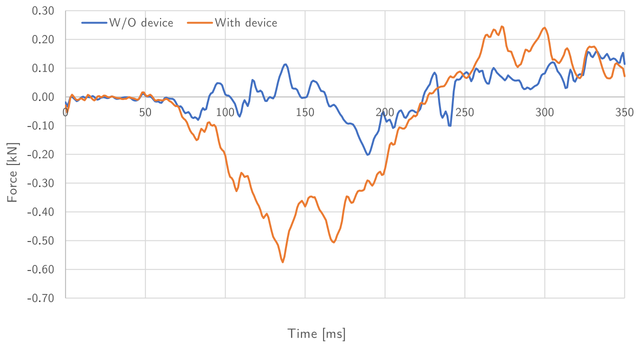

Figure A.54: Neck (X) Shear Force.

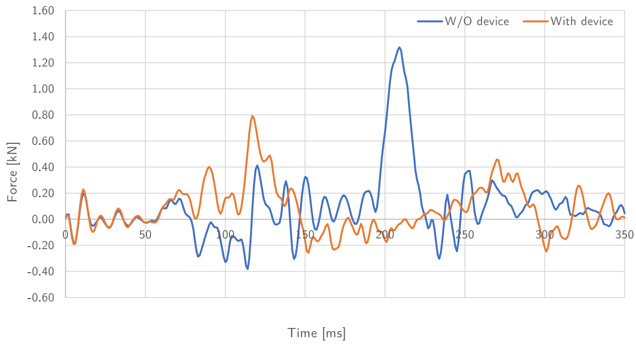

Figure A.55: Neck (Z) Axial Force.

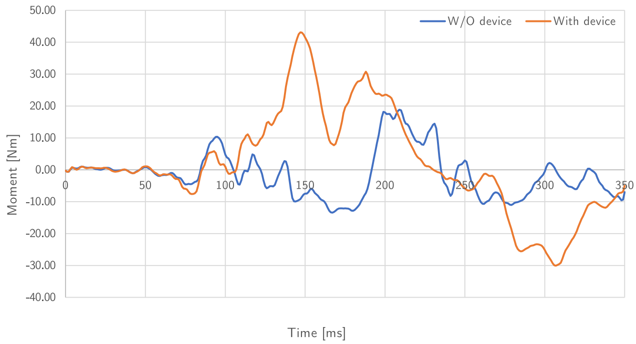

Figure A.56: Neck (Y) bending moment.

Appendix B

Rider's restraint system: tests and patents

In this appendix/chapter will be presented a little review on restraint systems/apparatus for restraining movement of a rider, and a little research of the state of the art on specific systems. In the specific, they will be described some crash tests carried out by a Swiss research centre and the most significant patents concerning this argument.

B.1 Safety Belt for Motorcyclists

In this section, the results obtained by Murri et al. (2008) at the Dynamic Test Center (DTC) in collaboration with the University of Bern, will be reported. In this study different technical options were analysed, which could limit the motorcyclist movement reducing the risk of injury in an accident. For the evaluation of the restraining system values the dummy was placed on a mechanical, simple and reversible system, using a passive operation (better acceptance). With this system, in case of falls or similar situations, if a restraining force was not activated the motorcyclist would not be affected by injuries and would get down the motorcycle in the usual way. The effectiveness of the belt system was tested during a series of motorcycle skidding trials and motorcycle impact trials, using light and heavy motorcycles against the side of stationary motor cars. These tests were performed under standard conditions (ISO 13232) and during a collision with double energy at 70 km/h. This study was carried out, because the author had reason to believe that a restraint force can cause less injury risks compared to a support force, because this last one could partially act on the head. In this regard the author had identified for restraint systems some advantages in comparison with airbags, for example:

1. it can autonomously work without other activation devices;
2. it is cheap and easy to achieve;
3. it is completely reversible in case of accidental activation;
4. it ensures major separation time (rider-motorcycle) compared to airbag.

On the other hand, to create an integrate belt restraint system, there should be a close cooperation between motorcycle and clothes manufacturers. In general the device purpose is to avoid the head impact against the car roof edge and anyway to reduce the rider's speed before the impact, in order to limit head, cervical spine and pelvis injuries. The device used for tests is characterized by a pair of belts acting on shoulders and another one acting on pelvis. These pairs are interlinked, and both have buckles to fast opening. To ensure more comfort for the rider, author suggest to embed the belts into the cloths. Before starting with real crash tests, the apparatus was preliminary tested on one sled, in order to assess the resistance of the motorcycle anchor points (see figure B.1).

Figure B.1: Preliminary tests with sled (*Source:* Murri et al. (2008)).

These preliminary tests, an increasing speed up to 50 *km/h*, showed that the bio-mechanical indexes did not exceed their limits. Furthermore, to avoid the uplift of the motorcycle rear part, author suggest a crash box installation in the frontal part of the vehicle. The first test was carried out on light motorcycle affecting a light van in configuration 413 Stationary/Moving. The speed used for these tests was 50 *km/h* (in figure B.2 it is visible the crash test frames at 100 *ms*).

To reduce the pitch moment as consequence of the impact, a simple sponge crash box was integrated in the frontal side of the PTW. The results obtained were convincing; indeed, the head of the dummy did not touch the lateral wall of the van although the impact speed was not low. The crash box had avoided the lifting of the motorcycle back. The rider's position remained almost vertical, and the head acceleration peak at 3 *ms* was 44.0 *g* (the limit is 80 *g*), and the *HIC* was equal to 314. All injury indexes registered in this test are reported in figure B.3.

In the second test, a touring motorcycle, a Honda CB 600 at 50 *km/h*, was crashed against a car with and without the device fitted. Also in this case, results show a significant injury reduction. Without the device fitted on the motorcycle, the dummy's head hits against the car roof edge. Contrary with the belts worn, the impact is practically avoided. This fact allows to have a substantial reduction of the head and neck forces. In figure B.4 a comparative frame of the Honda CB

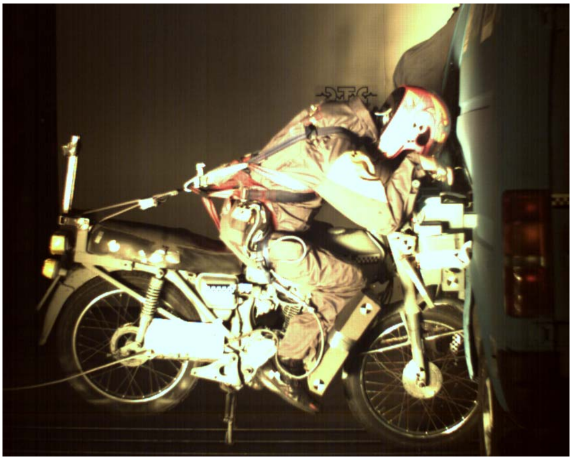

Figure B.2: Light motorcycle crash test at 100 *ms* (*Source:* Murri et al. (2008)).

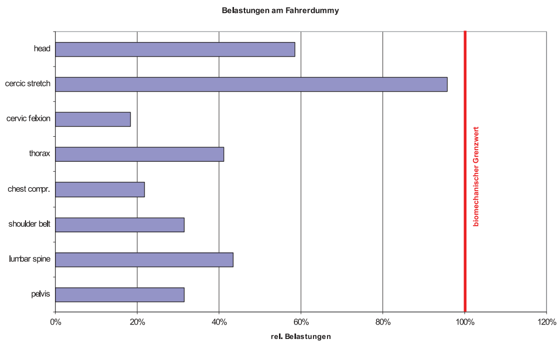

Figure B.3: Light motorcycle crash test: injury indexes registered (*Source:* Murri et al. (2008))

impact with and without the device are shown.

Figure B.4: CB 600 comparison: impact with the device and its relative head acceleration (on the left) and W/O the device and relative head acceleration (on the right) (*Source:* Murri et al. (2008)).

In the last test, carried out on motorcycle - once again a Honda CB 600 -, the speed was increased to 70 *km/h*. This test was performed for two reasons: to assess the effectiveness of the system independently from the impact speed, and to verify the frame resistance under very high load. Regarding the first point, the device effectiveness resulted confirmed although the impact speed was high. The lack of activation or inflating time of the device (for example airbags), allows the operation in more situations (due to different displacement speeds for different speed impact). The test showed a good behaviour of the MC frame. Frontal and rear (where the belts are fixed) motorcycle sides had resisted to the impact. The bio-mechanical injury indexes registered high values, and even if the head impact against the car was not completely avoided, the loads on head and injuries were on survival threshold. In figure B.5 frames of the impact test are shown.

Figure B.5: CB 600-car impact test at 70 *km/h* (*Source:* Murri et al. (2008)).

Other tests on light two-wheeler vehicles were carried out in this study to assess the possibility to extend the device use (Moped and bicycle). The results were showed the low frontal resistance offered by these types of vehicles. Furthermore, in event of rider's fall, the buckles are unlocked allowing a normal separation between the rider and the motorcycle. This study showed, with realistic tests, the potential of this type of safety device, giving an extra support to the work carried out in thesis.

B.2 Patents

In this section, patents relative to the last years which provide a connection between the rider and the motorcycle by a system of belts (to limit the rider's displacement during an accident), will be reported. Furthermore, some of these solutions shall integrate a system to release the rider from the PTW when specific condition do not require the system operation.

The first patent presented is relative to an invention of Matsuo (2008), of which Honda is the assignee. In this invention, it is provided a rider's restraint means capable of allowing a rider to freely leave a vehicle without a manual release operation when there is no need to restrain the rider to the vehicle. The rider's restraint means: includes a belt restraining a rider, buckles making the belt detachable, a guide rail making the buckles slidable, a retractor unit controlling the slide of the buckles, and coupling release means releasing coupling between the belt and the buckles in conjunction with the slide of the buckles. The coupling release means includes an inner wire, a wire stopper, and a wire end. The coupling release means releases the coupling between the belt and the buckles when the retractor unit loosens the winding after collision and the buckles slide by a predetermined distance or more or when the rider continues to pull the belt in a state other than collision and the buckles slide by a predetermined distance or more. In figure B.6 it is shown a motorcycle to which the device is applied.

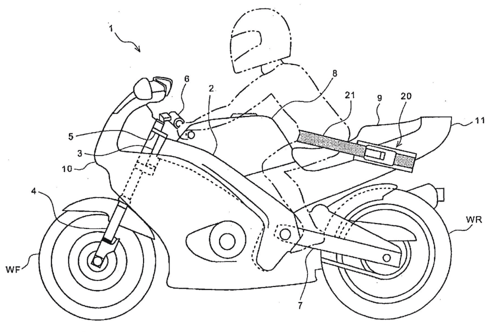

Figure B.6: A schematic view showing an entire rider's restraint apparatus (*Source:* Matsuo (2008)).

The restraint apparatus for restraining movement of a rider comprises the following:

- a seat belt-shaped rider restraint, restraining the rider;
- a detachable device, making the rider restraint detachable;
- a rail, making the detachable device slidable;
- a control, controlling sliding of the detachable device; and
- a coupling release device, releasing a coupling between the rider restraint and the detachable device in conjunction with the sliding of the detachable device, wherein the coupling release device releases the coupling between the restraint and the detachable device when the detachable device slides along the rail by a predetermined distance or more.

Figure B.7 shows a belt apparatus.

The rider restraint apparatus includes, at each of its ends, a coupling portion which is engaged with the detachable device, and a device allowing the coupling portion to be detached and a coupling release device are provided for the rail in a pair (see figures B.8).

The rider restraint apparatus is formed into a U-shape and it includes a wire attached to the detachable device, a wire end formed at an end of the wire, and a wire stopper restricting motion of the wire end, wherein an end of an outer tube is attached to the the detachable device, and the outer tube covers a part of the wire. Finally a rider restraint apparatus also includes:

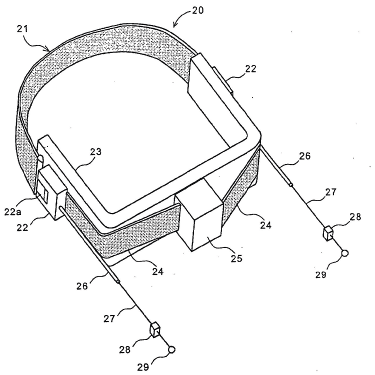

Figure B.7: A schematic view of the invention (*Source:* Matsuo (2008)).

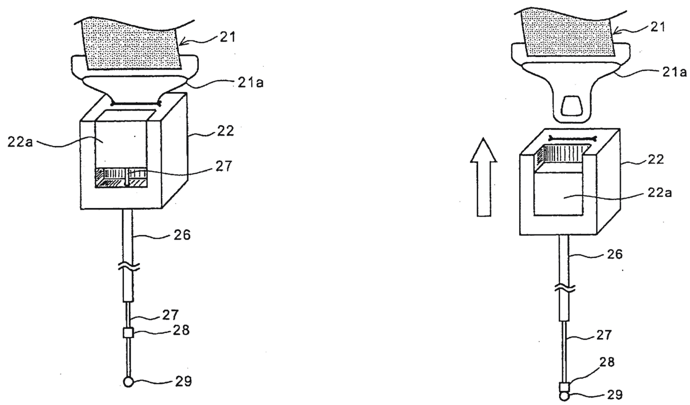

(a) Operation of a release button of the buckle coupled.

(b) Operation of the release button of the buckle released.

Figure B.8: Views of an operation of the release button (*Source:* Matsuo (2008)).

- a rail;
- at least one buckle, being slidable on the rail and the rider restraint belt being detachable from the rail by the at least one buckle;
- a retractor unit, the sliding of the at least one buckle on the rail being controlled by the retractor unit; and
- a coupling release device, the at least one buckle detaching the rider restraint belt when the at least one buckle slides along the rail by a predetermined distance or more.

The rider restraint apparatus includes a coupling portion at each of its ends, the coupling portions being respectively engaged with a pair of the at least one buckle, wherein there are a pair of the coupling release devices, the pair of coupling release devices being provided for the pair of buckles, respectively. The rail is formed into a substantially U-shape and the release device includes a wire attached to the buckle, a wire end formed at an end of the wire, and a wire stopper restricting motion of the wire end (see figure B.9).

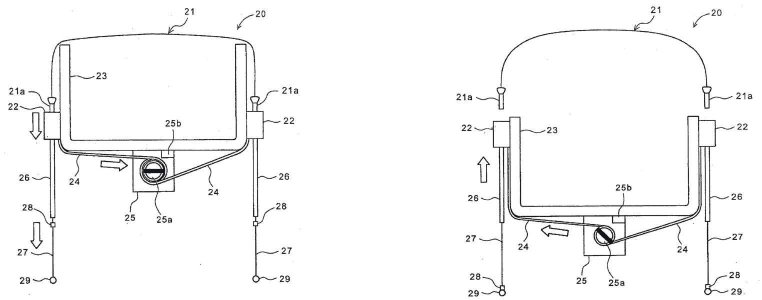

(a) A view of the safe apparatus when a winding belt is wound up.

(b) A view of the safe apparatus when a winding belt is released.

Figure B.9: Views of an operation of the release button (*Source:* Matsuo (2008)).

The applicant of the second patent reported is Marline Augustin Saint-Hilaire 2015. Its invention provides for a motorcycle safety belt device that secures a rider onto a motorcycle. The device includes a motorcycle having a main seat. A first strap has a first end and a second end. The first end of the first strap is coupled to the motorcycle proximate the main seat. The second end of the first strap is coupled to the motorcycle proximate the main seat such that the first strap is selectively positionable to extend over the main seat of the motorcycle. A buckle selectively couples a first section of the first strap to a second section of the first strap. In figure B.10 it is possible to see a perspective view of a motorcycle safety belt device.

With regards of figure B.10, the motorcycle and scooter safety belt device 10 generally comprises a motorcycle 12 having a main seat 14 and a passenger seat 16. For purposes of the application, the motorcycle 12 is defined as a motorized wheeled vehicle which includes scooters. A first strap 18 has a first end 20 and a second end 22. The first end 20 of the first strap 18 is coupled to the motorcycle 12 proximate the main seat 14. The second end 22 of the first strap 18 is coupled to the motorcycle 12 proximate the main seat 14 on an opposite side of the motorcycle such that the first strap 18 is selectively positionable to extend over the main seat 14 of the motorcycle 12. A first buckle 24 selectively couples a first section 26 of the first strap 18 to a second section 28 of the first strap 18. The first buckle 24 may employ a magnetic closure. A first tab 30 has a circular aperture 32 extending through the first tab 30. A bolt 34 is extended through the circular aperture 32 of the first tab 30. The bolt 34 extended through the circular aperture 32 of the

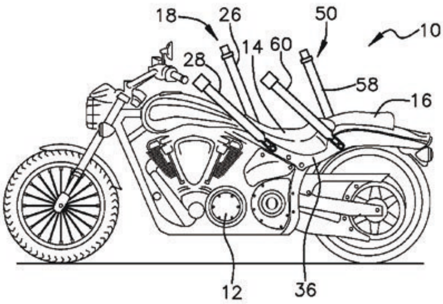

Figure B.10: A top front side perspective view of a motorcycle safety belt device (*Source:* Saint-Hilaire (2015)).

first tab 30 may be coupled to a frame 36 of the motorcycle 12 (see figure B.11).

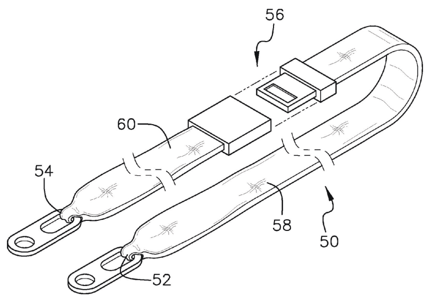

Figure B.11: A top front side detailed view of the bolted anchorage (*Source:* Saint-Hilaire (2015)).

A first loop 38 is positioned at the first end 20 of the first strap 18. A hole 40 extends through 15 the first tab 30 defining an arcuate bend 42 extending along an edge 44 of the first tab 30. The arcuate bend 42 of the first tab 30 extends through the first loop 38 wherein the first end 20 of the first strap 18 is securely coupled to the first tab 30. Similarly, a second tab 46 has the same structure as the first tab 30 for coupling the second end 22 of the first strap 18 to the second tab 46 and to the motorcycle 12. A second strap 50 may be provided having a first end 52 and a second end 54. The first end 52 of the second strap 50 is coupled to the motorcycle 12 proximate the passenger seat 16. The second end 54 of the second strap 50 is also coupled to the motorcycle 12 proximate the passenger seat 16 on a side opposite the first end 52 of the second strap 50 such that the second strap 50 is selectively positionable to extend over the passenger seat 16 of the motorcycle

12. A second buckle 56 selectively couples a first section 58 of the second strap 50 to a second section 60 of the second strap 50. Additional tabs may be employed to couple the first end 52 of the second strap 50 and the second end 54 of the second strap 50 to the motorcycle 12 in the same manner as described above for the first tab 30 and the second tab 46. In figure B.12 is shown a perspective view the belts.

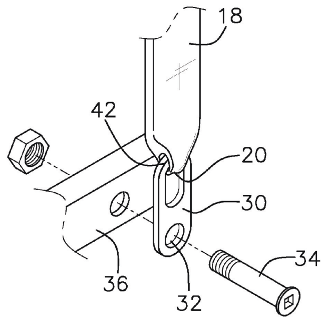

Figure B.12: A views of the belt (*Source:* Saint-Hilaire (2015)).

An alternative belt embodiment is shown in figure B.13, where a case 62 is coupled to the motorcycle 12. A reel 64 is positioned in the case 62. The device 10 is similarly structured to above except as noted wherein the first section 26 of the first strap 18 is coupled to the reel 64 such that the first section 26 of the first strap 18 is selectively extendable from and retractable into the case 62.

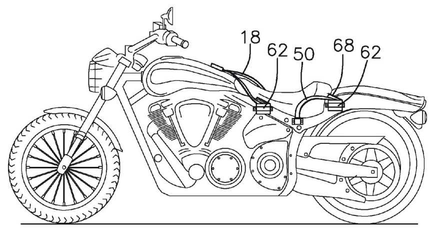

Figure B.13: An alternative belt embodiments (*Source:* Saint-Hilaire (2015)).

The case 62 may have an open top side 66. A cover 68 may be pivotally coupled to and selectively cover the open top side 66. A magnetic closure 70 may be provided having a first portion 72 coupled to the case 62 and a second portion 74 coupled to the cover 68 wherein the magnetic closure 70 selectively holds the cover 68 in a closed position over the open top 66 of the case 62 when the first portion

72 of the magnetic closure 70 magnetically engages the second portion 74 of the magnetic closure 70. Each of a pair of latches 76 may be coupled to a free end 78 of an associated one of the first section 26 of the first strap 18 and the second section 28 of the first strap 18. The first buckle 24 may be fixed to the motorcycle 12 and include a pair of slots 80. Each of the latches 76 may be selectively engageable to the first buckle 24 by insertion into an associated one of the slots 80 (see figure B.14).

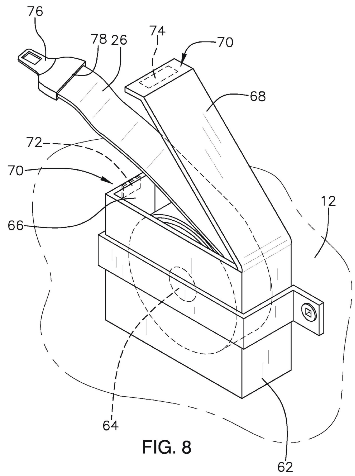

FIG. 8

Figure B.14: A top rear side perspective of device's detail (*Source:* Saint-Hilaire (2015)).

The third system presented relates to a restraining device for a rider of a vehicle, a garment for a rider of a vehicle, a safety system for the detachable binding of a rider to a vehicle, and a method for using a restraining device for a rider of a vehicle (Maka et al. (2015)). A general overview of the device is shown in figure B.15

A restraining device for a rider of a vehicle, comprises the following:

- a restraining belt that is integrable or is integrated at least partly into a garment of the rider, the restraining belt being configured so as to encompass at least one bodily region of the rider;
- a connecting element that is connectible or is connected to the restraining belt, and that is configured to bind the rider detach-ably to the vehicle.

The restraining device provides for the restraining belt configured to encompass at least one of a shoulder region, a chest region, and a pelvic region of the rider as bodily region (see figure B.16).

The connecting element has a belt buckle or an insertion tongue of a coupling system for coupling the restraining device to the vehicle. Furthermore, it has at least two electrical contact terminals. The first contact is configured to be

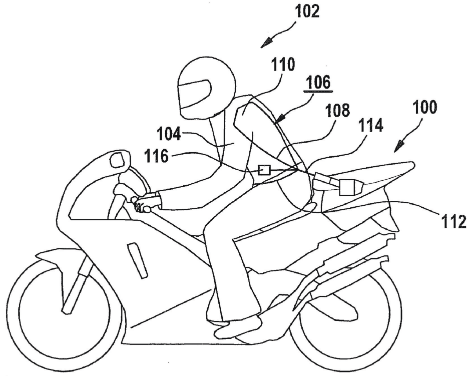

Figure B.15: A representation of a rider on a vehicle connected to a restraining device according to an exemplary embodiment of the present invention (*Source:* Maka et al. (2015)).

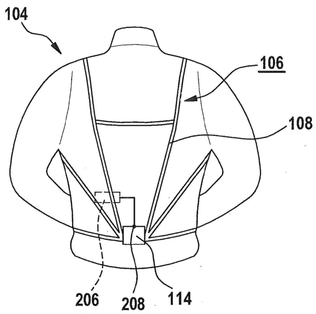

Figure B.16: A rear view of the restraining device (*Source:* Maka et al. (2015)).

connected to an energy supply line of the restraining device, and the second one is configured to be connected to a data transmission line of the restraining device. The restraining device further comprises an output contact terminal to transmit electrical voltage received from the first electrical contact terminal and/or from the further first electrical contact terminal to a rider protection device that is coupled or couple-able to the restraining device and is situated at a distance from the first electrical contact terminal and/or from the further first electrical contact terminal, or to a communication device that is coupled, or couple-able to the restraining device and that is situated at a distance from the first electrical contact terminal and/or from the further first electrical contact terminal. Another device characteristic is represented by a further connecting element to additionally bind the rider detach-ably to the vehicle. It comprises:

- a safety system arrangement; and

- a vehicle connecting element for coupling the safety system arrangement to a restraining device, the vehicle connecting element having at least one second electrical contact terminal; wherein the restraining device includes a restraining belt that is integrable or is integrated at least partly into a garment of the rider, the restraining belt being configured so as to encompass at least one bodily region of the rider, and a connecting element that is connectible or is connected to the restraining belt, and that is configured to bind the rider detach-ably to the vehicle.

Figure B.17 shows a belt system for coupling the restraining device to the vehicle according to an exemplary embodiment.

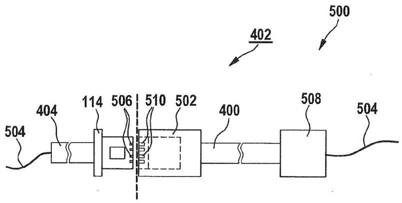

Figure B.17: A belt system for coupling the restraining device to the vehicle (*Source:* Maka et al. (2015)).

The last patent is a specific application to release the belt from motorcycle. Here, the device relates to a safety belt; more particularly, a motorcycle or equivalent vehicles safety belt for a rider or a passenger, which is extendable and retractable, but grasp the wearer in place when the vehicles come to an hasty halt or an impact, and self-releasable and extricates the wearer when the vehicles fall from an upright position to left or right side after the hasty halt or impact. The invention presented by Chen 2015 is shown in figure B.18.

The device is characterized by:

- a self-releasable safety belt (1) for a motorcycle or equivalent vehicles;
- a strap (2) defined by a finite length including a first end and a second end.
- a retractor (3) receiving the first end of the strap (2) for stowing and locking the strap (2) in a predetermined situation;
- a detachable joint (4) coupling the first end of the strap (2) to the rear of the motorcycle or the like, whereby the detachable joint (4) will detach when force is applied to the joint (4);
- a male connector (7) coupled to the second end of the strap (2);
- a female connector (8) including a pair of releasing devices (9) disposed on opposite sides of the female connector (8), for receiving the male connector (7);

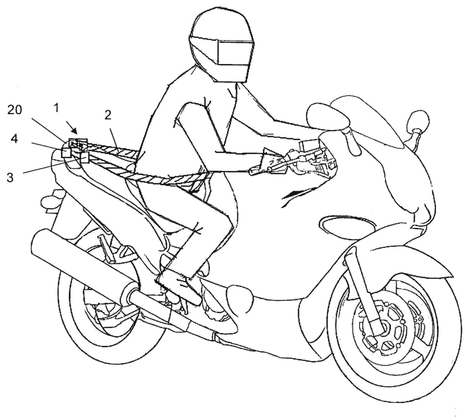

Figure B.18: The arrangement of a self-releasable safety belt used in a vehicle and employing a wearer (*Source:* Chen (2015)).

- a mounting device (10) coupling the female connector (8) to the rear of the motorcycle or the like; and
- a U-bracket (11) affixed on the mounting device (10) and having two arms (12) protruding towards the pair of releasing devices (9), whereby, the male connector (7) is ejected from the female connector (8) when the releasing devices (9) contact the arms (12) with force;

The safety belt (1) is extendable and retractable, but tightens up and holds the wearer in place when the motorcycle or the like comes to an abrupt halt or an impact, thereby preventing the wearer from being flung away. Furthermore, the safety belt is self-releasable and detachable, and disentangles the wearer when the motorcycle or the like falls from an upright position to the left or right side after the abrupt halt or impact, thereby preventing the wearer from being stuck in the motorcycle or the like which is still moving or knocked by the fallen motorcycle or the like when the rider lost control or balance after an abrupt halt or impact. The detachable joint (4) includes a shaft (5) and a socket (6), wherein the .shaft (5) is coupled to the first end of sold strap (2) and the socket (6) is coupled to the rear of the motorcycle or the like for receiving the shaft (5). The socket (6) includes a slit (13) to enable the shaft (5) to slide into the socket (6) and a retaining clip (14) mounted on both ends of the slit (13) to hinder the shaft (5) from sliding out from the socket (6) until a force snatches the strap (2) and detaches the shaft (5) from the socket. The detachable joint (4) and the mounting device (10) are preferably mounted on a U-bar (20) at the rear of a motorcycle or the like. The female connector (8) is coupled to the mounting device (10) by a pivot (15), thereby enabling the female connector (8) to swing horizontally. The releasing devices (9) are disposed on the left and right side of the female connector (8) as visible in figure B.19.

The arms (12) are aligned with the releasing devices (9) in order that when the

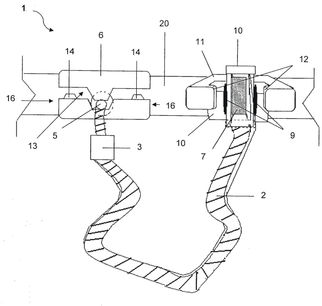

(a) Front view.

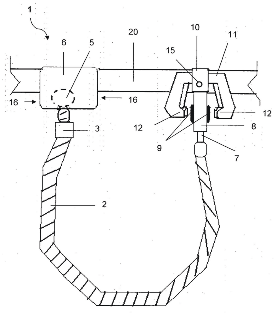

(b) Top view.

Figure B.19: Views of the self-releasable safety belt mounted on a U-bar at the rear of a motorcycle (*Source:* Chen (2015)).

wearer falls from upright position to the left or right side after the abrupt halt or impact, the releasing devices (9) will contact the arms (12) with force, resulting in the ejection of the male connector (7) from the female connector (8). The retractor (3) is preferably has an inertia reel system to resist acceleration during abrupt halt or impact (see figure B.20).

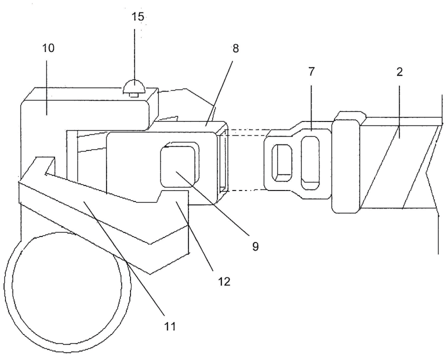

Figure B.20: A side perspective view illustrating the engagement of a male connector to a female connector that is coupled to a mounting device by a pivot (*Source:* Chen (2015)).

Bibliography

Aare, M. and Holst, H. (2003). Injuries from motorcycle-and moped crashes in sweden from 1987 to 1999. *Injury control and safety promotion*, 10(3):131–138.

Aare, M., Kleiven, S., and Halldin, P. (2004). Injury tolerances for oblique impact helmet testing. *International journal of crashworthiness*, 9(1):15–23.

Aikyo, Y., Kobayashi, Y., Akashi, T., and Ishiwatari, M. (2015). Feasibility study of airbag concept applicable to motorcycles without sufficient reaction structure. *Traffic injury prevention*, 16(sup1):S148–S152.

Aldman, B., Cacciola, I., Gustafsson, H., Nygren, A., and Wersall, J. (1981). The protective effect of different kinds of protective clothing worn by motorcyclists. In *Proceedings of the International Research Council on the Biomechanics of Injury conference*, volume 9, pages 1–9. International Research Council on Biomechanics of Injury.

Altshuller, G. (1986). To find an idea: introduction to the theory of inventive problem solving.

Altshuller, G. (1999). *The innovation algorithm: TRIZ, systematic innovation and technical creativity.* Technical Innovation Center, Inc.

Altshuller, G. S. (1969). Algorithm of invention. *Moscowskiy Rabochy, Moscow.*

Altshuller, G. S. (1984). *Creativity as an exact science: the theory of the solution of inventive problems.* Gordon and Breach.

Ankarath, S., Giannoudis, P. V., Barlow, I., Bellamy, M., Matthews, S., and Smith, R. (2002). Injury patterns associated with mortality following motorcycle crashes. *Injury*, 33(6):473–477.

Backaitis, S. H. and St-Laurent, A. (1986). Chest deflection characteristics of volunteers and hybrid iii dummies. Technical report, SAE Technical Paper.

Barbani, D., Baldanzini, N., and Pierini, M. (2014a). Development and validation of an fe model for motorcycle–car crash test simulations. *International journal of crashworthiness*, 19(3):244–263.

Barbani, D., Baldanzini, N., and Pierini, M. (2014b). Sensitivity analysis of a fe model for motorcycle-car full-scale crash test. Technical report, SAE Technical Paper.

Barbani, D., Baldanzini, N., Pierini, M., and Santucc, M. (2012a). Analisi e sviluppo di un modello fem di airbag integrato su motoveicolo. In *41 convegno nazionale AIAS - Associazione Italiana per l'Analisi delle Sollecitazioni, Vicenza.*

Barbani, D., Pierini, M., and Baldanzini, N. (2012b). Fe modelling of a motorcycle tyre for full-scale crash simulations. *International journal of crashworthiness*, 17(3):309–318.

Belin, M.-Å. (2012). *Public road safety policy change and its implementation-Vision Zero a road safety policy innovation.* Inst för folkhälsovetenskap/Dept of Public Health Sciences.

Berg, F., König, J., and Rücker, P. (2004). Profit and protection of the airbag to enhance the passive safety of motorcycles. Technical report, SAE Technical Paper, FISITA.

Berg, F., Rücker, P., and König, J. (2005). Motorcycle crash testsâan overview. *International Journal of Crashworthiness*, 10(4):327–339.

Berg, F. A., Bilrkle, H., Schmidts, F., Epple, J., and AG, D. A. (1998). Analysis of the passive safety of motorcycles using accident investigations and crash tests. In *16th International Technical Conference on the Enhanced Safety of Vehicles ESV, Windsor, Ontario, Canada*, volume 31.

Berger, C., Blauth, R., and Boger, D. (1993). âkanoâs methods for understanding customer customerdefined qualityââ. *Centre for Quality Management Science*, 17(1):66–88.

Borgianni, Y., Frillici, F. S., and Rotini, F. (2015). Integration of otsm-triz and analytic hierarchy process for choosing the right solution. *Procedia Engineering*, 131:388–400.

Bothwell, P., Knight, R., and Peterson, H. (1973). Dynamics of motorcycle impact 1971-1973. vol. 1. summary report-results of crash test program and computer simulation. Technical report.

Cavallucci, D., Khomenko, N., and Morel, C. (2005). Towards inventive design through management of contradictions. In *2005 CIRP International Design Seminar.*

Chen, W. O. (2015). Self-releasable safety belt. US Patent 9,061,723.

Chinn, B., Hopes, P., and Macaulay, M. (1985). Leg protection for riders of motorcycles. Technical report, SAE Technical Paper.

Chinn, B. and Macaulay, M. (1984). Leg protection for motorcyclists. In *Proceedings of the International Research Council on the Biomechanics of Injury conference*, volume 12, pages 265–278. International Research Council on Biomechanics of Injury.

Chinn, B., Okello, J., McDonough, P., and Grose, G. (1996). Development and testing of a purpose built motorcycle airbag restraint system. In *International Technical Conference on the Enhanced Safety of Vehicles, 15th, 1996, Melbourne, Victoria, Australia*, number DOT HS 808 465.

CNS EN (2014). European Commitee for Standartization - EN 1621-2 - motorcyclists' protective clothing against mechanical impact - part 2: Motorcyclists' back protectors - requirements and test methods.

Craig, G., Sleet, R., and Wood, S. (1983). Lower limb injuries in motorcycle accidents. *Injury*, 15(3):163–166.

CSN EN (2002). European Commitee for Standartization - EN 13595 - protective clothing for professional motorcycle riders - jackets, trousers and one piece or divided suits - part 1: General requirements.

CSN EN (2015). European Commitee for Standartization - EN 13594 - protective gloves for professional motorcycle riders - requirements and test methods.

de Rome, L., Ivers, R., Fitzharris, M., Du, W., Haworth, N., Heritier, S., and Richardson, D. (2011). Motorcycle protective clothing: protection from injury or just the weather? *Accident Analysis and Prevention*, 43(6):1893–1900.

Deguchi, M. (2005). Simulation of motorcycle-car collision. In *19th International Technical Conference on the Enhanced Safety of Vehicles*, pages 6–9.

Deutermann, W. (2004). Motorcycle helmet effectiveness revisited. Technical report.

Di Genova, F., de Manes, M., Di Mare, G., Ioele, M., Cioffi, V., Ferrara, F., Caraceni, A., Marcacci, M., Baracchino, L., Bernardi, L., et al. (2007). Hardware in the loop validation of the piaggio mp3. Technical report, SAE Technical Paper.

DIN EN (2013). European Commitee for Standartization - EN 1621-1 - motorcyclists' protective clothing against mechanical impact - part 1: Motorcyclists' limb joint impact protectors - requirements and test methods.

DIN EN (2015). European Commitee for Standartization - EN 1621-3 - motorradfahrerschutzkleidung gegen mechanische belastung - teil 3: Anforderungen und prÃ¼fverfahren fÃ¼r brustprotektoren; deutsche und englische fassung pren 1621-3:2015.

DIN EN (2016). European Commitee for Standartization - EN 13634 - protective footwear for professional motorcycle riders - requirements and test methods.

Directive 96/79/EC (1996). Directive 96/79/ec on the protection of occupants of motor vehicles in the event of a frontal impact and amending directive 70/156/eec.

Elvik, R. (2009). *The Power Model of the relationship between speed and road safety: update and new analyses.* Number 1034/2009.

Eppinger, R., Sun, E., Bandak, F., Haffner, M., Khaewpong, N., Maltese, M., Kuppa, S., Nguyen, T., Takhounts, E., Tannous, R., et al. (1999). Development of improved injury criteria for the assessment of advanced automotive restraint systems–ii. *National Highway Traffic Safety Administration*, pages 1–70.

EU Commission (2001). Motorcycle safety helmets. final report of the action. Technical report.

EU Commission (2016). *Traffic Safety Basic Facts on Motorcycles Mopeds, European Commission.* Directorate General for Transport.

Evans, L. and Frick, M. C. (1988). Helmet effectiveness in preventing motorcycle driver and passenger fatalities. *Accident Analysis & Prevention*, 20(6):447–458.

Feldkamp, G., Prall, W., Buehler, G., and Junghanns, K. (1977). Motorcycle accidents-eidemiology, clinical aspects and protective measures-a follow-up and prospective study (author's transl). *Unfallheilkunde*, 80(1):1–19.

Finnis, M. P. (1990). Air bags and motorcycles: Are they compatible? Technical report, SAE Technical Paper.

Foret-Bruno, J., Trosseille, X., Le Coz, J., Bendjellal, F., Steyer, C., Phalempin, T., Villeforceix, D., Dandres, P., and Got, C. (1998). Thoracic injury risk in frontal car crashes with occupant restrained with belt load limiter. Technical report, SAE Technical Paper.

Foret-Bruno, J.-Y., Trosseille, X., Page, Y., Huère, J.-F., Le Coz, J., Bendjellal, F., Diboine, A., Phalempin, T., Villeforceix, D., Baudrit, P., et al. (2001). Comparison of thoracic injury risk in frontal car crashes for occupant restrained without belt load limiters and those restrained with 6 kn and 4 kn belt load limiters. *Stapp car crash journal*, 45:205–224.

Gadd, C. W. (1962). Criteria for injury potential. *Impact Acceleration Stress*, 977:141.

Gadd, C. W. (1966). Use of a weighted-impulse criterion for estimating injury hazard. Technical report, SAE Technical Paper.

Gehre, C., Vetter, D., and Appek, H. (2001). Protection of the lower extremities in two and three wheelers with safety cell. In *International Conference on the Enhanced Safety of Vehicles. ECV.*

Geisinger, A., Kreitmeier, H., Leatt, C., Diehl-Thiele, T., Bachmann, J., and Muller, P. (2007). Innovations at bmw motorrad in the development of equipment for motorcycle riders to reduce the risk of injuries based on the example of the neck brace system. *Development trends of motorcycles: With*, 10:199.

Gennarelli, T. A. and Wodzin, E. (2015). *Abbreviated injury scale 2005: update 2015*. Russ Reeder.

Griffin, A. and Hauser, J. R. (1993). The voice of the customer. *Marketing science*, 12(1):1–27.

Guha, S. (2014). Lstc_ncac hybrid iii 50th dummy positioning & post-processing. *Livermore Software Technology Corporation Michigan, Michigan*.

Gurdjian, E., Webster, J., and Lissner, H. (1955). Observations on the mechanism of brain concussion, contusion, and laceration. *Surgery, gynecology & obstetrics*, 101(6):680.

Gustafsson, A., Ekdahl, F., and Edvardsson, B. (1999). Customer focused service development in practice–a case study at scandinavian airlines system (sas). *International Journal of Service Industry Management*, 10(4):344–358.

Halldin, P., Gilchrist, A., and Mills, N. (2001). A new oblique impact test for motorcycle helmets. *International Journal of Crashworthiness*, 6(1):53–64.

Halquist, J. (2007). Ls-dyna keyword userâs manual version 971. *Livermore Software Technology Corporation, Livermore, CA*.

Happian-Smith, J. and Chinn, B. (1990). Simulation of airbag restraint systems in forward impacts of motorcycles. Technical report, SAE Technical Paper.

Happian-Smith, J., Macaulay, M., and Chinn, B. (1987). Motorcycle impact simulation and practical verification. *11th ESV*.

Hell, T. and Lob, G. (1993). Typical injury patterns of motorcyclists in different crash types: Effectiveness and improvements of countermeasures. In *Proceedings: Association for the Advancement of Automotive Medicine Annual Conference*, volume 37, pages 77–86. Association for the Advancement of Automotive Medicine.

Hirsch, A. and Bothwell, P. (1973). Air bag crash protection for motorcycle application. In *MECHANICAL ENGINEERING*, volume 96, pages 70–70. ASME-AMER SOC MECHANICAL ENG 345 E 47TH ST, NEW YORK, NY 10017.

Hirsch, A. and Bothwell, P. (1974). Air bag crash protection for motorcycle application. In *MECHANICAL ENGINEERING*, volume 96, pages 70–70. ASME-AMER SOC MECHANICAL ENG 345 E 47TH ST, NEW YORK, NY 10017.

Hobbs, C. (2001). Priorities for motor vehicle safety design. *Brussels (Belgium): European Traffic Safety Council*.

Hobbs, C., Gloyns, P., Rattenbury, S., and Roberts, J. (1997). European new car assessment program (euro-ncap).

Hole, G. J., Tyrrell, L., and Langham, M. (1996). Some factors affecting motorcyclists' conspicuity. *Ergonomics*, 39(7):946–965.

Holgate, J., Redant, K., De Solere, H., Van Elslande, P., Margaritis, D., Yannis, G., De Craen, S., Haslie, L. I., Muguiro, J., Granstrom, P.-O. G., et al. (2015). Improving safety for motorcycle, scooter and moped riders.

Hollmotz, L., Sohr, S., and Johannsen, H. (2005). Clever–a three wheel vehicle with a passive safety comparable to conventional cars. In *The 19th international technical conference on the enhanced safety of vehicles (ESV)-Washington DC June 6-9*.

Hurt, H., Ouellet, J. V., and Wagar, I. (1981). Effectiveness of motorcycle safety helmets and protective clothing. In *Proceedings: American Association for Automotive Medicine Annual Conference*, volume 25, pages 223–235. Association for the Advancement of Automotive Medicine.

Hutchinson, J., Kaiser, M. J., and Lankarani, H. M. (1998). The head injury criterion (hic) functional. *Applied mathematics and computation*, 96(1):1–16.

Ibitoye, A., Hamouda, A. M. S., Wong, S. V., and Radin, R. (2006). Simulation of motorcyclist's kinematics during impact with w-beam guardrail. *Advances in engineering Software*, 37(1):56–61.

IIHS (2009). *Frontal offset crashworthiness evaluation - guidelines for rating injury measures.* Insurance Institute for Highway Safety, Alington VA, USA.

ISO (2005). International Standard of Organization - ISO 13232 (2005) - Motorcycles - Test and analysis procedures for research evaluation of rider crash protective devices fitted to motorcycles - Second Edition.

ITF (2015). Improving safety for motorcycle, scooter and moped riders.

Kalliske, I. and Albus, C. (1998). Safety potential of future two-wheel concepts-a challenge. In *16th ESV Conference.*

Kanbe, S., Deguchi, M., and Hannya, Y. (2007). Basic research for a new airbag system for motorcycles. In *Proceedings of the 20th International Conference on Enhanced Safety of Vehicles, Lyons, France.*

Kano, N. (1984). Attractive quality and must-be quality. *J. Jpn. Soc. Quality Control*, 14:39–48.

Kent, R., Lessley, D., Shaw, G., and Crandall, J. (2003). The utility of hybrid iii and thor chest deflection for discriminating between standard and force-limiting belt systems. *Stapp car crash journal*, 47:267.

Khomenko, N. (1984). Modeling of problem situation. In *Conference on methodology and techniques of engineering creativity.*

Khomenko, N. (1987). Selection of the minimal task. *Design research in progress.*

Khomenko, N. (1988a). Contradiction as a system of elementary contradictions. In *Conference on Engineering creativity. USSR, Miass,(Year).*

Khomenko, N. (1988b). Software for inventive problem solving training classes. In *Conference on Engineering creativity.*

Khomenko, N. (1988c). Using multi dimension space of features for system description. In *Conference on Engineering creativity*, pages 1980–1997.

Khomenko, N. (1997). Working materials for otsm development: State of art 1980–1997. *LG-Electronics Learning Center, Piangteck, South Korea (in English).*

Khomenko, N. (1999). Education materials for otsm development: State of art 1980–1997. *LG-Electronics Learning Center, Piangteck, South Korea (in English).*

Khomenko, N. (2014). Otsm network of problems: Draft for discussion and improvements. In *OTSM Network of Problems: Draft for Discussion and improvements.*

Khomenko, N. and De Guio, R. (2007). Otsm network of problems for representing and analysing problem situations with computer support. *Trends in Computer Aided Innovation*, pages 77–88.

Khomenko, N., De Guio, R., Lelait, L., and Kaikov, I. (2007). A framework for otsm? triz-based computer support to be used in complex problem management. *International Journal of Computer Applications in Technology*, 30(1-2):88–104.

Khomenko, N., Kucharavy, D., and LRPS, E. (2002). Otsm-triz problem solving process: solutions and their classification. In *Proceedings of TRIZ Future Conference*, pages 6–8.

Khomenko, N., Schenk, E., and Kaikov, I. (2006). Otsm-triz problem network technique: application to the history of german high-speed trains. In *TRIZ Future 2006 Conference. Belgium, Kortijk.*

Khomenko, N. and Tsourikov, V. (1988). Contradiction resolution in artificial intelligence software for concept design stage of product developing. In *Conference on CAD system for product development.*

Khosroshahi, S. F., Ghajari, M., and Galvanetto, U. (2016). Finite element simulation of neck brace protective equipment for motorcycle riders.

Kis, M., Saunders, F., Ten Hove, M., and Leslie, J. (2004). Rotational acceleration measurements-evaluating helmet protection. *Canadian journal of neurological sciences*, 31(4):499–503.

Kis, M., Saunders, F. W., Kis Sr, M., Irrcher, I., Tator, C. H., Bishop, P. J., and Martin, W. (2013). A method of evaluating helmet rotational acceleration protection using the kingston impact simulator (kis unit). *Clinical Journal of Sport Medicine*, 23(6):470–477.

Kleinberger, M., Sun, E., Eppinger, R., Kuppa, S., and Saul, R. (1998). Development of improved injury criteria for the assessment of advanced automotive restraint systems. *NHTSA Docket*, (1998-4405):9.

Klinich, K., Saul, R., Auguste, G., Backaitis, S., and Kleinberger, M. (1996). Techniques for developing child dummy protection reference values.

Kroell, C. K., Schneider, D. C., and Nahum, A. M. (1971). Impact tolerance and response of the human thorax i. Technical report, SAE Technical Paper.

Kroell, C. K., Schneider, D. C., and Nahum, A. M. (1974). Impact tolerance and response of the human thorax ii. Technical report, SAE Technical Paper.

Kuppa, S., Wang, J., Haffner, M., and Eppinger, R. (2001). Lower extremity injuries and associated injury criteria. In *17^{th} International Technical Conference on the Enhanced Safety of Vehicles*, number 457, Amsterdam, Paesi Bassi.

Lau, I. V. and Viano, D. C. (1986). The viscous criterion-bases and applications of an injury severity index for soft tissues. Technical report, SAE Technical Paper.

Leatt, C., de Jongh, C., and Keevy, P. (2012). White paper: Research and development efforts towards the production of the leatt-brace® moto gpx. Unrestrained torso neck brace. Technical report, Leatt Corporation®.

Lissner, H., Lebow, M., and Evans, F. (1960). Experimental studies on the relation between acceleration and intracranial pressure changes in man. *Surgery, gynecology & obstetrics*, 111:329–338.

Liu, B. C., Ivers, R., Norton, R., Boufous, S., Blows, S., and Lo, S. K. (2008). Helmets for preventing injury in motorcycle riders. *The Cochrane Library.*

López-Valdés, F. and Juste-Lorente, O. (2015). Innovative restraints to prevent chest injuries in frontal impacts. In *Proceedings of the 24: th Technical Conference on the Enhanced Safety of Vehicles, Gothenburg. Paper*, number 15-0381.

Lubock, P. and Goldsmith, W. (1980). Experimental cavitation studies in a model head-neck system. *Journal of Biomechanics*, 13(12):10411049–10471052.

MAIDS (2009). MAIDS 2.0 In-depth investigations of accidents involving powered to wheelers. Technical report, Bruxelles, Belgio.

Maka, T., Wahl, A., and Cuvillier, M. (2015). Restraining device for a rider of a vehicle, method for using such a restraining device, garment for a rider of a vehicle, and safety system for the detachable binding of a rider to a vehicle. US Patent 9,139,158.

Matsuo, H. (2008). Rider restraint apparatus. US Patent 7,370,887.

Matzler, K. and Hinterhuber, H. H. (1998). How to make product development projects more successful by integrating kano's model of customer satisfaction into quality function deployment. *Technovation*, 18(1):25–38.

Mertz, H. (1993). Anthropomorphic test devices. accidental injury-biomechanics and prevention chapter 4.

Mertz, H., Hodgson, V., Thomas, L. M., and Nyquist, G. (1978). An assessment of compressive neck loads under injury-producing conditions. *The Physician and Sportsmedicine*, 6(11):95–106.

Mertz, H., Irwin, A., Melvin, J., Stanaker, R., and Beebe, M. (1989). Size, weight and biomechanical impact response requirements for adult size small female and large male dummies. Technical report, SAE Technical Paper.

Mertz, H. J., , and Irwin, A. (1994). Brain injury risk assessment of frontal crash test results. Technical report, SAE Technical Paper.

Mertz, H. J. and Gadd, C. W. (1971). Thoracic tolerance to whole-body deceleration. Technical report, SAE Technical Paper.

Mertz, H. J. and Patrick, L. M. (1971). Strength and response of the human neck. Technical report, SAE Technical Paper.

Mooren, L., Grzebieta, R., and Job, S. (2011). Safe system–comparisons of this approach in australia. In *Australasian College of Road Safety National Conference, Melbourne.*

Mote, S., Kulkarni, V., and Narkhede, B. (2016). Kano model application in new service development and customer satisfaction. *IOSR Journal of Business and Management*, 18:10–14.

Murri, R., Martinbianco, R., and Gerster, B. (2008). Sicherheitsgurt fuer motorradfahrer. *FORSCHUNGSHEFTE ZWEIRADSICHERHEIT*, (13).

Nahum, A. M., Schneider, D. C., and Kroell, C. K. (1975). Cadaver skeletal response to blunt thoracic impact. Technical report, SAE Technical Paper.

Nairn, R. (1993). *Motor Cycle Safety Research Literature Review: 1987 to 1991*. Federal Office of Road Safety.

Neathery, R. F., Kroell, C. K., and Mertz, H. J. (1975). Prediction of thoracic injury from dummy responses. Technical report, SAE Technical Paper.

NHTSA (1993). 49 CFR Part 572, Anthropomorphic test devices, Subpart E - Hybrid III Test Dummy.

Nieboer, J., Wismans, J., Versmissen, A., Van Slagmaat, M., Kurawaki, I., and Ohara, N. (1993). Motorcycle crash test modelling. Technical report, SAE Technical Paper.

Nyquist, G., Begman, P., King, A., and Mertz, H. (1980). Correlation of field injuries and gm hybrid hi dummy responses for lap-shoulder belt restraint. *Journal of biomechanical engineering*, 102:103.

OECD (2008). *Towards Zero: Ambitious Road Safety Targets and the Safe System Approach*. Organisation for Economic Co-operation and Development.

Osendorfer, H. and Rauscher, S. (2001). The development of a new class of two-wheeler vehicles. In *Proceedings of the 17th International Conference on the Enhanced Safety of Vehicle (ESV), Amsterdam, Netherlands*.

Otte, D. (1994). Biomechanics of impacts to the legs of motorcyclists and constructional demands for leg protectors on the motorcycle. In *Proceedings of the International Research Council on the Biomechanics of Injury conference*, volume 22, pages 271–290. International Research Council on Biomechanics of Injury.

Otte, D., Chinn, B., Doyle, D., Mäkitupa, S., Sturrock, K., and Schuller, E. (1999). Contribution to final report of cost 327 project. *University of Hannover*.

Otte, D. and Middelhauve, V. (1987). Quantification of protective effects of special synthetic protectors in clothing for motorcyclists. In *Interntional IRCOBI conference on the*.

Otte, D., Schroeder, G., and Richter, M. (2001). Possibilities for load reductions using garment leg protectors for motorcyclists–a technical, medical and biomechanical approach. *Annual proceedings/Association for the Advancement of Automotive Medicine. Association for the Advancement of Automotive Medicine*, 46:367–385.

Ouellet, J. V. (1982). Environmental hazards in motorcycle accidents. In *Proceedings of the 26th annual meeting of the american association for automotive medicine, Ottawa, Ontario, Canada*, volume 325.

Ouellet, J. V. (1990). Appropriate and inappropriate strategies for injury reduction in motorcycle accidents. Technical report, SAE Technical Paper.

Phillips, K. D. (2004). Protective headgear and protective armour and a method of modifying protective headgear and protective armour. US Patent 8,615,817.

Piantini, S., Pierini, M., Delogu, M., Baldanzini, N., Franci, A., Mangini, M., and Peris, A. (2016). Injury analysis of powered two-wheeler versus other-vehicle urban accidents. In *IRCOBI Conference., Malaga, Spain*.

Pipkorn, B., López-Valdés, F. J., Juste-Lorente, O., Insausti, R., Lundgren, C., and Sunnevång, C. (2016). Assessment of an innovative seat belt with independent control of the shoulder and lap portions using thor tests, the thums model, and pmhs tests. *Traffic injury prevention*, 17(sup1):124–130.

Pohekar, S. and Ramachandran, M. (2004). Application of multi-criteria decision making to sustainable energy planningâa review. *Renewable and sustainable energy reviews*, 8(4):365–381.

Prasad, P. and Daniel, R. P. (1984). A biomechanical analysis of head, neck, and torso injuries to child surrogates due to sudden torso acceleration. Technical report, SAE Technical Paper.

Prasad, P. and Mertz, H. J. (1985). The position of the united states delegation to the iso working group 6 on the use of hic in the automotive environment. Technical report, SAE Technical Paper.

Pratellesi, A., Turrin, S., Haag, T., Scippa, A., and Baldanzini, N. (2011). On the effect of testing uncertainties in the homologation tests of motorcycle helmets according to ece 22.05. *International journal of crashworthiness*, 16(5):523–536.

Richter, M., Otte, D., Lehmann, U., Chinn, B., Schuller, E., Doyle, D., Sturrock, K., and Krettek, C. (2001). Head injury mechanisms in helmet-protected motorcyclists: prospective multicenter study. *Journal of Trauma and Acute Care Surgery*, 51(5):949–958.

Rodgers, G. B. (1990). The effectiveness of helmets in reducing all-terrain vehicle injuries and deaths. *Accident Analysis & Prevention*, 22(1):47–58.

Rogers, C., Pagliarello, G., McLellan, B., and Nelson, W. (1991). Mechanism of injury influences the pattern of injuries sustained by patients involved in vehicular trauma. *Canadian journal of surgery. Journal canadien de chirurgie*, 34(3):283–286.

Rogers, N. M. and Zellner, J. W. (1998). An overall evaluation of ukds motorcyclist leg protectors based on is0 13232. In *16th Enhanced Safety of Vehicles Conference*.

Ross, D. J. (1983). The prevention of leg injuries in motorcycle accidents. *Injury*, 15(2):75–77.

Rouhana, S. W., Bedewi, P. G., Kankanala, S. V., Prasad, P., et al. (2003). Biomechanics of 4-point seat belt systems in frontal impacts. *Stapp Car Crash Journal*, 47:367.

RTO (2007). Test methodology for protection of vehicle occupants against anti-vehicular landmine effects. Technical Report RTO-TR-HFM-090.

Sage, A. P. and Rouse, W. B. (1999). *An introduction to systems engineering and systems management*. John Wiley & Sons, Inc., New York.

Saint-Hilaire, M. (2015). Motorcycle safety belt device. US Patent 8,925,669.

Santucci, M., Pieve, M., Koenig, J., Bianco, E., et al. (2009). Powered-two-wheeler integrated safety-first results of the sim project. In *Proceedings: International Technical Conference on the Enhanced Safety of Vehicles*, volume 2009. National Highway Traffic Safety Administration.

Sauerwein, E., Bailom, F., Matzler, K., and Hinterhuber, H. H. (1996). The kano model: How to delight your customers. In *International Working Seminar on Production Economics*, volume 1, pages 313–327.

Schuller, E., Beier, G., and Spann, W. (1982). Effectiveness of protective clothing in munich area motorcycle accidents. Technical report, SAE Technical Paper.

Schuller, E., Beier, G., and Spann, W. (1986). Disability and impairment of protected and unprotected motorcycle riders. Technical report, SAE Technical Paper.

Senge, P. (1990). The fifty discipline: the art and practice of the learning organizationâ, doubleday/currency, new york.

Servadei, F., Begliomini, C., Gardini, E., Giustini, M., Taggi, F., and Kraus, J. (2003). Effect of italyâs motorcycle helmet law on traumatic brain injuries. *Injury prevention*, 9(3):257–260.

Shiba, S. (1993). *New American TQM*. Productivity press.

Sponziello, A., Frendo, F., and Guiggiani, M. (2008). Stability analysis of a three-wheeled motorcycle. *SAE International Journal of Engines*, 1(2008-32-0062):1396–1401.

Sporner, A., Langwieder, K., and Polauke, J. (1990). Passive safety for motorcyclists-from the legprotector to the airbag. Technical report, SAE Technical Paper.

Stalnaker, R., McElhaney, J., Roberts, V., and Trollope, M. (1973). Human torso response to blunt trauma. In *Human Impact Response*, pages 181–199. Springer.

Stapp, J. P. (1970). Voluntary human tolerance levels. in impact injury and crash protections.

Tadokoro, H., Fukuda, S., and Miyazaki, K. (1985). A study of motorcycle leg protection. Technical report, SAE Technical Paper.

Terninko, J., Zusman, A., and Zlotin, B. (1998). *Systematic innovation: an introduction to TRIZ (theory of inventive problem solving)*. CRC press.

United Nations (2000). ECE/ONU 22 Rev.05 - Uniform provisions concerning the approval of protective helmets and of their visors for drivers and passengers of motor cycles and mopeds.

Van Auken, R. M., Zellner, J. W., Smith, T., and Rogers, N. M. (2005). Development of an improved neck injury assessment criteria for the iso 13232 motorcyclist anthropometric test dummy. In *19th International Technical Conference on the Enhanced Safety of Vehicles (ESV)*, number 05-0227.

Van Driessche, H. (1994). Development of an iso standard for motorcycle research impact test procedures. In *Proceedings of the 14th International Technical Conference on the Enhanced Safety of Vehicles*, pages 23–26.

Veena, D. K., Devaraj, D., Rajasree, P., and Oberoi, A. (2014). A compact sensor system for concussion mitigation in helmets-a concept prototype. In *Contemporary Computing and Informatics (IC3I), 2014 International Conference on*, pages 363–366. IEEE.

Versace, J. (1971). A review of the severity index. Technical report, SAE Technical Paper.

Viano, D. C. (1978). Evaluation of biomechanical response and potential injury from thoracic impact. *Aviation, space, and environmental medicine*, 49(1 Pt. 2):125–135.

Viano, D. C. and Lau, I. V. (1988). A viscous tolerance criterion for soft tissue injury assessment. *Journal of Biomechanics*, 21(5):387–399.

von Rosenberg, W., Chanwimalueang, T., Looney, D., and Mandic, D. P. (2015). Vital signs from inside a helmet: A multichannel face-lead study. In *Acoustics, Speech and Signal Processing (ICASSP), 2015 IEEE International Conference on*, pages 982–986. IEEE.

Watson, G. H. (2003). Customer focus and competitiveness. *Six Sigma and Related Studies in the Quality Disciplines*, pages 59–66.

Watson, P. (1990). Motorcycle casualties-a time bomb? how long is the fuse? *Journal of traffic medicine*, 18(HS-041 056).

WHO (2005). United nations road safety collaboration: a handbook of partner profiles.

WHO (2015). *Global status report on road safety 2015*. World Health Organization.

WHO (2017). Powered two-and three-wheeler safety: a road safety manual for decision-makers and practitioners.

Wiechel, J. F., Bell, S., Pritz, H., and Guenther, D. A. (1985). Enhancement of the hybrid iii dummy thorax. Technical report, SAE Technical Paper.

Withnall, C., Shewchenko, N., Wiley, K., and Rogers, N. (2003). An improved dummy neck for the iso 13232 motorcycle anthropometric test dummy. In *proceedings of the 18th International Technical Conference on the Enhanced Safety of Vehicles, Nagoya, Japan, National Highway Traffic Safety Administration, Washington DC*.

Yamada, H. and Evans, F. (1970). Strength of biological materials (baltimore, md: Williams and wilkins).

Yamazaki, T., Iijima, S., and Yamamoto, T. (2001). Exploratory study of an airbag concept for a large touring motorcycle: Further research. In *17 th International Technical Conference on the Enhanced Safety of Vehicles*.

Yettram, A., Happian-Smith, J., Mo, L., MACAULEY, M., and Chinn, B. (1994). Computer simulation of motorcycle crash tests.

Yoganandan, N., Pintar, F. A., Zhang, J., Gennarelli, T. A., and Beuse, N. (2005). Biomechanical aspects of blunt and penentrating head injuries. In *IUTAM Symposium on impact biomechanics: From fundamental insights to applications*, pages 173–184. Springer.

Zettas, J. P., Zettas, P., and Thanasophon, B. (1979). Injury patterns in motorcycle accidents. *Journal of Trauma and Acute Care Surgery*, 19(11):833–836.

Zhu, D.-S., Lin, C., Tsai, C., and Wu, J. (2010). A study on the evaluation of customersâ satisfaction–the perspective of quality. In *4th international quality conference. Center for Quality, Faculty of Mechanical Engineering, University of Kragujevac*, volume 19.

Acknowledgments

Un grazie a tutti coloro che, con un gesto, una parola, un consiglio o un'azione, hanno contribuito affinchè potessi raggiungere questo prestigioso traguardo. Spero possiate in qualche modo gioirne ed esserne fieri.

GRAZIE!